A pre-feasibility study of a concentrating solar power system to offset electricity consumption at the Spier Estate

by

Matti Lubkoll

Master's project presented in partial fulfilment of the requirements for the degree Master of Engineering at Stellenbosch University

Department of Mechanical and Mechatronic Engineering

Stellenbosch University

Faculty of Engineering

Supervisor: Mr. Paul Gauché

Co-supervisor: Prof. Alan C. Brent

December 2011

Declaration

By submitting this thesis electronically, I declare that the entirety of the work contained therein is my own, original work, that I am the sole author thereof (save to the extent explicitly otherwise stated), that reproduction and publication thereof by Stellenbosch University will not infringe any third party rights and that I have not previously in its entirety or in part submitted it for obtaining any qualification.

December 2011

ABSTRACT

The Spier Estate - a wine estate in the Western Cape Province of South Africa - is engaged in a transition towards operating according to the principles of sustainable development. Besides changes in social and other environmental aspects, the company has set itself the goal to be carbon neutral by 2017. To this end, Spier is considering the on-site generation of electricity from renewable energy sources. This study was initiated to explore the technical and economic feasibility of a concentrating solar power plant for this purpose on the estate.

The investigation was carried out to identify the most appropriate solar thermal energy technology and the dimensions of a system that fulfils the carbon-offset requirements of the estate. In particular, potential to offset the annual electricity consumption of the currently 5 570 MWh needed at Spier, using a concentrating solar power (CSP) system, was investigated. Due to rising utility-provided electricity prices, and the expected initial higher cost of the generated power, it is assumed that implemented efficiency measures would lead to a reduction in demand of 50% by 2017. However, sufficient suitable land was identified to allow electricity production exceeding today's demand.

The outcome of this study is the recommendation of a linear Fresnel collector field without additional heat storage and a saturated steam Rankine cycle power block with evaporative wet cooling. This decision was based on the system's minimal impact on the sensitive environment in combination with the highest potential for local development. A simulation model was written to evaluate the plant performance, dimension and cost. The analysis was based on a literature review of prototype system behaviour and system simulations. The direct normal irradiation (DNI) data that was used is based on calibrated satellite data. The result of the study is a levelised cost of electricity (LCOE) of R2.74[1] per kWh, which is cost competitive to the power provided by diesel generators, but more expensive than current and predicted near-future utility rates. The system contains a 1.8 ha aperture area and a 2.0 MWe power block. Operating the plant as a research facility would provide significant potential for LCOE reduction with R2.01 per kWh or less (favourable funding conditions would allow for LCOE of R1.49 per kWh) appearing feasible, which results in cost competitiveness in comparison a photovoltaic (PV) solution. Depending on tariff development, Eskom rates are predicted to reach a similar level between 2017, the time of commissioning, and the year 2025. The downside is that the plant would not solely serve the purpose of electricity offsetting for Spier, which may result in a reduced amount of electricity that may be generated.

Further studies are proposed to refine the full potential of cost reduction by local development and manufacturing as well as external funding. This includes identification of suitable technology vendors for plant construction. An EIA is required to be triggered at an early stage to compensate for its long preparation.

[1] All conversion rates are calculated with R7.3 per $ and R9.5 per €. R = South African Rand (ZAR)

OPSOMMING

Die Spier wynlandgoed in die Wes-Kaap Provinsie van Suid-Afrika is tans in ‘n oorgangsfase tot besigheids-praktyke gebaseer op volhoubare ontwikkeling. Afgesien van die sosiale en omgewingsaspekte het die groep hom ook ten doel gestel om koolstof neutraal te wees teen 2017. Ten einde hierdie doel te bereik, moet die maatskappy sy algehele elektrisiteitsverbruik vervang met hernubare bronne. Hierdie studie is dus geloods om die tegniese en ekonomiese uitvoer-baarheid van 'n gekonsentreerde sonkragstasie op die landgoed te ondersoek.

Hierdie ondersoek is gedoen om die mees toepaslike sontermiese tegnologie en die grootte van 'n termiese sonkragstelsel te bepaal, wat aan die koolstof vereistes van die landgoed voldoen. Die potensiaal om die jaarlikse elektrisiteitsverbruik van 5 570 MWh met 'n gekonsentreerde elektriese sonkrag-stelsel te vervang, is ondersoek. Weens die toename in die elektrisiteitsprys en die verwagte hoërkoste van opgewekte elektrisiteit word aanvaar dat die implementering van voorgestelde doeltreffendheidsverbeteringe, sal lei tot 'n afname in die aanvraag na elektrisiteit van tot 50% teen die jaar 2017. Voldoende beskikbare grond is geïdentifiseer om genoeg elektrisiteit te produseer om die huidige vraag na elektrisiteit te oorskry.

Die uitkoms van die studie is die aanbeveling van 'n lineêre Fresnel kollektorveld sonder addisionele warmte storing, asook 'n versadigde stoom Rankine siklus-kragblok met ‘n nat-verdamping verkoelingstelsel. Die besluit is gebaseer op die stelsel se minimale impak op die omgewing, tesame met die hoogste potensiaal vir plaaslike ontwikkeling. 'n Simulasie is ontwikkel om die aanleg se werkverrigting, grootte en koste te evalueer. Die analise is gebaseer op 'n literatuuroorsig van 'n prototipe stelsel gedrag en stelsel-simulasies. Die direkte normale sonstralings data wat gebruik is, is gebaseer op gekalibreerde satelliet data. Die bevinding van die studie is 'n gebalanseerd koste van elektrisiteit van R2.74 per kWh, wat mededingend is met die koste van elektrisiteit wat deur diesel kragopwekkers verskaf word, maar is aansienlik duurder as die huidige en toekomstige voorspellings van Eskom-tariewe. Die stelsel bevat 'n 1.8 ha son kollektor oppervlakte en 'n 2.0 MWe krag-blok. Daarbenewens, sal die gebruik van die aanleg as 'n navorsingsfasiliteit die potensiaal hê om die gebalanseerd koste van elektrisiteit te verminder na R2.01 per kWh of minder (gunstig befondsing voorwaardes sal gebalanseerd koste van elektrisiteit van R1.49 per kWh tot gevolg hê), wat mededingend is met die koste van 'n fotovoltaïese alternatief. Daar word voorspel dat Eskom-tariewe dieselfde sal bly vanaf 2017, die jaar van inbedryfstelling van die aanleg, tot en met die jaar 2025. Die nadeel is dat die aanleg nie noodwendig uitsluitlik vir die opwek van elektrisiteit vir Spier gebruik sal word nie, en daarom kan dit lei tot 'n vermindering in die hoeveelheid elektrisiteit wat deur die aanleg opgewek word.

Daar word voorgestel dat verdere studies onderneem word om die moontlikheid van koste-besparings vir die aanleg te ondersoek deur gebruik te maak van plaaslike ontwikkeling en vervaardiging, asook eksterne befondsing. Dit sluit die identifisering van geskikte tegnologie verskaffers vir die aanleg-kostruksie in. 'n Omgewingsimpakstudie, volgens die EIA regulasies, moet ook so gou as moontlik gedoen word aangesien dit n langsame proses is.

PLAGIARISM DECLARATION

I know that plagiarism is wrong.

Plagiarism is to use another's work (even if it is summarised, translated or rephrased) and pretend that it is one's own.

This assignment is my own work.

Each contribution to and quotation (e.g. "cut and paste") in this assignment from the work(s) of other people has been explicitly attributed, and has been cited and referenced. In addition to being explicitly attributed, all quotations are enclosed in inverted commas, and long quotations are additionally in indented paragraphs.

I have not allowed, and will not allow, anyone to use my work (in paper, graphics, electronic, verbal or any other format) with the intention of passing it off as his/her own work.

I know that a mark of zero may be awarded to assignments with plagiarism and also that no opportunity will be given to submit an improved assignment.

I know that students involved in plagiarism will be reported to the Registrar and/or the Central Disciplinary Committee.

Name: Matti Lubkoll

Student no: 16105974

Signature:

Date: 25.07.2011

ACKNOWLEDGEMENTS

First I would like to thank my study supervision team: Prof. Alan C. Brent for his excellent guidance throughout this project, and Mr. Paul Gauché for his continued support and valuable input.

Further gratitude is directed to the Spier Estate in general, and Ms. Cherie Immelman, Ms. Christie Kruger and Mr. Orlando Filander in particular for their continued accessibility and friendly support.

I would also thank Mrs. Welma Liebenberg, Mr. Riaan Meyer and the entire team of CRSES for their continued assistance throughout my entire degree and during this project specifically.

And lastly, special recognition is directed to the German Academic Exchange Service (DAAD) for the generous funding of my studies at Stellenbosch University.

TABLE OF CONTENTS

Page

LIST OF FIGURES

Page

LIST OF TABLES

NOMENCLATURE

A	Area (aperture/plant/surface)
a	year
CENERG	Centre Energétique et Procédés
CRSES	Centre for Renewable and Sustainable Energy Studies
CDM	Clean development mechanism
CF	Capacity factor
CFD	Computational fluid dynamics
CLFR	Compact linear Fresnel
CRF	Capital recovery factor
CPC	Compound parabolic concentrator
CSP	Concentrating solar power
d	Day
DLR	Deutsches Zentrum für Luft- und Raumfahrt
DNI	Direct normal irradiation
DSG	Direct steam generation
DOE	Department of Energy
E_{beam}	Insolation
E_{net}	Net energy production
EC	European Commission
EOT	Equation of time
GHG	Greenhouse gas
GIS	Geographic information system

GMT	Greenwich mean time
GWP	Global warming potential
h	hour
h	convection heat transfer coefficient.
HTF	Heat transfer fluid
I	Irradiance
$I_{reflected}$	Reflected irradiance
I_{usable}	Usable irradiance
IAM	Incidence angle modifier
IAM_{COS}	Incidence angle modifier cosine effect
IAM_{l}	Incidence angle modifier for longitudinal incidence angles
IAM_{t}	Incidence angle modifier for transversal incidence angles
IPP	Independent power producer
k	Thermal conductivity
k_d	Real debt interest rate
k_{fuel}	Annual fuel cost
k_{invest}	total investment of plant
$k_{insurance}$	Annual insurance rate
$k_{O\&M}$	Annual Operation & Maintenance cost
LCA	Life cycle assessment
LCOE	Levelized cost of electricity
LCT	Local clock time
n	year
N	day of the year

NERSA	National Energy Regulator of South Africa
NREL	National Renewable Energy Research Laboratory
O&M	Operation and maintenance
ORC	Organic Rankine cycle
$P_{thermal}$	Thermal load
$\dot{q}'_{cond}$	Conduction heat loss rate
$\dot{q}'_{conv}$	Convection heat loss rate
$\dot{q}'_{Heat\ loss}$	Heat loss rate
$\dot{q}'_{in}$	Heat input rate
$\dot{q}'_{loss}$	Heat loss rate
$\dot{q}'_{rad}$	Radiation heat loss rate
$\dot{q}'_{SolAbs}$	Solar irradiation absorption rate
$\dot{q}'_{thermal\ in}$	Heat input rate on heat transfer fluid
RC	Rankine cycle
SAM	Solar Adviser Module
SEGS	Solar Energy Generating Systems
t	Pipe wall thickness
$T_{absorber}$	Absorber temperature
$T_{ambient}$	Ambient temperature
T_C	Condenser temperature
T_H	Temperature of hot reservoir
T_{iH}	Temperature of internal hot reservoir
T_{iL}	Temperature of internal cold reservoir
T_L	Temperature of cold reservoir

t_s	Solar time
t_{sr}	Sidereal time
u	Heat loss coefficient
W	Work
x	Function of the day
ZAR	South African Rand

η	Efficiency
η_{Carnot}	Carnot efficiency
η_{CN}	Chambadal-Novikov efficiency
η_O	Optical efficiency
η_{pb}	Power block performance
$\eta_{reflector}$	Optical efficiency of reflector
$\eta_{transenv}$	Transmissivity of envelope
θ	Incidence angle of the sun
θ_l	Longitudinal incidence angle
θ_t	Transversal incidence angle
θ_z	Zenith angle
ω	Hour angle

INTRODUCTION

The Spier Estate (hereafter referred to as Spier) is a wine estate located in the Cape Winelands region of the Western Cape Province of South Africa. It is actively engaged in transforming its enterprise into a company operating under the principles of sustainable development. The company's vision is to "make a real difference to society and the planet" (Spier 2008). This statement indicates that, besides seeking a more equal and just society, Spier is committed to changing the way in which it consumes natural resources, as a source and as a sink. In this context, the short-term, self-imposed targets comprise, amongst others, plans for more environmental friendly farming, zero waste water production and a carbon neutral footprint by 2017 (Spier 2008). With more than 60% of Spier's carbon emissions caused by electricity consumption, renewable power generation provides the biggest lever towards the proposed target. The total CO_2 emissions in the business year 2007-08 was 6 055 tonnes (Spier 2008).

Currently the electricity consumed by Spier is provided by Eskom, which generates more than 90% of its energy from coal, the worst source in terms of greenhouse gas (GHG) emissions (Fröhlich, Schwarz 2009). To offset its share of emissions caused by electricity, Spier is committed to generating its own electricity by means of renewable energies.

Individual investigations and proposals have been initiated in the past to satisfy the power demand of parts of the estate. These projects include a biomass fired power station and a PV solution mounted on the roof of buildings. Spier rejected those proposals mainly due to funding problems (Pahwa 2011). Interest in concentrating solar power (CSP) has emerged as it appears to be one of the most promising, cost effective technologies for electricity production. This project is Spier's first attempt to investigate satisfaction of the demand of the entire estate.

The target of this study was to identify a suitable CSP system tailored for the Spier context and evaluate the cost of construction and operation. The technologies need to conform to Spier's ethos of sustainability and South Africa's industrial environment. Additionally, Spier will be provided with material to decide how to further approach their targets and whether to initiate a full scale feasibility study.

A CSP plant at Spier would not only represent the first operating solar thermal power plant in South Africa, but one with ideal public exposure. Spier is situated between Stellenbosch and Cape Town (two towns well known for their universities, wineries, and sought after climate) and is popular among tourists. Furthermore, due to Spier's proximity to parliament in Cape Town and Cape Town International Airport, it is easily accessible to national and international political representatives. For these reasons, a CSP plant at Spier would have high strategic and representative value.

The work in this paper is based on several underlying assumptions. Firstly, it was assumed that the municipality of Stellenbosch would buy excess electricity in times of peak production and sell back grid electricity at times of higher demand. This procedure was assumed with equal prices for selling and buying. It is difficult to predict how electricity demand will behave between the time of this study and 2017; however, rapidly increasing Eskom rates for the following years are likely to boost the trend towards energy efficiency. Because Spier has not yet developed a roadmap toward their target to achieve zero emissions, there was no strategy in place to determine the extent energy efficiency measures will be deployed to reduce the need for energy production. Therefore, it was agreed for this study that offsetting half of the current electricity consumption would be a sufficient target. In addition, an analysis of available land was conducted in the event that Spier required higher than assumed demand or other consumers showed an interest in purchasing renewable energy at the time.

CHAPTER 1: CONTEXTUAL REVIEW

The contextual review provides a background to this project's objective. The first section supplies information about Spier, including their reasoning to initiate this research and an overview on the estate's efforts to date. The electricity consumption and trends thereof conclude the background on the estate. The second part of the contextual review outlines the availability of key resources required for a solar thermal power plant. These resources are the amount of suitable land, the availability of water for cooling purposes and the insolation on the farm. The contextual review is completed with the project objective and the research methodology.

1.1 Spier background

Spier is situated in South Africa's Winelands of the Western Cape. As shown in Figure 1 the estate is located just outside Cape Town. It is surrounded by the town of Stellenbosch to the North, the R310 (Baden Powell Drive) to the West, Annandale Road to the South and nearly stretches to the R44 on the east.

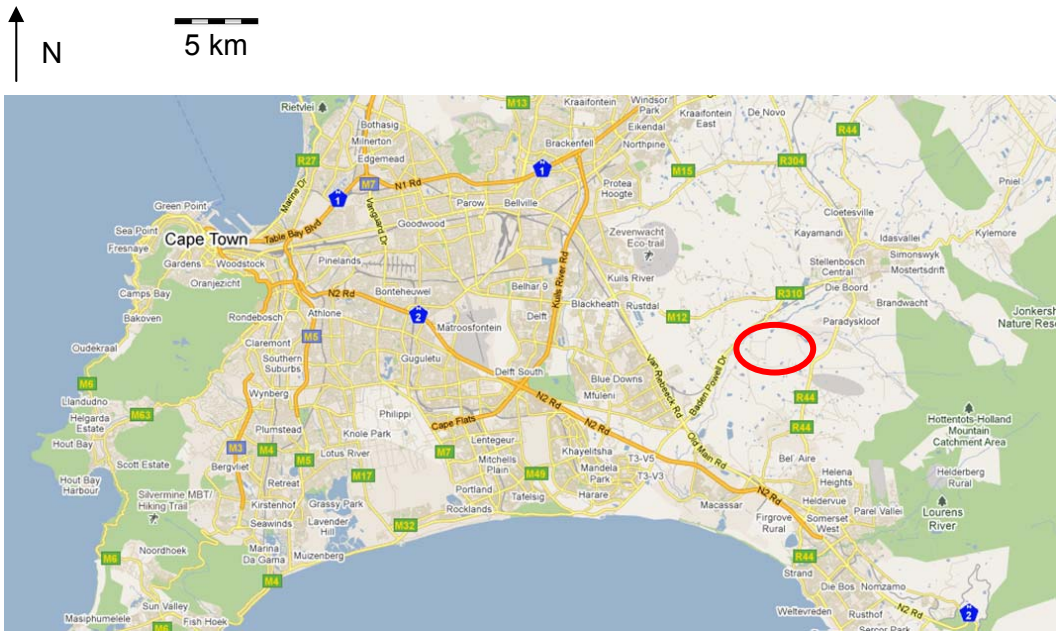

Figure 1: Location of Spier home farm (Google Maps 2010)

Spier is not solely a producer of wine. The estate also operates a hotel, several restaurants, a conference centre and recreational facilities. The entire Spier Estate, with all its units, is prescribing a way toward a sustainable future. To this end, Spier has initiated multiple projects in the many facets of sustainable development, and the company is publishing the progress in sustainability

reports. In order to clarify the aim and purpose of these developments, Spier's ambitious macro-targets are discussed in the following section along with a discussion of their previous work and approaches on energy efficiency and renewable energy production.

1.1.1 Macro-targets

The aim of the macro-goals is to enhance the transition of the company towards a sustainably operated business by 2017 (Spier 2008). Winkler (2007) highlights the three columns of sustainable development that need to go hand-in-hand to achieve the transition towards a prosperous sustainable business: economic, social and environmental development, as illustrated in Figure 2.

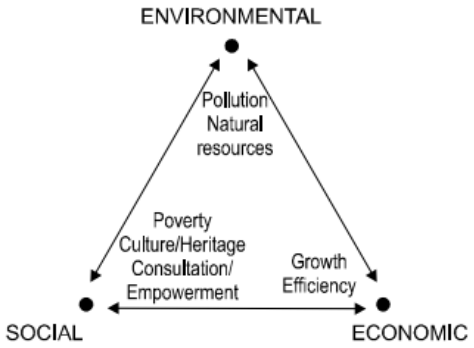

Figure 2: Elements of sustainable development (Winkler 2007)

For Spier, the elements of sustainable development are subdivided into the two groups of climate change goals (environmental) and poverty alleviation goals (social), while the economic goals are a matter for Spier as a private enterprise. The social and environmental targets are highlighted in the sustainability report (Spier 2008). Spier's social macro goals comprise matters such as local job creation, social security, improvement of living conditions, empowerment and education (Spier 2008). The environmental elements of sustainable development are combined as climate change goals and consist of carbon neutrality, zero waste solids, zero waste water, water sustainability, biodiversity enhancement and environmentally friendly farming (Spier 2008). The latter five aims deal with sustainable utilisation of resources and improvement of the farm's direct impact on the environment. The first point of carbon neutrality, however, contains the most ambitious of all the targets. Spier is planning to achieve a zero carbon footprint by 2017 by deploying energy efficiency measures and shifting from utility generated electricity to renewable energy (Spier 2008). The mid-term target for achieving carbon neutrality is a 50% emission reduction by 2012 (Pahwa 2011). As discussed in the following section, this target is unlikely to be reached.

1.1.2 Previous work

In the year 2007, Spier set the macro-goal of achieving carbon neutrality by 2017. A variety of energy efficiency and energy generation projects have been initiated by now. In 2008, the installation of timers on hotel geysers, accompanied by a trigger matrix to switch off hotel sections during periods of low booking, was the only project that had been realised (Immelman 2010). Further proposals were requested from industry and the Centre for Renewable and Sustainable Energy

Studies (CRSES), but none was pursued mainly due to funding difficulties (Pahwa 2011).

Energy efficiency

Spier's hotel facilities were initially equipped with solar water heaters. Due to poor positioning, the output was less than expected and the systems remained unused; as a result, maintenance was neglected (Immelman 2010). Refurbishment of the solar water heater systems was considered in 2008 but not implemented (Pahwa 2011). Further proposals in 2009 to install solar water heaters on the conference and banqueting buildings failed for financial reasons (Pahwa 2011). In 2010, solutions were explored to replace the hotel's individual electric geysers for each room with two heat pumps that would meet the combined hotel hot water demand (Tekniheat 2010). In the same year, however, the proposals were dropped due to insufficient funds (Pahwa 2011).

Renewable energy production

In 2006, the first project on renewable energy production was the investigation of a biodiesel production plant. This project was halted in 2007 as unexpected supply reductions lead to project failure (Pahwa 2011). The subsequent year, energy production based on biomass digesters was analysed. This project included on-site plantation of usable wood, but it was not pursued due to economic reasons and a decision to utilise the land necessary for tree plantation for other purposes (Pahwa 2011). The first solar energy project was investigated in 2009 when proposals to offset about 10% of the banqueting and conference centre's electricity demand were requested (Pahwa 2011). Despite the dropping prices for PV systems, these projects were never realised due to financial reasons (Pahwa 2011).

Independent of these developments, Spier's winemaker, Frans Smit, pursued his own track towards increased energy efficiency. His work includes projects such as improved insulation of wine chillers. His boundary was a payback period of one to two years (Smit 2010). This restriction prevented the feasibility of many attempts.

1.1.3 Electricity demand

The demand for electricity at Spier can be broken down into four basic sectors of consumption: the resort, winery, hotel and farming. The consumption of each unit and the total demand for the business year 2008-09 are given in Figure 3. The average annual electricity consumption over the past five years was 5 570 MWh (Kruger 2010).

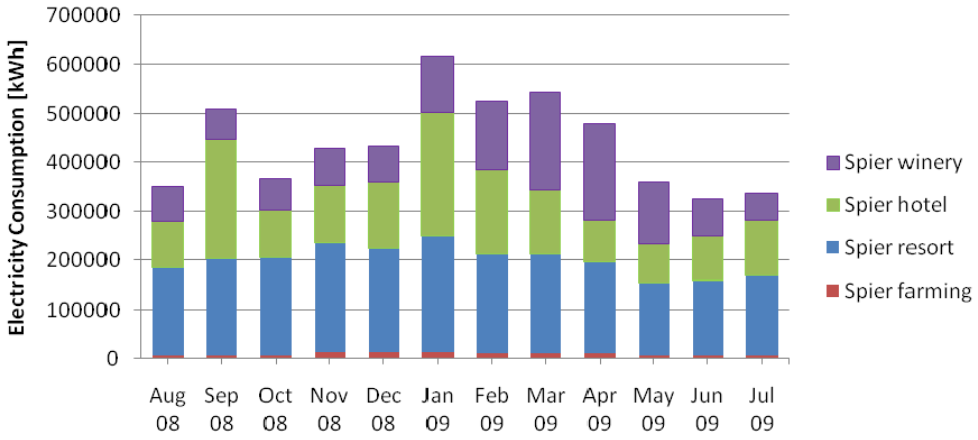

Figure 3: Spier electricity consumption for business year 2008/2009

A peaking of consumption can be observed during the summer months (January to March) mainly caused by the hotel and the winery. The hotel demand is largely dependent on bookings which peak in the summer holidays (and occasionally due to conferences), while the winery demand peaks after the harvest when the grapes and wine barrels need to be chilled (Smit 2010).

1.1.4 Metered electricity consumption patterns

The highest electricity consumption of the winery occurs during March and April. However, available metering data for the peak month of March, 2008, shows no significant correlation between electricity demand and time of the day, as shown in Appendix A. The electricity consumption of the hotel was metered in early March, 2008. As illustrated in Appendix B, a continuous pattern of peak consumption can be seen in the morning around 09h00 and again in the evening hours after 18h00; at the same time, the amount of peak consumption varied from day-to-day. The pattern of hotel electricity consumption is explained by customer behaviour. Guests showering in the morning before leaving the hotel cause the morning peak. In the evening, when they return from the day's activities and prepare for dinner, a second peak consumption is generated (Immelman 2010). The data logged for the hotel has lead to the described installation of automatic shut offs and geyser timers. This information should be viewed with caution, but the implemented changes do appear to affect the overall consumption rather than the demand pattern.

1.2 General resource availability

For the development of every technological product, several key boundary conditions need to be determined in order to select the appropriate technology and accurate sizing thereof. First, the size and limitations of suitable land is important as this defines the maximum dimensions of a plant and can influence the technology selection. Next to consider is the solar irradiation. As the natural

power source that drives the plant, the insolation data leads to appropriate sizing of plant components. Lastly, the availability of water is needed to be known to allow decision on the appropriate cooling technology.

1.2.1 Available land

A variety of solar thermal power plant technologies has been developed in recent decades. Every approach has its specific requirements on land quality and size. For this reason it is important to investigate the availability of land as a first step as this gives a required boundary for selecting the appropriate solar thermal technology. Investigating land availability included analysing current land use, such as whether it is being used as farmland or has existing structures (i.e., buildings, power lines), and the slope on the remaining available areas. This investigation was based on geographic information system (GIS) data. The GIS maps were made available by Spier and allow access to information about structures, vineyards, roads, dams and power lines, as well as topographic information regarding slopes on the property.

A satellite image of Spier is shown in Figure 4 (a large scale picture is given in Appendix C). The network of green lines indicates farm roads. The two main entrances to the estate are the southern entrance off of Annandale Road, and the western entrance off of Baden Powell Drive. Houses and other structures are marked black on the map. Dams are turquoise, vineyards are orange and grazing areas are marked by blue and green fields. Red lines represent power lines..

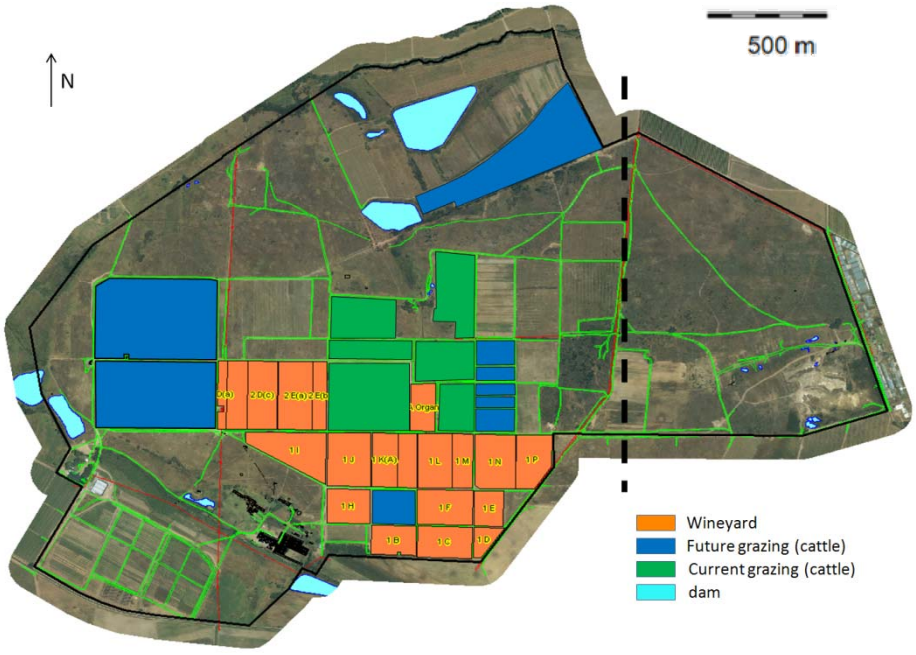

Figure 4: Spier Home Farm

A black dashed line on the right hand side of Figure 4 indicates a limitation of the possible extension for the power plant to the east, as from there on the power plant structure would be directly visible from the De Zalze Winelands Golf Estate. Such conspicuousness is not desired as it would lead to a foreseeable clash of interests that bears the risk of project failure. At the moment, the land that is not marked orange is mainly used for grazing and partially included in future planning schemes. These schemes are flexible and can be shaped around the implementation of a solar thermal power plant, as only irrigation infrastructure is involved (Filander 2010). Figure 4 indicates that the majority of the land - including the green and blue areas - is potentially available to accommodate a solar thermal power plant.

The second point of interest after principal land availability was the slope of the land. Different technologies are restricted by different maximal gradients. Note however, that a slope of 1% to 1.75% can accommodate any available technology. Feasible locations were determined by looking at the GIS slope map, given in Appendix D. In Appendix D, the magnitude of the slope is indicated by different colours of the map. Contour lines are shown with 1 m of altitude difference. The farm is built mainly on uneven undulating terrain. Nevertheless, there are three spots identified with a slope of less than 1%. One is situated in a valley on the south-eastern edge of the farm, in an area exposed to De Zalze Winelands Golf Estate. The other two are situated in the farm centre, directly north of the vineyards and marked in a larger scaled illustration in Figure 5.

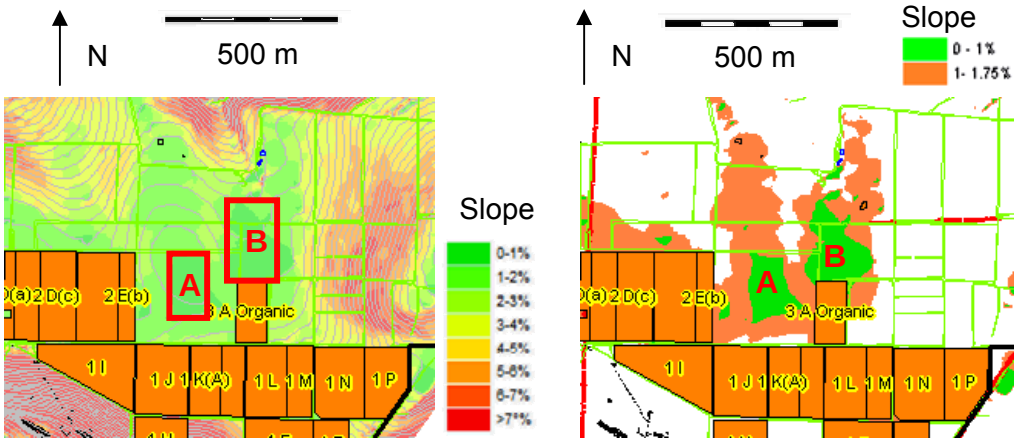

Figure 5: Zoomed in image of site with low slope

The south-western area A encloses about 2.3 hectares, while field B measures about 3.3 hectares. At 1.75% slope, the size of field B will not change significantly, whereas the initially smaller field A will increase up to more than 10 hectares. The land available for more slope-tolerant technologies is estimated in Appendix E.

1.2.2 Water resource

Water availability is a requirement that determines whether a power plant is wet cooled or evaporative cooled. The alternative is a dry cooled power station which leads to higher levelised cost of electricity (LCOE) for the consumer due to lower system efficiency.

From a historic view, the total water consumption of Spier has decreased by 71% from 1 364.7 million liters in 2004 to 391.4 million liters in 2009 (Kruger 2010). This decrease has led to a significant spare capacity of water (Filander 2010). The Spier farm is equipped with several underground irrigation pipelines built to supply 2 m³ of water per hectare of land per hour (Filander 2010). In the surrounding areas of the suitable locations highlighted in Figure 5 are two access points to the farms pipeline system, marked by blue circles in Figure 6. The available usable capacity for the south-western supply line is 84 m³ per hour and for the central supply line 45 m³/h (Filander 2010). The indicated water pipelines are part of the farms irrigation system and can be tapped without further permission from the external irrigation board (Filander 2010). In short, an amount of 129 m³/h of water can be accessed in the immediate area of the suitable locations on the farm.

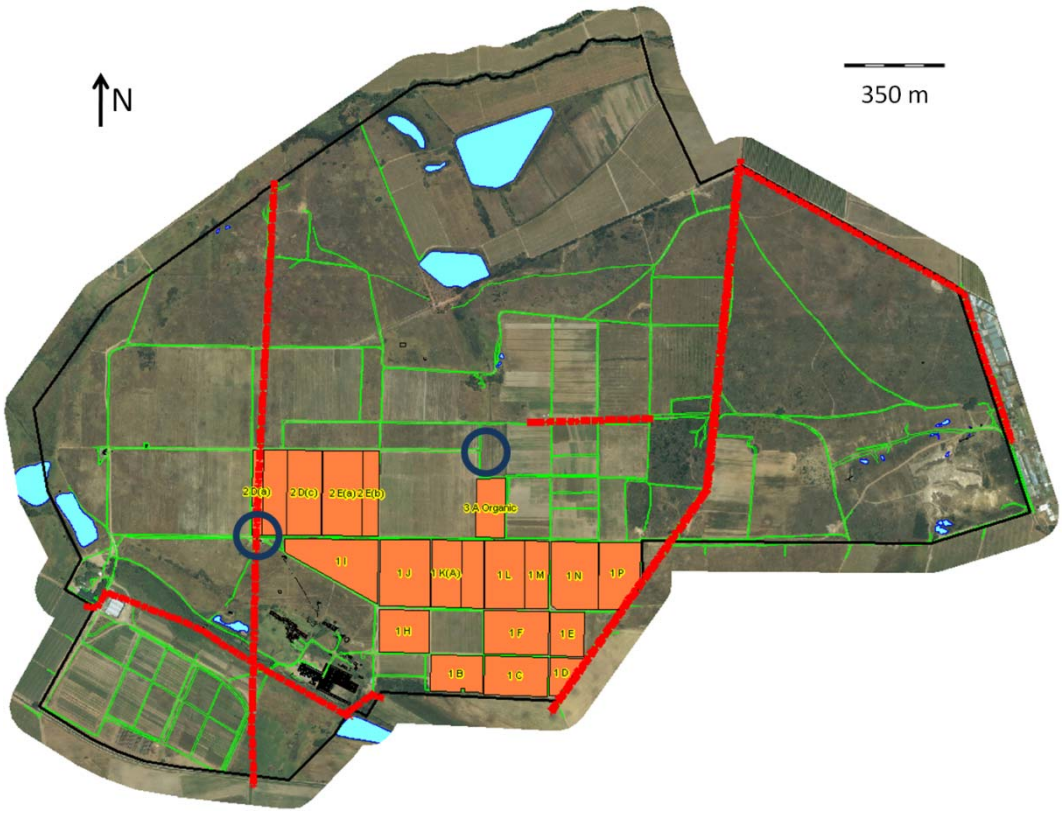

Figure 6: Irrigation pipe access marked by blue circles

1.2.3 Grid connection

The Eskom grid is highlighted by red lines in figure 6. Eskom not only allows the connection of a renewable energy production plant via a main transmission system substation or a distribution substation, it also permits a generation plant to be directly looped into an existing transmission line (ESKOM 2010a). As shown in Figure 6, every location on the farm is in proximity to transmission lines (red lines). By 2012 the Eskom grid will be able to support 4 100 MW of additionally supplied electricity in the Western Cape (ESKOM 2010a). Although the National Energy Regulator of South Africa (NERSA) allows grid connection for IPPs outside the REFIT program (NERSA 2008), the technology needs to be designed to fulfil the Distribution Code, the SA Grid Code and possibly additional codes (ESKOM 2011).

1.2.4 Solar resource

The insolation on an investigated site is important for appropriate sizing of the technology. For concentrating solar power, the direct normal irradiation (DNI) is of interest due to the CSP technologies being based on reflection and concentration of light beams. The common process is to utilise DNI data over a period of up to 30 years and develop a mean year out of that data. That mean year has the closest possible average DNI to the average of the investigated 30 years, but consists as a composition of actual measured months (Stine, Geyer 2001). A dataset of a full year with hourly DNI information can be used to size the plant.

For information on the DNI data source used and its quality, the reader is referred to Appendix F. The best fit for the Spier mean average year is given in Figure 7. The resulting average annual DNI of the best fit is 2 342.0 kWh/m², a good value compared to the actual average of 2 347.7 kWh/m². The used source provides full years data from 2005 onward. Ideally, the average year is fitted over a time frame of 30 years, but with limited available data and the scope of this study, five years is sufficient.

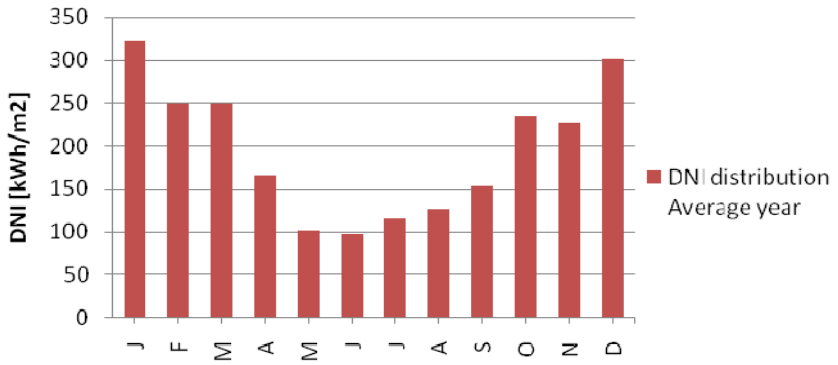

Figure 7: Average DNI (years 2005 to 2010)

1.3 Objective

The objective of this study is to supply Spier with a pre-feasibility study on its vision to offset its electricity production by operation of a CSP plant. Part of this work is to identify and provide the following:

- Appropriate technology
- Proposed power plant configuration
- Capital cost for plant installation
- Levelised cost of electricity
- Appropriate site for the power plant
- Environmental effect
- Recommendation on the way forward

The other stimulating effects of possibly the first operating CSP plant in South Africa on marketing and sales of the Spier Estate are not discussed in this report.

For clarity, the acronym CSP, or concentrating solar power, refers to solar thermal electricity generation. It must not be confused with concentrating PV applications that are usually abbreviated with CPV (concentrating photovoltaic) or CSPV (concentrating solar photovoltaic). This project does not compare the developed CSP solution with other sources of renewable energy generation such as biomass, photovoltaic or wind power. Spier requested different proposals for alternatives in the past.

1.4 Research methodology

The research methodology for this work is structured to gain reliable and comprehensive results in order to develop a pre-feasibility study to serve as a tool for decision making at Spier.

As a basis for research on a solar thermal power plant for the estate, an investigation was completed on Spier's electricity consumption and its past development. Additionally, interviews with Spier employees were used to understand the company's targets, approach and work done to date.

The resources at the Spier farm were analysed by different satellite based tools. A solar map was developed and insolation data of the previous years investigated. Based on GIS data, the land resource was evaluated. Through interviews with the farm manager, the land availability and water supply situation is discussed.

The selection of a suitable technology was done mainly based on a literature review of technology. A power plant simulation model was developed to extract the best sizing of the power block and the collector field. This model was developed on an approach using theory and simulation results from the literature and was built on hourly steady state calculations. The physical background

predicted the sun position and, accordingly, manipulated the insolation data; simulation results of linear Fresnel systems and power block behaviour were based on findings from the literature. The simulation was also supplied with cost information extracted from literature. In this way, results in sizing, capital cost and LCOE were gained. The simulation was verified by comparison to simulation results on a linear Fresnel prototype system as no operational experiences were available.

The cost results were then analysed and, based on the findings, opportunities for cost reduction are discussed. This chapter is followed up by a brief investigation of environmental impacts and a concluding recommendation on how to improve the chances of project realisation.

1.5 Conclusion

Spier has set itself ambitious targets towards a sustainable future. In the sector of renewable energy supply it is noted that the set goals are high. A path towards those goals was prepared which led to a history of many project approaches and rejections. Additionally, no money for renewable energy projects were previously allocated, leaving planners to operate with left-over budgets at the end of financial years that were ultimately insufficient. Consequently, a risk exists for a CSP project to be dismissed as well. Nonetheless, the current situation provides a basis to focus on one large scale renewable energy project instead of many small installations. In such a cost intensive context, the management has to decide on a path to go forward and the entire company must become part of the change.

This contextual review further shows that suitable land at Spier is available in two locations at 2.3 hectares and 3.3 hectares. The solar resource is higher than in Spain, where currently a large number of CSP projects are in operation, under construction or in development. The accessible water supply is 168 million liters per hour.

The winery's energy consumption pattern does not emphasise a continuous demand pattern. By contrast, the hotel consumption shows a recurring pattern with peaks in the morning and evening hours.

To gain solid conclusions, in terms of energy to be produced by 2017 and the then given potential for cogeneration, a full energy audit is needed on the entire estate. A roadmap to achieve the estimated consumption reductions by the implementation of efficiency measures should then be developed.

CHAPTER 2: TECHNOLOGY REVIEW

This chapter begins with an overview on the market situation of commercial small scale CSP products, and their appropriateness is judged. Following this overview is a discussion of different CSP collectors and appropriate power blocks in order to identify the most suitable solution for Spier. The criteria for a plant situated on the Spier home farm are elaborated on in Chapter 2.1.

2.1 Technology selection criteria

As stated in the contextual review, development at Spier endeavours to follow the principle of sustainability. This noted effort leads to important criteria when it comes to the selection of an appropriate solar thermal power plant technology. Besides the economic matters of capital cost, LCOE and operation and maintenance (O&M) cost selection is based on:

- Potential for local development
- Technology maturity
- Minimal risk of soil contamination
- Minimal risk of fire and explosion
- Low system complexity

2.2 Estimated plant dimension

Preliminary plant dimension was determined, based on typical capacity factors CF, annual production W in kWh of solar thermal power plants and the potential production hours of one year (24 hours per day at 365 days per year):

$$P_{rated} = \frac{W}{8760\frac{h}{a} \cdot CF} \quad (1)$$

The capacity factors for CSP plants range from 12% (plant SEGSII without storage) to 36% (plant Andasol I with storage) (NREL 2010). All other reported CSP plants range in between these figures. Applying this to equation (1) leads to a required plant dimension of 0.91 MWe to 2.7 MWe.

2.3 Commercial CSP systems in suitable dimension

The main focus of CSP developers lies in utility sized power plants. The SEGS plants were the first commercial systems and were built in sizes from 13.8 MWe (SEGSI) to 80 MWe (SEGSVIII & SEGSIX). Nevertheless, a few small scale CSP plants have been developed for commercial purposes. The Israeli company, Aora-Solar, offers a central receiver system of 100 kW size that is based on a gas turbine (Aora-Solar 2011). Due to its small size, a series of such systems would be needed to produce sufficient power for Spier. The Aora-Solar receiver is mounted on a 30 m high tower. As detailed in the technology review, the visual

impact of the high towers' central receiver plants makes such solutions infeasible for application the Spier environment. Furthermore, Hawaiian company, Sopogy, offers low temperature parabolic trough systems with an organic Rankine cycle (ORC) power block (Sopogy 2011). However, due to its ORC power block which contains risk of explosion and the used refrigerants that are harmful to the environment (see technology review on ORC), this system is also not a practical solution for Spier.

Currently the small market of CSP systems in the right dimension does not deliver a product which would fit the Spier environment. The central receiver system has a high visual impact, and the parabolic trough system utilises a power block that is based on a risky technology and contains materials that do not correlate with the Spier ethos of a sustainable future.

2.4 Concentrator technologies

A variety of different concentrator technologies has been investigated in recent decades, and four promising systems have evolved and reached prototype status or commercial CSP applications. These are the parabolic dish, central receiver, parabolic trough and linear Fresnel concentrator. The parabolic dish and central receiver technologies are called point concentrators since they focus the sun-beams onto a single receiver point (surface). The two other systems, linear Fresnel and parabolic trough, are categorised as line focus since the concentrators reflect the incoming sun-beams onto a linear receiver.

2.4.1 Parabolic dish

Parabolic dish systems are point-focusing systems which track the sun around two axes. Dish applications are almost exclusively reported in conjunction with Stirling engines and therefore are treated as a combination of the two in the following paragraphs. Other attempts utilising dish applications in large interconnected systems showed no further proof of economic competitiveness (Derby, Lazzara s.a.).

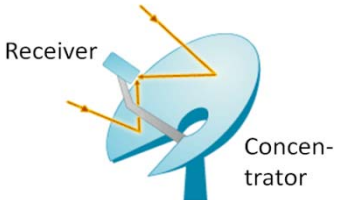

Figure 8: Dish Stirling system (Abengoa Solar 2008)

Parabolic dishes are stand-alone applications with a machine consisting of one dish and one heat engine, either a Stirling engine or potentially a Brayton turbine (Kaltschmitt 2007). System output is limited to 9 kWe to 25 kWe (Kaltschmitt 2007).The modularity of the structures allows individual deployment for off-grid or small-scale solutions, as well as more cost effective, mass-produced solar dish farms (SolarPACES 1998). As a result, parabolic dish applications are only cost competitive when mass produced. With a production rate of 2 000 modules per production model, capital costs of R41 610 per kWe are given (SolarPACES 1998) and Kaltschmitt (2007) assumes R47 500 per kWe

at 1 000 modules. The LCOE of the latter model is R1.71 per kWh at an assumed insolation of 2 700 kWh/m²a (Kaltschmitt 2007).

One advantage of dish Stirling applications is that the individual dishes have low requirements on the land as no flattening is required. This leads to land slopes of up to 10% being usable (Tessera Solar 2011a). Unfortunately, such systems are commercially unavailable and developing an individual system from the ground up is very costly. With a number between 40 and 108 dishes (at 25 kWe) required for the Spier application, the system cost was deemed high due to the diseconomies of the small scale, even when technology development was taken into account. The only planned large scale multi MW plants have recently been terminated (Tessera Solar 2011b, Business Wire 2010).

2.4.2 Central receiver

The central receiver technology is a point focusing, solar thermal collector system where multiple sun-tracking mirrors (heliostats) reflect the sunlight onto a collector at the top of a tower (Figure 9). Due to the principle of point focus, concentration ratios of up to 1 500 can be achieved in praxis (Kalogirou 2004). This, in combination with little heat losses in the absorber due to its relatively small size, leads to high solar-thermal efficiencies of above 15% in operating plants (NREL 2010) with future predictions of around 20% with Rankine cycle power blocks. Many different heat transfer fluids (HTF) have proven feasibility in central receiver applications. Besides Molten salts, such as Nitrate and Hitec (Tyner, Sutherland & Gould 1995), direct steam generation (DSG) (NREL 2010) and air (Haeger et al. 1994) have found application in prototype systems. In addition to the power block based on a conventional Rankine cycle (RC), developments also focus on solar Brayton cycles which promise high efficiency without water consumption for condensing (Stancich 2010b) as well as efficiencies of up to and 25% (Richter et al. 2010).

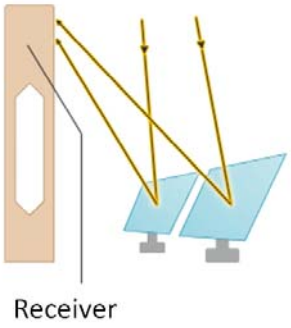

Figure 9: Central receiver system (Abengoa Solar 2008)

While central receiver systems operate at relatively high efficiency in terms of utilization of aperture area, the efficiency of land usage is averse. With the installed power plants, the total land area is larger than the actual aperture area by a factor of five (PS10) to 7 (PS20) (NREL 2010). The targeted LCOE ranges from R0.58 per kWh for a 100 MWe plant to R1.17 per kWh for a 15 MWe power station (Romero, Buck & Pacheco 2002). Total project cost without thermal storage is estimated at R17 341, but can reach up to R40 500 per kWe, including a 15 h storage system (Romero, Buck & Pacheco 2002).

The disadvantages of a central receiver system are the high visual impact due to the height of the tower and the biggest land usage of all collector technologies. The receiver mounted on the tower is elevated above the ground to a height of

30 m for a 100 kWe plant (Aora-Solar 2011) and up to 165 m for a 20 MWe plant (NREL 2010). The height of several built central receiver power plants is given in Figure 10.

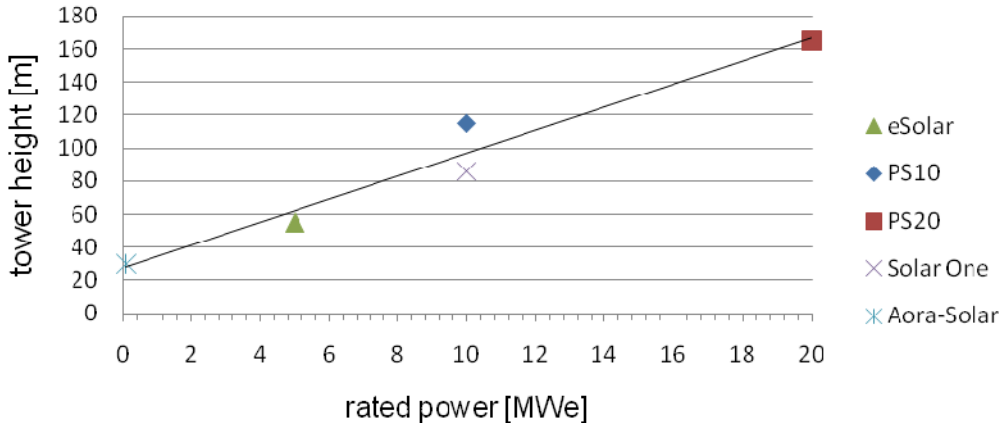

Figure 10: Tower height over rated power plant output

There is an apparent correlation between power plant size and tower height, as indicated with the black linear best fit through the five investigated plants. With an expected dimension of around 1 MWe to 2.7 MWe (contextual review), the tower height, following Figure 10, is expected to be between 35 m and 45 m.

2.4.3 Parabolic trough

CSP plants with the parabolic trough receiver technology (Figure 11) are the most mature solar thermal technology plants. With 354 installed MWe in the SEGS plants in California, they also represent the world's largest CSP installation by far (Nixon, Dey & Davies 2010).

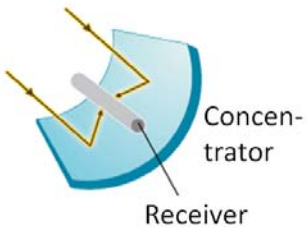

Figure 11: Parabolic trough system (Abengoa Solar 2008)

The range of installation cost for parabolic trough plants operating on superheated steam RC is from R30 324 per kWe (for Solar One) for non-storage plants and up to R60 914 per kWe (for Arcosol 50) for plants equipped with thermal storage systems (NREL 2010). Production cost predictions vary from R0.51 to R1.17 per kWh (Cohen 2006).

What all currently operating RC power stations and plants under construction have in common is the utilisation solely of HTF's based on biphenyl/diphenyl oxide blends. The flash point is given at 117°C (DOW 2001) and in combination

with operating temperatures of 393°C to 395°C (NREL 2010), leads to risk of fire. This situation also applies to lower temperature parabolic trough applications such as plants with an organic Rankine cycle (ORC) power block. These plants allow utilisation of mineral oils such as Xceltherm 600 as HTF (Sinai, Fisher 2008), which is a nontoxic white mineral oil approved for incidental food contact (Tecsia Lubricants 2010). The material's flash point is 193°C, which is well below the fluid temperature in the plant operation (Tecsia Lubricants 2010) and thus also involves risk of fire in case of leakage.

The only exception is the smallest parabolic trough plant, the 1 MWe Saguaro plant operated by Arizona Public Service in the USA (Sinai, Fisher 2008). This plant utilises a 1 MWe ORC power block originally designed for geothermal applications. The reduced requirements onto the HTF allow utilisation of mineral oils. The ORC and all current RC systems operate the heat transfer fluid above flash point and are thus exposed to technical risk. In 1999, a disaster occurred when a heat storage tank of the SEGS II plant in California caught fire and exploded (Los Angeles Times 1999).

A typical approach to construction phases of a parabolic trough plant is illustrated in the Solargenix Energy report on the Nevada Solar One parabolic trough plant (Cohen 2006). The process requires flattening of the land which makes slopes of above 1% uneconomical (Turchi 2010). To reduce complexity, risk and cost, future research is aimed at direct steam power plants where water, as heat transfer fluid, is directly converted into steam which drives the turbine in one loop (Mills 2004). Steam temperatures of up to 500°C allow increased power block efficiency (Abengoa Solar 2008), however, this field of research is currently in an initial prototype phase (Zarza et al. 2004).

2.4.4 Linear Fresnel

While linear Fresnel systems have as yet only been built for testing and prototyping, they increasingly gain academic attention. Books and papers written up until the early 21st century mostly overlooked this technology as no prototype systems were erected during the oil crisis of the 1970's, the period when other CSP technologies gained attention (Ford 2008). More recent investigations see the potential of linear Fresnel systems representing one of the most important solar thermal collector technologies (Viebahn, Lechon & Trieb 2010). The physical principle of a linear Fresnel collector (Figure 12) is similar to parabolic trough technology in which the mirrors focus the light onto a linear absorber. Although, unlike the parabolic shape of the trough collector, the mirrors of the linear Fresnel collector are fixed in a plane reflecting the sunbeams onto the absorber, that is mounted onto a tower.

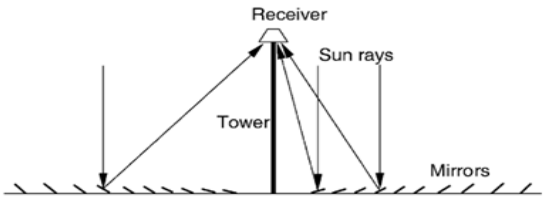

Figure 12: Linear Fresnel collector (Kalogirou 2004)

The vision behind the development of linear Fresnel power plants is to significantly reduce the cost of plant construction and thus, despite lower efficiency, provide cheaper electricity to the customer (Mills 2004). One cost effective benefit of linear Fresnel technology is that flat mirrors can be used, making sophisticated, expensive mirror shaping and support structures obsolete. The LCOE has been estimated at R0.71 per kWh for application in Egypt with a DNI of 2 782 kWh/m²a and a 50 MWe power block (Häberle et al. 2002). Besides the lower construction costs, Fresnel plants also have lower O&M costs compared to parabolic trough applications. Häberle et al. (2002) assumes that O&M costs reach R330 per kWe installed. This assumption is mainly due to the easier accessibility of the flat mirrors for cleaning and the reduced failure due to less wind load (Häberle et al. 2002). Additionally, automated waterless mirror cleaning technologies have been developed (Paul 2008). Therefore, the construction cost of a utility-sized linear Fresnel plant of 50 MWe size is assumed to be around R14 000 per kWe installed (Häberle et al. 2002).

Linear Fresnel systems are also promising to have the highest output per land usage (Sierra Club 2008) with plants tolerating a slope of up to 1.75% (Nixon, Dey & Davies 2010). Another advantage of the linear Fresnel technology is that, due to its low wind load, it has the potential of elevating the mirror field above the ground in a way that allows double usage of the underlying land (Häberle et al. 2002, Scoccini 2010). Examples of potential land usage are shown in Figure 13.

Figure 13: Potential land usage below the mirrors (Scoccini 2010)

The pilot and prototype plants are based on DSG (NREL 2010, Häberle et al. 2002, Küsgen, Küser 2009). The annual solar-to-electric efficiencies are estimated at 10.4% (Lerchenmüller et al. 2004) to 11.3% (Häberle et al. 2002) for a superheated steam Rankine cycle system at 393°C steam temperature, while

the 1.39 MWe saturated steam plant in the Spanish Murcia produces at 6.4% with 270°C steam temperature (NREL 2010). There were still obstacles to be overcome in the development of direct steam plants, and maturity was not reached in 2004 according to Lerchenmüller (2004). Linear Fresnel prototype plants experienced unexpected problems, such as dust intruding in the collector (Gauché, 2010). As utility sized plants are under development, such problems seem to have been overcome. A 30 MWe saturated steam linear Fresnel plant is under construction by Novatec (NREL 2010, Novatec Biosol 2010). Current developments target collectors producing superheated steam at 450°C for higher efficiencies (Küsgen, Küser 2009, Price 2010).

2.4.5 Conclusion on collector technology

Of the four collector technologies discussed, the most suitable choice for Spier is the linear Fresnel system. The dual land usage is a unique advantage of the linear Fresnel collector as other technologies do not allow elevation of the mirror field due to strong wind loads on the structure (Brost 2010). Linear Fresnel systems without evacuated tube absorbers allow the highest amount of local manufacturing of the collector. The mirrors can either be mounted flat or, for higher concentration, be mechanically bent at the mounting. No handling of advanced engineering materials or manufacturing processes is required (Ford 2008). Besides these positive aspects, a linear Fresnel plant has the potential to deliver electricity at lower cost compared to the other collectors. The technology allows low cost direct steam application where no environmentally harmful HTF's are necessary. Requirements regarding slope are less restrictive than for a parabolic trough. The potential for dual usage of the ground and the predicted lowest production cost make the linear Fresnel system the most suitable technology for the Spier application.

Dish Stirling can be an excellent solution in a time when mass production of thousands of systems leads to market availability of systems for small scale applications (which cannot otherwise be identified for the near future). On the small required scale, development and manufacturing of a small batch is not economically feasible due to the high system cost.

The central receiver system is dependent on the absorber mounted on a tower. According to the Municipality of Stellenbosch, construction of any structure needs to go through approval by a municipal committee to gain admission of building plans (Akhoma 2010). Approval is unlikely for a structure with high visual impact, such as a tower dozens of meters high (Akhoma 2010). The high tower is also a concern due to its visual nuisance to surrounding farms and residential areas, such as the De Zalze Winelands Golf Estate. If approval is achieved, the potential for resistance from surrounding residents can lead to undesired negative publicity. For these reasons, a system based on the central receiver concept is not seen as a suitable solution.

The parabolic trough technologies available to date are exposed to risk of fire and soil contamination in case of leakage of HTF. Additionally, the requirements for slope are the strictest of the collector technologies. The essential land flattening

and the unavoidable risk of contamination and explosion rule out the parabolic trough as an appropriate collector technology for Spier.

Concluding this comparative analysis, the linear Fresnel collector is the only suitable technology for Spier and therefore proposed.

2.5 Thermodynamic cycles

In this chapter, the thermodynamic cycles used for solar thermal applications were reviewed to identify the most suitable system for the proposed linear Fresnel collector. Thus far, four different working principles have successfully found application in commercial and prototype solar thermal plants: the Rankine cycle, the organic Rankine cycle, the solar Brayton turbine, and the Stirling engine. The typical application range for each of these principles is illustrated in Figure 14.

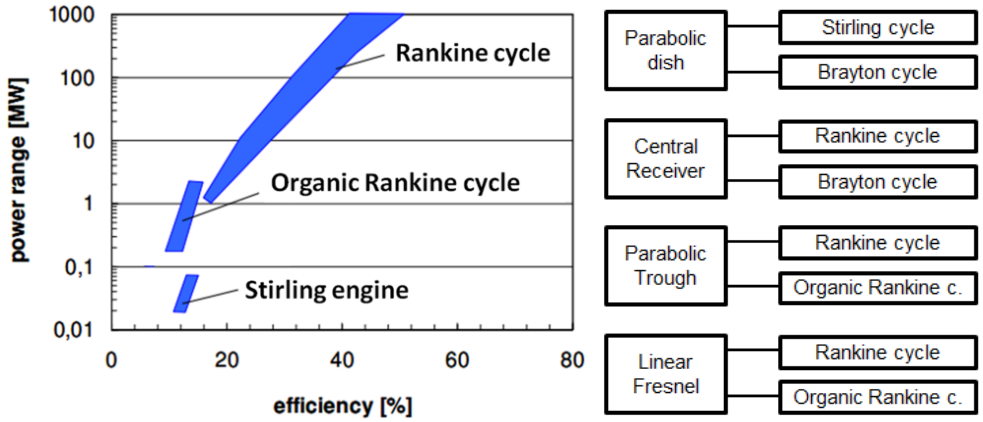

Figure 14: Plant efficiency over power range (left, adapted from (Spliethoff 2006)) and collector technologies and compatible thermodynamic cycles (right)

Figure 14 shows, how different technologies are more appropriate for different power ranges. As outlined earlier, a power block size of about one to three MW is needed. This requirement leaves the applicability of the Rankine cycle; the organic Rankine cycle; the solar Brayton turbine, which is feasible at any size from microscopic applications (Stauffer 2006) to large power plant systems, such as the 148.3 MWe gas turbines operated by Eskom in Ankerlig and Gourikwa (Eskom s.a.); and a series of Stirling engines.

2.5.1 Rankine cycle

The Rankine cycle is the basic thermodynamic cycle commonly utilised in thermal power stations, such as coal, nuclear or CSP power plants. It is based on water/steam as the working fluid and thus requires high input temperatures. Usually, the Rankine cycle is driven by superheated steam to eliminate the risk of droplet erosion of the turbine blades when steam condenses to water. In contrast, saturated steam turbines operate in the non-superheated region, as illustrated in Figure 15, and are suitable for operation at lower temperature and pressure.

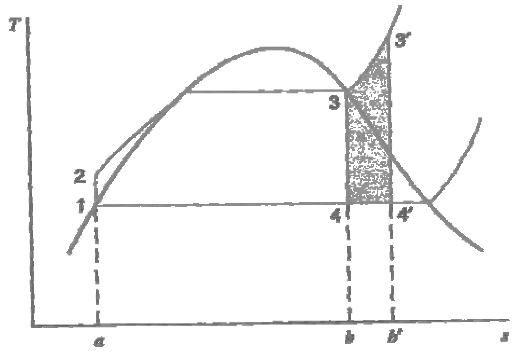

Figure 15: T-s diagram of saturated (1-2-3-4-1) and superheated steam (1-2-3'-4'-1) Rankine cycles (van Wylen, Sonntag & Borgnakke 1994)

Rankine cycle superheated steam

The superheated steam Rankine cycle is the most common cycle in large-scale fossil fired and solar thermal power plants (NREL 2010). A schematic diagram of a possible Rankine cycle configuration of a parabolic trough CSP plant with a superheating section is illustrated in Figure 16. After the initial solar steam generator, a second heat exchanger serves the purpose of providing the required superheated steam quality.

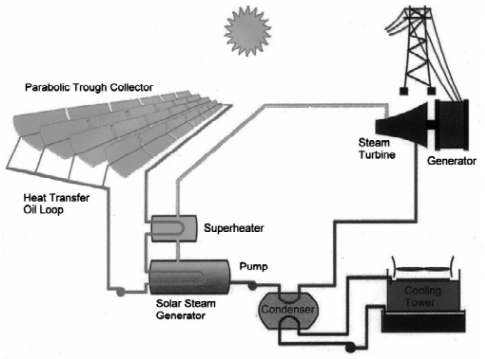

Figure 16: Scheme of a solar only solar thermal power plant with superheater (Broesamle et al. 2001)

All currently operating RC parabolic trough plants utilise synthetic oils, such as Therminol VP-1, as heat transfer fluid (NREL 2010). Due to restricted thermal stability, these fluids lead to a solar field outlet with a temperature limitation of around 390°C (Eck, Hennecke 2007) at an operational pressure of

12 bar to 16 bar (Kaltschmitt 2007). The steam temperature is thus constrained to around 370°C which results in a practical maximum efficiency of the power block of 38% (Eck, Hennecke 2007), achieved by the later SEGS plants and many proposed power plants (NREL 2010). The relating steam pressure in the working cycle reaches up to 100 bar (NREL 2010). As mentioned above, the efficiency of the current generation of solar thermal power plants is restricted by the characteristics of the heat transfer fluid. By comparison, in the new coal fired power stations, Medupi and Kusile, steam temperatures reach up to 560°C at 241 bar (Fouilloux, Otto 2009). Steam temperatures of the DSG Ferrostaal linear Fresnel prototype reach 450°C (Küsgen, Küser 2009). Provision of superheated steam at continuous quality makes sophisticated plant configuration necessary, and usually an additional collector field is dedicated for superheating.

Rankine cycle with saturated steam

A typical Rankine cycle operation with superheated steam was discussed in the previous section. In contrast to the superheated steam application, saturated steam turbines operate in the non-superheated region, as illustrated in Figure 15. Such systems can operate at lower temperatures between 200°C to 300°C (Mills 2004). The technology of saturated steam turbines is well developed and has been proven in the nuclear power industry where efficiencies of up to 33% are reached (Mills 2004). One of the main benefits of saturated steam solar thermal power plants is that since no additional stage for superheating is required a simplified plant layout can be used, such as shown in Figure 17 (Eck, Zarza 2006). In this case, the water is pumped into the collector field where it vaporizes. The generated steam at saturation temperature, or slightly above, is then directed into the turbine. To maintain steam quality, a water separator is installed in front of the turbine as well as in between the turbine stages. The saturated steam systems of Ausra and Novatec Biosol in the solar thermal environment are operated at 250°C to 300°C, with steam pressures of 35 bar to 45 bar (NREL 2010).

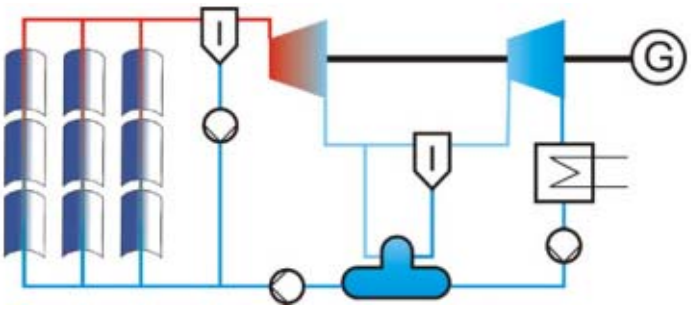

Figure 17: A simple saturated steam plant (Eck, Zarza 2006)

Both the saturated and superheated steam Rankine cycle are operated with water/steam as the working fluid. This type of system eliminates the problems

inherent with system leakage in terms of contamination or fire. Nevertheless, improper O&M of a high pressure steam system can lead to explosion. Additionally, the recent accident at South Africa's Duvha power station has shown that a poorly maintained and operated turbine has the potential to cause severe damage (Donnelly 2011). Steam systems are well understood and accidents are rare, but their potential must not be underestimated.

2.5.2 Organic Rankine cycle

Organic Rankine cycles use the same working principle as the standard Rankine cycle, but instead of water/steam, fluids with vaporisation at lower temperatures are used as working fluids. For this reason, Prabhu (2006) identifies it as a suitable technology for small scale applications. He also states that in geothermal energy extraction, the ORC has been used successfully at HTF temperatures of 150°C. Lower O&M costs are identified due to a high degree of automation possible for ORC systems (Prabhu 2006).

The net efficiency of an ORC power block has been simulated for complex cascaded toluene/butane cycles with 28% at 390°C HTF temperature and up to 23.9% at 293°C HTF temperature (Prabhu 2006). However, the only operating ORC CSP plant, in Saguaro (Arizona, USA), operates at 20.7% power block efficiency (Sinai, Fisher 2008). The non-cascaded plant is supplied with a HTF at a temperature of 300°C and runs with n-pentane as the working fluid (Sinai, Fisher 2008). The achieved annual solar-to-electric efficiency of the parabolic trough plant is 7.3% (based on NREL 2010).

The working fluid used in the 1 MWe Saguaro plant is n-pentane (Sinai, Fisher 2008), a material that is toxic (MEGS 2000) and potentially explosive from -49°C on (Oxford University 2009). Other possible working fluids are refrigerants, such as R-245fa which is also toxic and has a global warming potential (GWP) of 900 (Unitor 2008). Based on these findings, this study determined that the ORC could not be seen as a suitable solution for a renewable energy power plant at Spier.

Further development of the ORC technology for solar thermal electricity generation seems to have stopped in commercial on-grid applications, as the small scale gives diseconomies of production for manufacturers and the high installation costs lead to a high LCOE (Orosz 2010). Niche markets for off-grid solutions have been identified for rural clinics and institutions where electricity and hot water can be provided in cogeneration (Orosz 2010).

2.5.3 Solar Brayton cycle

A Brayton cycle is commonly known as a gas turbine in which air is compressed in a compressor stage and then added fuel is burned. Due to the heat generated and accompanying expansion of the gas, the turbine is driven and mechanical power is generated. The Solar Brayton turbine can operate in an open cycle which leads to no water consumption for cooling purposes. Solar Brayton cycles can be sized in small-scale, with an engine in kW-size mounted onto a parabolic

dish point receiver (Kaltschmitt 2007), as well as in large-scale utility size, mounted onto a central receiver utilising heliostat fields (EC 2005). With required air temperatures at the turbine inlet of above 1 000°C, an additional combustion chamber in a gas hybrid system has so far been necessary to increase the air temperature by means of burning fuel such as natural gas or biogas (EC 2005). Materials and systems research is done to increase the solar energy input and allow solar only operation (EC 2005). A solar Brayton cycle configuration is shown in Appendix G.

Due to the required high temperatures, the technology is suited for collector technologies with high concentration ratios such as the central receiver or parabolic dish. The European Commission's Solgate project required fossil fuel combustion, despite gas temperatures of 1 000°C at the receiver outlet (EC 2005).

2.5.4 Stirling engine

Applications for Stirling machines are limited to small-scale solutions and find application exclusively in parabolic dishes (NREL 2010). Due to the working principle, the Stirling motor is not feasible in large dimensions, with a 330 kW engines the biggest reported machine (von Wedel 2011). The dimension of Stirling engine systems for CSP applications ranges between 9 kWe and 25 kWe (Kaltschmitt 2007). Big scale applications, therefore, make use of multiple individual dish systems. Despite the absence of any fluids threatening soil contamination and its high operational hours (Kaltschmitt 2007), the Stirling motor is not suitable for application in conjunction with a linear Fresnel plant. This is explained by the low efficiency at supply able temperatures and dimensional limitations of such an engine.

2.5.5 Conclusion on thermodynamic cycle

Of the four thermodynamic cycles discussed, the popular Rankine cycle is identified as the most suitable system for Spier.

The ORC technology is not feasible for the system foreseen at Spier for several reasons. While reasonable efficiencies at lower temperatures are achievable, this comes at the expense of a complex cascaded power block configuration. The usable fluids do not correspond with the Spier target of sustainability, as possible working fluids are toxic and harmful to the atmosphere. Furthermore, a risk of soil contamination and explosion exists from the power block.

In regards to the Solar Brayton cycle and the Stirling cycle, the system's essential high temperatures cannot be supplied by a linear Fresnel collector.

The Rankine cycle with superheated steam also requires high temperatures and steam pressures which lead to higher design requirements and a complicated system configuration. The linear Fresnel system developers, Ausra and Novatec Biosol, decided to design their first prototype installations specifically for

saturated steam Rankine cycle operation. However, the future target is to reach high temperature superheated steam conditions with improved system understanding and maturity (Price 2010, Stancich 2010a).

The low system temperature and pressure of saturated steam technologies allow less complex solar field configuration and reduced risks. Therefore, the saturated steam RC is seen as the best combination for a linear Fresnel collector at Spier.

2.6 Simulation tools for a linear Fresnel CSP plant

A variety of tools has been developed to assist developers in analysing desired technologies. The best known system is the software SAM (solar adviser model), developed by NREL. SAM is restricted to simulation of parabolic trough and central receiver power plants and cannot be used for linear Fresnel systems (Gilman et al. 2008). The optical behaviour of the collector field of linear Fresnel plants is usually done using ray tracing software (Häberle et al. 2002; Brost 2010; Mertins 2009; Facão, Oliveira 2009). Due to high computational requirements of ray tracing models, statistical simulation tools have been developed, taking sun-shape, mirror error and glass properties into account (Morin et al. 2006). The thermodynamic part of a linear Fresnel plant is then modelled using computational fluid dynamics (CFD). CFD simulations based on TRNSYS models or ColSim applications found use in CSP simulations. Both are sophisticated systems that require detailed modelling and information input. A software named “greenius”, similar to SAM, has been developed by the German DLR. Greenius is available in a cost free version, greeniusFREE, which is not capable of simulating linear Fresnel power plants. The input variables for greenius are very limited. The available used simulation software ranges from sophisticated very detailed models, such as ColSim and the statistical models, to very user-friendly versions, such as SAM and greenius where the user has only limited influence in the specifications. It was, therefore, decided to develop an independent linear Fresnel simulation model that allows simulating the desired system at the desired depth.

2.7 Conclusion

Parabolic dish applications are only feasible in high numbers (i.e., thousands of dishes), making this kind of system development unfeasible for the Spier application. Furthermore, central receiver collectors are ruled out due to the inevitable high visual exposure of the receiver tower. While a parabolic trough is the collector with the highest operational experience, technologies have yet to advance to allow electricity production without environmentally harmful heat transfer fluids. At the current state of technology, the linear Fresnel collector is the only system that allows delivering a solution to fulfil the Spier requirements. The linear Fresnel technology permits application at suitable dimensions with environmentally friendly steam as the heat transfer fluid. Additionally, the system has the lowest land usage as well as the potential for dual usage of the covered land. The optimum power block for the linear Fresnel system is identified in a saturated steam system. A simulation tool is required to be developed as no commercial software was identified to fit the requirements.

CHAPTER 3: POWER PLANT CONFIGURATION

In this chapter, the most suitable linear Fresnel power plant configuration for the Spier environment is developed.

3.1 Rankine cycle configuration

Each power plant utilising the Rankine cycle consists of a boiler (collector), the turbine and generator, the condenser and a pump, as illustrated in Figure 18. In efforts to increase power plant efficiencies, developers have investigated numerous variations with many steam reheating sections. Where superheated steam is used, an additional part of the solar field can also be dedicated to that purpose. Based on a linear Fresnel application, Mertins (2009) compares a simple power plant layout with a more sophisticated version, as shown in Figure 19. The figure on the left illustrates the simple layout where the entire field is used to heat the water and generate superheated steam in the same absorber tube. The scheme on the right describes a complicated system with a separated superheater stage and five reheater sections in an attempt to increase efficiency.

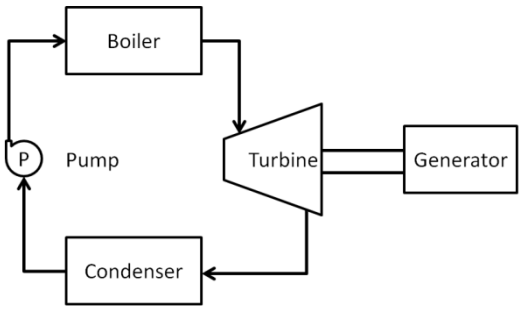

Figure 18: Rankine cycle based power plant

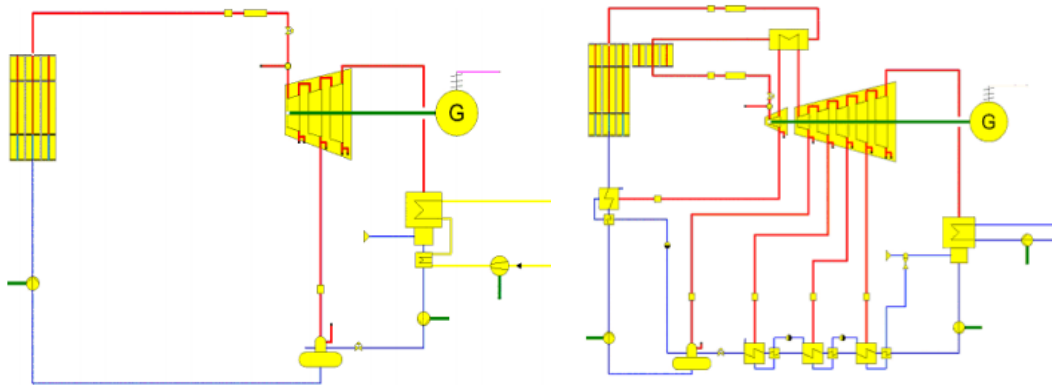

Figure 19: Simple plant layout (left) and complex layout with five reheater sections (right) (Mertins 2009)

While the more complex system offers higher solar-thermal efficiency, it does not result in considerably lower LCOE as the bottom line is less than one percent

lower cost (Mertins 2009). Mertins concludes that the average higher collector temperatures in the complex setup lead to increased heat losses that counter the higher efficiency of the Rankine cycle. One has to keep in mind that a solar power plant at Spier is intended to be a newly developed plant, so unexpected errors and higher downtime than with a mature commercial plant could occur. Possibly opening the facility towards research by institutions such as Universities would lead to further downtime due to experiments. The significantly higher capital cost of the complex plant could easily lead to higher LCOE when production targets are not reached. Also, a less costly power plant would reduce investor risk. In conclusion, the simple plant layout is proposed for the Spier application.

3.2 Cooling

The most efficient and economic way to cool a power plant is once through direct water cooling followed by evaporative wet cooling, while the least efficient and most expensive technology is dry cooling (EPRI 2002). The cooling technology for the Rankine cycle is therefore chosen based on the availability of water. In a first step once through cooling was ruled out for the lack of large water carrying systems in the proximity. The water consumption of evaporative cooling plants can be approximated by using the known consumption of a RC power plant in combination with application of thermodynamic theory. For comparison, a RC coal fired plant at 550°C turbine inlet temperature and a water consumption of 2.0 l per kWh was noted (evaporative cooling) (IEA 2010). The water consumption of the linear Fresnel plant can be approximated with

$$\dot{V}_{water} = 2.0 \frac{l}{kWh} \cdot \frac{550°\mathrm{C} - T_C}{T_H - T_C} \qquad (2)$$

where T_H is the steam temperature at turbine inlet of the investigated plant and T_C is the condenser temperature, which was for this calculation assumed with 45°C. The typical operating temperature of the saturated steam prototypes is 270°C (NREL 2010). This results in a water consumption of 4.5 l per kWh or 8 978 l per hour (9.98 m^3/h) at peak load. The results are in a similar region to the estimated 3.8 l/kWh estimated by the U.S. department of energy (DOE) (DOE 2009). The annual water requirement for wet cooling is then 12.5 million litres. This represents less than 4% of Spier's total water usage based on 2009 water consumption readings. The farm manager reported that an amount of 20 million litres per year is readily available and not a matter of concern (Filander 2010). The required amount, in terms of annual and peak consumption, can be supplied by the irrigation system. Therefore, it is proposed that the power plant be equipped with evaporative wet cooling technology.

3.3 Reflector configuration

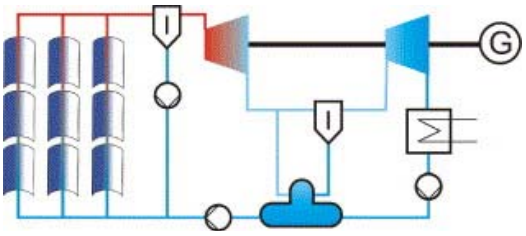

Figure 20: Parabolic trough Saturated steam plant setup (Eck, Zarza 2006)

The setup of the plant is shown in Figure 20. In times of insufficient heat input to run the turbine, the HTF is circulated back into the collector. The power plant is a simple once-trough setup with a recirculation bypass. In order to improve efficiency by reducing of shading of two adjacent mirrors the technology compact linear Fresnel reflector (CLFR) has been proposed by researchers at the University of Sydney (Mills 2004). The conventional linear Fresnel and the CFLR principle are illustrated in Figure 21. With this system multiple linear Fresnel fields are placed next to each other and computer algorithms decide for each mirror on which receiver to reflect.

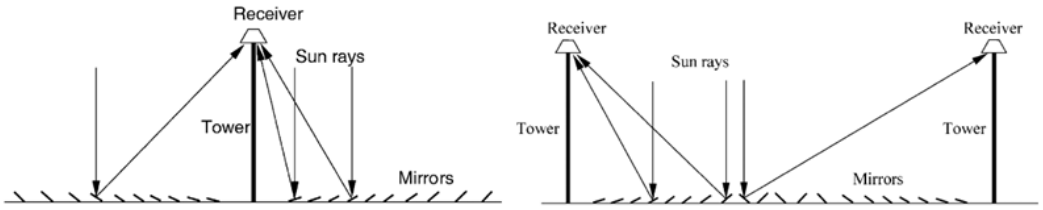

Figure 21: Linear Fresnel (left) and compact linear Fresnel (right) (Kalogirou 2004)

Mertins (2009) concludes, however, that the disadvantages due to additional complexity outweigh the benefits of the CLFR solution and the principle has not been realised in prototypes (NREL 2010). For that reason, the Spier system is simulated as a conventional linear Fresnel plant.

3.4 Receiver configuration

Receiver type

The linear Fresnel reflector consists of multiple flat or slightly bent mirrors. Consequently, it does not focus the reflected beams on an ideal line as accurately as a parabolic trough system. The result is that reflected beams illuminate a bigger cross section surface on the receiver. Different receiver types are proposed to cope with that requirement. Two basic receiver principles are shown in Figure 22.

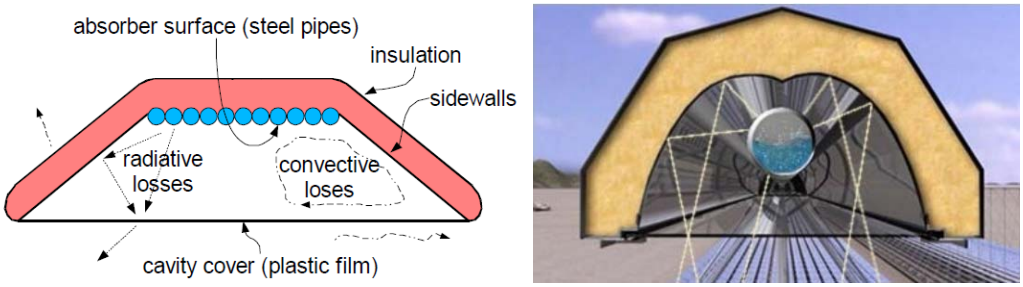

Figure 22: Receiver with multiple pipes (left) (Pye, Morrison & Behnia 2003) and single-tube receiver (right) (Selig 2009)

The receiver illustrated on the left features multiple pipes in parallel to cover the area of incoming reflected beams. Steel pipes (Pye, Morrison & Behnia 2003) as well as evacuated tubes (Mills, Morrison 2000) are proposed. The disadvantage of this approach is that each pipe receives a different amount of heat input which leads to complicated system behaviour.

The other system shown on the right in Figure 22 is equipped with a single but much larger tube. The wide distribution of incoming beams is partially captured by the large pipe, while the passing beams are reflected by a secondary compound parabolic concentrator (CPC). This system can also be either equipped with a steel pipe absorber or an evacuated tube. The single-tube receiver is a less complicated solution than one with multiple pipes and allows for simplified controls. It is also has the potential to yield 10% more energy than the multi-tube system (Morin et al. 2006). For these reasons the single-tube absorber is proposed for the linear Fresnel system at Spier.

Absorber type

The single-tube cavity receiver can either be equipped with a steel pipe, as shown in Figure 22, or an evacuated tube. An evacuated tube features superior heat-loss behaviour compared to the steel pipe. However, the steel pipe is a continuous tube welded on-site, and by that, able to absorb energy over the entire pipe length. In contrast, an evacuated tube is transported to the site in factory assembled units. These pre-assembled evacuated tube systems have bellowed endings on each pipe side, as required by the technology. Manufacturer Schott Solar states that these endings of their PTR 70 system result in shading losses of less than 4% (Burkholder, Kutscher 2009). As shown in the following, depending on system layout and the DNI, the shading losses can overcome the benefit of the superior heat loss behaviour of the evacuated tube. A comparison was done with the simulated results of the Solarmundo linear Fresnel system (steel pipe) and measured data of the Schott PTR 70 evacuated tube receiver. It has to be noted that the PTR 70 system is neither designed for DSG nor linear Fresnel application. As it is developed for parabolic trough systems, the PTR 70's

inner pipe diameter measures 6.6 cm (Burkholder, Kutscher 2009), while a linear Fresnel single-tube receiver's inner pipe diameter is about 18 cm (Häberle et al. 2002). Increase in tube diameter leads to increased heat loss (Stine *et al*., 2001) which results in this comparison privileging the PTR 70 system.

The absorber temperature of a solar thermal power plant is about 10°C above the HTF temperature for power plants operating on synthetic oils (Burkholder, Kutscher 2009). For two phase flow in a DSG plant, a simplified 15°C is assumed as sufficient approximation for the scope of this study. Further, the mean absorber temperature is assumed as the average between absorber inlet and outlet temperature. The PE1 saturated steam power plant in Spain operates at 270°C outlet and 140°C inlet temperature (Selig 2009). This leads to a mean absorber temperature of 230°C for the DSG system. The heat loss per meter of absorber pipe at a mean absorber temperature of 230°C is around 50 W/m for the evacuated tube (Burkholder, Kutscher 2009) and 380 W/m for the cavity receiver (Häberle et al. 2002). The difference in heat loss per m is 330 W/m. The evacuated tube system's heat loss superiority increases with increasing operating temperature.

The effect of shading was calculated by using the Solarmundo system layout, leading to an aperture of 24 m (Häberle et al. 2002). With an optical efficiency of 61% (Häberle et al. 2002) for the systems (the same optical efficiency is assumed, as the sun beams pass through one level of glazing, the evacuated tube envelope, or the glass pane of the conventional cavity receiver), the mentioned 4% shading loss leads to 586 W/m at a DNI of 1 000 W/m². This is higher than its heat loss advantage. The effect of shading reduces with dropping DNI. The DNI where shading and heat loss advantage of the evacuated tube equal is 563.5 W/m².

The cavity receiver with steel pipe consists of standard engineering material with an on-site welded absorber tube (with selective coating), an insulated secondary reflector and a glass pane on the bottom to reduce heat loss. By contrast, the evacuated tube receiver is an imported system that still requires the secondary reflector. Savings on other receiver elements can, thus, only be realised on the backside insulation.

This overview leads to the conclusion that the single-tube cavity receiver with steel pipe is not only the more energy efficient solution, but also implies less cost due to simpler technology. Furthermore, the solution with the steel pipe allows a higher value gain in the country as system imports are reduced. With a higher operating temperature, the heat loss advantage of the evacuated tube increases while the shading penalty remains the same, leading to a higher feasibility of the latter system. For this reason, the evacuated tube manufacturer, Schott Solar, announced development of systems suitable for high temperature linear Fresnel applications with production of superheated steam in DSG and testing at Novatec's PE1 power plant at up to 450°C (Schott 2010). Conversely, the linear Fresnel developer, Ausra, is intending to produce superheated steam plants with a conventional steel pipe cavity receiver as they aim to avoid the high costs involved (Deign 2010).

3.5 Thermal storage

A number of existing solar thermal power plants are equipped with on-site thermal storage to allow a high capacity factor without the combustion of fossil fuels. The most important benefits of thermal storage are the controllability of the output (the operator is more independent to fit production to demand), which improves dispatchability (World Bank 1999). Furthermore, due to an increased capacity factor, the need for fossil fuels becomes obsolete and a solar-only utility size generation becomes more feasible (World Bank 1999). The heat transfer fluid can be used directly for storage by pumping the hot fluid into insulated tanks with a round trip efficiency of up to 99% (SolarPACES s.a.). The capital cost of the mature molten salt storage system is given with a minimum of R225 per kWh of storage capacity for large multi MWh sized tanks and is highly dependent on storage sizing (Herrmann, Kelly & Price 2004). The major portion of that cost lies in the tank structure. A well-sized molten salt storage system can reduce the LCOE by 10% (Herrmann, Kelly & Price 2004) to 20% (Kearney et al. 2003). This is due to improved capacity factors rising from 12% for non-storage, to 40% for plants equipped with storage (based on NREL 2010). As a result, the initial capital cost can increase almost by a factor of two (Herrmann, Kelly & Price 2004).

Different mixtures of salts are available with freezing points between 120°C for Hitec XL® and 220°C for a binary salt mixture of $NaNO_3$ and KNO_3 (Herrmann, Kelly & Price 2004). The operating temperature of the cold tank is around 290°C (Herrmann, Kelly & Price 2004), and the hot tank is up to operational HTF temperature with a peak salt temperature of 390°C (Mills 2004). In case of a salt being operated as HTF, additional heating devices need to be included into the plant design to avoid freezing overnight.

Thermal tank storage is not proposed for this project as it is only cost effective in large scale. Also, with molten salts at an operating temperature of the cold tank around the typical peak steam temperature of saturated steam plants, the most cost effective solution becomes unusable. Otherwise, a relatively little gain in LCOE is achieved with a large additional initial capital invest. Thermal storage, therefore, becomes applicable for mature utility scaled projects to improve profit and base load abilities. For a first solar thermal power plant, additional complicated elements are not reasonable, especially when the economic feasibility depends on guaranteed high reliability.

However, it needs to be understood that thermodynamic systems like CSP plants feature built-in thermal storage in the form of thermal inertia. This effect can be enhanced by a larger steam seperator which provides in its standard version several minutes of storage (Eck, Zarza 2006). Inertia storage is excellent to overcome insolation interruptions by clouds. It can be implemented at minimal capital cost and does not add to a more complicated plant setup. It was therefore identified that inertia storage is the suitable storage solution for a linear Fresnel system at Spier.

CHAPTER 4: SIMULATION OF POWER PLANT

A simulation model of the performance of a saturated steam linear Fresnel plant is developed to obtain information about plant dimensions, component sizing and the costs involved. The simulation is built upon hourly insolation data and used theoretical approximation for the power block efficiency with measured and simulated system behaviour from the literature for the concentrator. The applied power plant configuration was discussed in the previous section.

4.1 Simulation approach

A full year data based on the mean average year in hourly solar information resolution is used as the simulation input (origin of DNI data, see contextual review/Appendix F). The hourly DNI data is processed in a static system simulation to approximate the variable nature of the resource and resultant power production. The sum of the outputs then gives the electricity produced by the plant. The principle of the approach is illustrated in Figure 23.

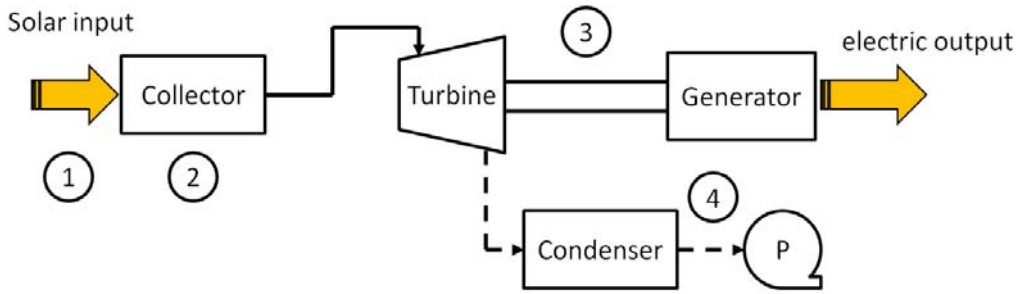

Figure 23: Linear simulation configuration

The simulation is built upon four main elements which include (1) the modification of satellite derived DNI, (2) the collector model, (3) the power block model and (4) a final model containing parasitic losses and other assumptions. This is a comparable simulation approach to the one used by the DLR to develop the greenius simulation environment (Quaschning et al. s.a.).

In the first step, the clock time at which insolation measurements are available is converted into solar time. This is necessary to accurately calculate the position of the sun. Information about sun position is used for DNI manipulation as well as efficiency calculation of the collector. The usable insolation is actual solar power reaching the plant aperture, taking the cosine effect into account. The solar beams are reflected by the mirror field onto the absorber where the energy content is converted into thermal power which heats the water and converts it into steam. This process is accompanied by losses (such as shading and heat losses) which are incorporated into the collector model. The thermal power is then

delivered in the form of steam to the power block where it is converted into electric energy via a turbine-generator set.

4.2 Insolation manipulation

As described in the contextual review, a year's DNI is available in hourly intervals. DNI is solar power measured per square meter of a surface perpendicular to the sun beams. Only direct beams from the sun are considered. The change of the suns position needs to be taken into account to determine the usable energy reaching the collector (cosine losses). To calculate the angle of the sun in reference to the power plant, its position needs to be known at a given time. This calculation is based on the sidereal[2] time. The then computed angle is used to calculate the effect of the angle of the sun.

The effect of sun angle onto a linear Fresnel collector performance is incorporated in the collector model.

4.2.1 Sidereal time

The position of the sun needs to be calculated for every full hour when DNI information needs to be manipulated. To be able to calculate that location of the sun accurately, the actual time (sidereal time) at the power plant location has to be known. The sidereal time is the time for a location that defines 12h00 as the time where the sun is at its zenith; while clock time is an artificial time, that is the same across South Africa, with GMT+1 (Greenwich mean time) as the reference.

Sidereal time is more accurate than solar time and its calculation is a refinement of solar time (Stine *et al*., 2001). Solar time uses the coordinates of a site to correct the clock time to get to a time system in which the sun is in zenith at 12h00. Since the planet rotates by 360° every 24 hours, 15° represents one hour. Thus, solar time t_s can be calculated by equation (3), where *LCT* represents local clock time and ω the hour angle, which describes the angle between the meridian containing the plant location and a meridian that is defined as a 15th of 360° (Stine, Geyer 2001). The selection of the reference meridian is dependent on the applied time zone.

$$t_s = \frac{\omega}{15°} + LCT \tag{3}$$

For example, when the clock time says that noon at Spier is 12h00, the more accurate solar time concludes that solar noon is actually at 12 h, 15 min, 9 sec on the clock. But solar time neglects the effect of the earth not rotating around the sun in a perfect circle and is thus not accurate. The deviation to the actual solar

[2] Different definitions of solar time and sidereal time are used in literature, such as (Duffie, Beckman 2006).

noon is up to 16 min, 24 sec (Stine, Geyer 2001). The deviation of solar time compared to the solar time is given over a year in Figure 24.

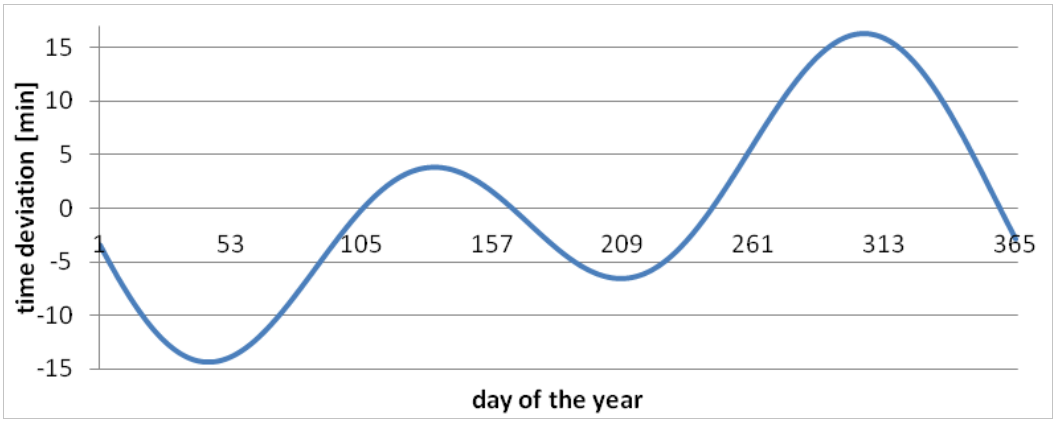

Figure 24: Deviation of solar time to sidereal time

This deviation leads to the necessity to include another correction step in order to calculate the sun's position. The equation of time *(EOT* in minutes) is used to manipulate the solar time and given as (Stine *et al*., 2001)

$$EOT = 0.258 \cdot cosx - 7.416 \cdot sinx - 3.648 \cdot cos2x - 9.228 \cdot sin2x \qquad (4)$$

where x (in degrees) is an equation affected by the day of the year, as given

$$x = \frac{360 \cdot (N - 1)}{365.242} \qquad (5)$$

N represents the day number of the year (1st of January: *N* = 1, 31st of December: *N* = 365). The manipulated accurate solar time is named sidereal time t_{sr} and calculated as follows.

$$t_{sr} = t_s - \frac{EOT}{60} + LCT \qquad (6)$$

The demonstrated *EOT* equation gives an accuracy of 30 seconds (Stine, Geyer 2001). More accurate, but also more complex, *EOT* models exist and become necessary when highly detailed applications are investigated, such as sun tracking (Stine, Geyer 2001). This accuracy is not necessary for this simulation as hourly static computations are done for purposes of a pre-feasibility investigation. Accurate computation for tracking is required at the later stage of a real plant design.

4.2.2 Usable solar energy

Direct normal irradiation is given for a surface tracking the sun's position. DNI is measured in W/m^2. The measurement is taken in parallel to the sun's rays, therefore at an angle θ_z to the ground, as illustrated in Figure 25.

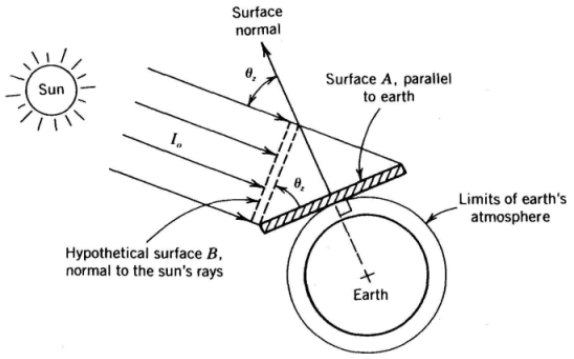

Figure 25: Illustration of cosine effect (Stine, Geyer 2001)

Depending on the location of the power plant, the sun's angle θ_z might never be 0°. The amount of energy actually reaching a square meter on the ground is thus less than the measured DNI per square meter. The usable solar irradiation is obtained by correcting the DNI by an incidence angle modifier (IAM), representing the cosine of the sun's angle. The correction is done by applying equation (7).

$$IAM_{COS} = cos(\theta_z) \tag{7}$$

The incidence angle of the sun is dependent on the sidereal time, the day of the year and the coordinates of the plant on the planet. For more information about how the incidence angle θ_z of the sun is calculated in respect to the plant location, the reader is referred to the book "Power From The Sun" (Stine, Geyer 2001). Applying equation (7), the usable insolation on a plant site is

$$I_{usable} = \mathrm{DNI}_{measured} \cdot IAM_{COS} \tag{8}$$

4.3 Collector model

This section discusses the implementation of the collector efficiency behaviour. The first part deals with the influence of the incidence angle of sun beams on the collector efficiency. In the second part of the collector model, the heat losses of the absorber pipe are implemented. Elements are based on research outcome of the Solarmundo prototype system in Belgium.

4.3.1 Reflector efficiency

The efficiency of the reflector is dependent on the direction at which the sun beams hit the collector field. The incidence angle of the sun beams is split into the transversal and the longitudinal angle. The transversal angle θ_t is on a plane perpendicular to the tracking axis, and the longitudinal angle θ_l is on a vertical plane parallel to the tracking axis (thus θ_l = 90° equals the tracking axis) as shown in Figure 26. Both angles are dependent on the position of the sun with reference to the power plant. Therefore, the calculations of the θ_t and θ_l are based on Stine *et al*. (2001) and further trigonometric manipulation. To correct the influence of the incidence angle, the collector efficiency of the power plant is adjusted by an incidence angle modifier as given in equation (9) (Häberle et al. 2002)

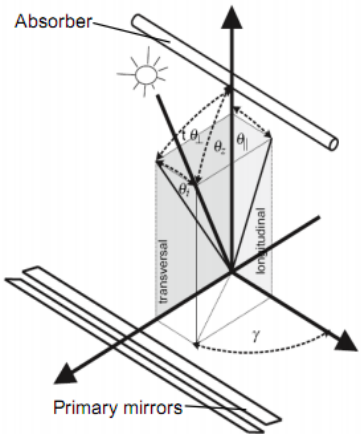

Figure 26: Definition of transversal and longitudinal angle (Morin et al. 2008)

$$\eta(\theta) = IAM \cdot \eta(\theta = 0) \tag{9}$$

where $\eta(\theta = 0)$ is the solar thermal efficiency for vertical insolation. To integrate both θ_t and θ_l into equation (9), it can be rewritten as

$$\eta(\theta_t, \theta_l) = IAM_t(\theta_t) \cdot IAM_l(\theta_l) \cdot \eta(\theta = 0) \tag{10}$$

The influence of longitudinal and latitudinal change in angle of insolation is discussed by Häberle et al. (2002) as given in Figure 27.

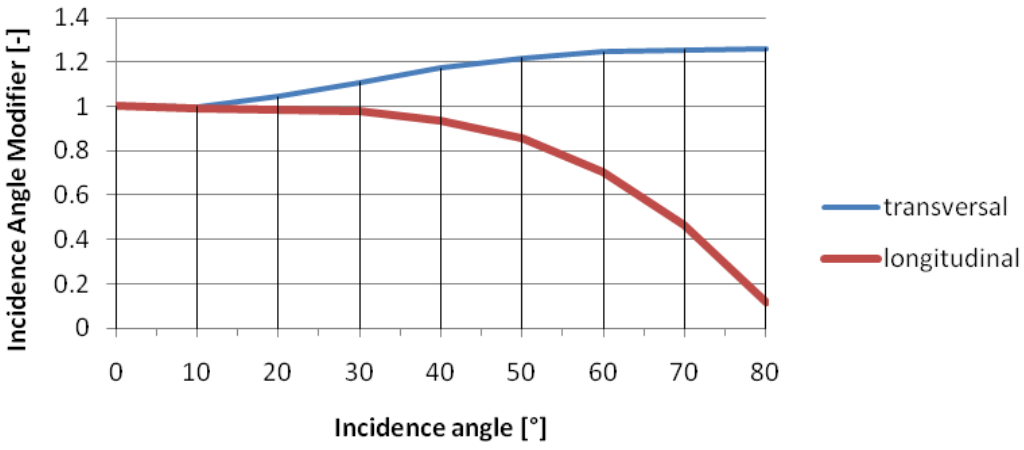

Figure 27: Dependence of IAM of incidence angle of the sun beams

An increasing *IAM* for increasing transversal angles is mainly explained by less reflection onto the back of neighbouring mirrors and the decreasing gaps between the mirrors (Häberle et al. 2002). Therefore, the solar-thermal efficiency of the system can actually be higher than the efficiency at 12h00, when the sun is closest to zenith (note that IAM is not the efficiency, it is its modifier: the actual efficiency is discussed in the following section).

For the collector model in the simulation, IAM_t and IAM_l are converted into functions by applying a polynomial best fit onto the curves. The fitted functions are given in equation (G1) and (G2) in Appendix H. The result is that the solar energy absorbed can be written as a combination of equations (8) and (9)

$$I_{absorbed} = \eta(\theta_t, \theta_l) \cdot I_{usable} \tag{11}$$

4.3.2 Receiver efficiency

A theoretical background on calculation of heat losses of an evacuated tube receiver is given in Appendix I. For the scope of this work, it was sufficient to apply the simulated efficiency from the Solarmundo project's cavity receiver as represented in equation (12). The used model gives the solar-thermal efficiency of the collector for the sun in zenith. For other incidence angles, the previously described *IAM* is applied. The solar thermal efficiency of the Solarmundo linear Fresnel prototype can be calculated by equation (12) (Häberle et al. 2002).

$$\eta(T_{absorber}) = \eta_0 - u \cdot \frac{T_{absorber} - T_{ambient}}{E_{beam}} \tag{12}$$

where E_{beam} is the DNI in W/m², η_0 the optical efficiency of 61% and u the temperature dependent heat loss coefficient as calculated in equation (13) (Häberle et al. 2002).

$$u = 3.8 \cdot 10^{-4} \cdot (T_{absorber} - T_{ambient}) \tag{13}$$

The solar thermal efficiency is plotted in Figure 28 for multiple DNI's (at 30°C ambient temperature $T_{ambient}$). The absorber temperature is described by $T_{absorber}$ where it is assumed that the absorber temperature is 15°C higher than the water/steam temperature inside. For absorbers with oil as HTF, a temperature difference of 10°C has been measured (Forristall 2003). However it is assumed that due to two partial phase flow in the DSG plant, a higher average deviation occurs.

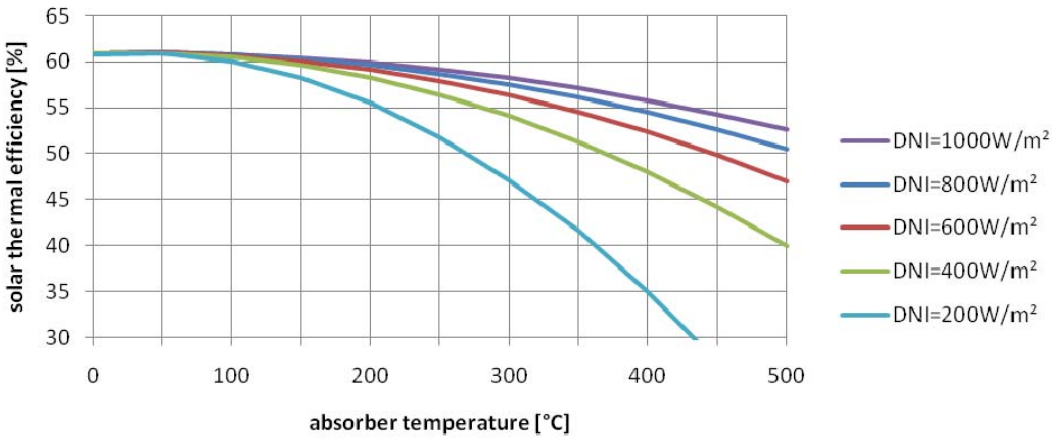

Figure 28: Collector efficiency curve for vertical insolation

In Figure 28 it can be seen that the efficiency drops with increased absorber temperature. This is explained with the increased heat losses occurring due to the higher difference to the ambient temperature. The collector efficiency also drops with reduced DNI due to the higher percentage of absorbed energy necessary to eliminate the occurring heat losses. The collector is modeled as a single element. The non-linearity of the absorber efficiency suggests an investigation of the absorber pipe in segments for better accuracy. For the scope of this work, it is sufficient to see the pipe as one element at intermediate temperatures. The effect of more accurate non-linear behavior is mostly linked to part load stages with low DNI. The effect is negligible for saturated steam application with an outlet temperature of 270°C (Selig 2009).

4.4 Power block model

The power block model represents the behaviour of the steam turbine. The efficiency of the turbine was based on the theoretical Chambadal-Novikov efficiency because no specific turbine was selected at this stage of the project. As the output of a solar thermal power plant is dependent on intermittent insolation, a sufficient steam supply to operate the steam turbine at the design point cannot be guaranteed. For that reason, the part load behaviour of a saturated steam Rankine cycle is discussed and implemented into the simulation.

4.4.1 Chambadal-Novikov efficiency

At this stage of the project, no actual turbine system has been earmarked for the application, and the turbine efficiency needs to be evaluated based on theoretical background. The ideal efficiency of a heat engine is the Carnot efficiency, calculated as shown in (14),

$$\eta_{Carnot} = 1 - \frac{T_L}{T_H} \tag{14}$$

with T_H being the temperature of the hot reservoir and T_L the temperature of the cold reservoir, as illustrated in Figure 29.

Figure 29: Reversible heat engine cycle (left) (van Wylen, Sonntag & Borgnakke 1994) and Novikov engine as reversible Carnot engine, with irreversible link to heat source T_H (right) (Wagner 2008)

The Carnot engine as an internally reversible process, operates between two fixed heat reservoirs (van Wylen, Sonntag & Borgnakke 1994). This is an ideal process and cannot be achieved in practice. A comparison of the efficiency of the Carnot engine, compared to actual power plant applications, is given in Table 1.

Table 1: Comparison of Carnot and observed efficiency (Curzon, Ahlborn 1975)

Power source	T_L [°C]	T_H [°C]	η – Carnot [%]	η – observed [%]
West Thurrock (U.K.) coal fired steam plant	25	565	64.1	36
CANDU (Canada) nuclear reactor	25	300	48	30
Larderello (Italy) geothermal steam plant	80	250	32.3	16

It is obvious that the Carnot efficiency provides a significant deviation to the actual achieved efficiency of the operating plant.

In an attempt to develop a theoretical efficiency that provides results that represent actual applications, a modified efficiency has been developed. Assuming that heat losses occur in between the reservoirs and the actual heat

engine, making the process externally irreversible, Van Wylen (1994) and Wagner (2008) derived a modified Carnot efficiency for heat engine systems, as stated in (15).

$$\eta_{CN} = 1 - \sqrt{\frac{T_L}{T_H}} \tag{15}$$

In the literature, equation (15) is also referred to as the Chambadal-Novikov efficiency. The associated illustration is shown on the right of Figure 29, where T_{iH} and T_{iL} represent the actual temperatures at the turbine in- and outlet.

Van Wylen's approach is slightly different from Wagner's, given that in his approach the Novikov engine also has an irreversible connection to the lower temperature source. After lengthy derivation, however, both approaches conclude with the same efficiency, as seen in equation (24). The Chambadal-Novikov efficiency is an approximation for heat engines and gives a good fit for real power blocks, shown in Table 2.

Table 2: Comparison of Chambadal-Novikov efficiency with observed efficiency (Curzon, Ahlborn 1975)

Power source	T_L [°C]	T_H [°C]	η–Chambadal-Novikov [%]	η – observed [%]
West Thurrock (U.K.) coal fired steam plant	25	565	40	36
CANDU (Canada) nuclear reactor	25	300	28	30
Larderello (Italy) geothermal steam plant	80	250	17.5	16

It can be seen that the Chambadal-Novikov efficiency provides a significantly better fit to the observed values than the Carnot efficiency. It still has to be mentioned that the highest deviation in the three observed power plants is above 10% for the coal fired power station.

Concluding, for this study, the Chambadal-Novikov efficiency provides a good approach for real efficiencies of heat engines that can be implemented into simulation codes in an analysis state where a turbine manufacturer, and thus detailed specifications, are not available.

4.4.2 Part load behaviour

The part load behaviour of the power block needed to be considered in the simulation because it is not linearly dependent on steam input. Eck (2006)

compares power block efficiencies for various operational modes over DNI variation. Derived from his model, and supported by Mertin's (2009), the result is a curve representing the power block performance over the thermal input for fixed pressure operation, as illustrated in Figure 30. This curve also includes the generator behaviour.

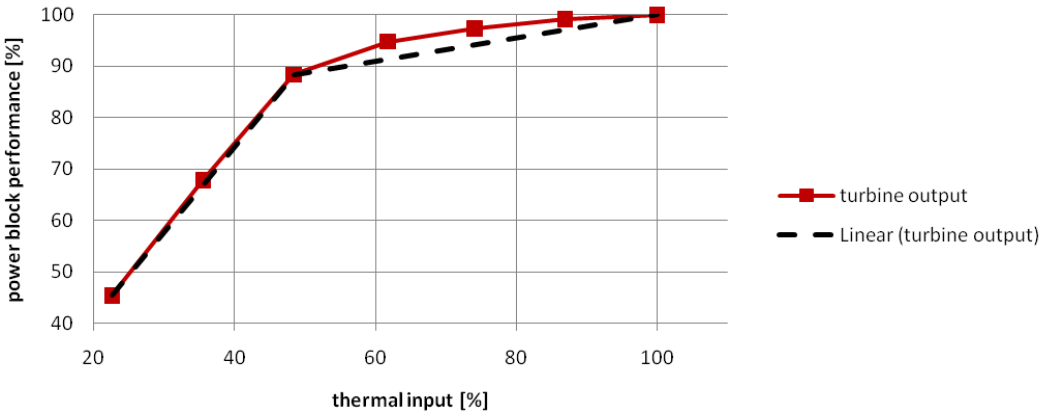

Figure 30: Power block performance over thermal input

Thermal power input of 100% gives 100% of the power block performance. The turbine efficiency drops with decreasing thermal input, thus the plant is running on part load. An Interesting observation is a high efficiency until 48.4% thermal; after which it drops steeply. The turbine output curve, as given in Figure 30, cannot accurately be represented by a low order polynomial function for the simulation. This makes it necessary to approximate the turbine output with two linear functions. For both functions, the bending point at around 50% thermal input was combined with the end of the turbine output curve at around 22% and 100%, respectively. This leads to a conservative model because the turbine output is of a convex shape throughout the thermal input spectrum. A best fit linear approach would lead to peak efficiency of above 100%.

The equation for the line below 48.4% thermal input is

$$\eta_{pb} = 1{,}666 \cdot P_{thermal} + 7{,}739\ \% \qquad (16)$$

where $P_{thermal}$ is the percentage of thermal input referred to 100% input at rated power. For the part of turbine efficiency simulation between 48.4% and 100% thermal input, the equation is

$$\eta_{pb} = 0{,}226 \cdot P_{thermal} + 77{,}43\ \% \qquad (17)$$

The lowest usable value for thermal input is 22.6%, which represents the lowest available figure. This value implies that the power block model includes a shut off

at below 22.6% of thermal input. The selected shut down due to insufficient steam supply is set at 30% of thermal input. Typical values from the literature range from 20% to 30% (Häberle et al. 2002, Eck, Hennecke 2007, Eck, Zarza 2006, Mertins 2009).

4.5 Additional assumptions

This chapter explains several assumptions implemented into the simulation. These are the generator efficiency, the run up phase of the power plant, the parasitic losses and the piping losses.

4.5.1 Generator efficiency

As with the steam turbine, no actual generator can be selected for the project at this stage. Therefore, a typical value from the literature was selected. The peak efficiency of the generator was assumed to be 96%. This value was used, as it reflects the typical value for generators in the low MW size range (Eck, Zarza 2006).

4.5.2 Run up phase of the plant

During night times, the heat transfer fluid in the collector field loses the contained heat to the ambient air and cools down. Such loss makes energy input necessary in the morning until the plant reaches an operational condition. Since the start-up procedure of a solar thermal power plant itself is highly complex and little has been published on it, a rule-of-thumb was used for this phase. In general it can be said that approximately the first hour of sunlight goes fully into preheating the power plant (Gauché 2010). This rule-of-thumb is supported by the working experience of the linear Fresnel prototype PE1 by Novatec Biosol (Selig 2009). Therefore, the simulation assumes that the first hour of thermal energy input of each day is used for inertial heating.

4.5.3 Parasitic losses

Linear Fresnel power plants only exist in prototype status. Operational information about the parasitic losses of linear Fresnel plants have therefore not been published as experience from commercial operation of power plants is not available. For this study parasitic losses of 9% were therefore assumed, based on DLR simulation for linear Fresnel and parabolic trough systems (Pitz-Paal 2007).

4.5.4 Piping losses

The pipe elements of the power plant are subject to heat losses. Piping is required between the power block and the solar field, as well as in between

collector fields, depending on the plant setup. The major heat loss of conduction and convection are included in the simulation, while radiation is neglected. The heat loss calculation is given in equation (18)

$$Q = \frac{T_{pipe} - T_{ambient}}{R_{cond} + R_{conv}} \tag{18}$$

with

$$R_{cond} = \frac{t}{k \cdot A} \tag{19}$$

and

$$R_{conv} = \frac{1}{h \cdot A} \tag{20}$$

where *t* is the thickness of the insulation material, *k* is the insulation material's thermal conductivity, *A* the pipe's surface and *h* the materials convection heat transfer coefficient (for used values see Table 4: Simulation input data, page 45).

4.6 Levelised cost of electricity

The benchmark for electricity producing technologies is the LCOE. This number provides a basis for comparison of technologies by giving costs per kWh of produced electricity. The LCOE is calculated as following the NREL guideline (Short, Packey & Holt 1995)

$$LCOE = \frac{CRF \cdot k_{invest} + k_{O\&M} + k_{fuel}}{E_{net}} \tag{21}$$

with the capital recovery factor (*CRF*) calculated as

$$CRF = \frac{k_d \cdot (1 + k_d)^n}{(1 + k_d)^n - 1} + k_{insurance} \tag{22}$$

with k_{invest} as the total investment of the plant in ZAR, $k_{O\&M}$ the annual operation and maintenance cost in percent of direct investment and k_{fuel} the annual fuel cost in ZAR - which is zero in case of a solar only plant. E_{net} is the annual net electricity output in kWh and k_d the debt interest rate. With n representing depreciation period in years (hence the planned lifetime of the power plant) and $k_{insurance}$ the annual insurance rate in percent of direct investment, the LCOE can be calculated.

4.7 Simulation verification

To approve the quality and usability of the above developed simulation, it was tested on the linear Fresnel prototype PE1, operated by Novatec Biosol in Calasparra, Spain. This prototype plant was commissioned in 2009 (Selig 2009). Production output from 2009 and 2010 is not published. The results for comparison were therefore not measured, but predicted by the developer. The plant configuration is with a once through saturated steam system similar to the proposed technology at Spier. The data input for the simulation is given in Table 3.

Table 3: PE1 power plant specifications

Element	Unit	Quantity
Power block	[MW]	1.4[1]
Collector area	[m^2]	25 792[1]
Steam temperature	[°C]	270[1]
Condenser temperature	[°C]	40-70[2]
Solar field inlet temperature	[°C]	140[2]
Collector loops	[-]	2[1]
Longitude	[°]	-1.60028[1]
Latitude	[°]	38.27841[1]

[1)] (NREL 2010) [2)] (Selig 2009)

The above data was fed into the simulation, including hourly DNI for the plant location. The planned output given at NREL (2010) was 2 800 MWh per year. The model described in this section predicted 2 738.4 MWh per year, thus deviating by 2.2% compared with the given target. This indicated that the analysis was acceptable for a pre-feasibility investigation.

The interpretability of the comparison was limited, however. The DNI source used in this simulation (satellite data of the HelioClim HC3v3 database) was not verified with ground measurement and it was unknown what quality of data was used for the given prediction. The collector field model was based on results of the Solarmundo prototype plant and design differences to the Novatec Biosol collector could not be implemented. Similarly, there were also uncertainties about the turbine, such as shut down at which percentage of steam supply. Additionally, the exact behaviour of the solar field was unknown, as well as the turbine efficiency, the part load behaviour and field piping.

CHAPTER 5: SIMULATION RESULTS, INTERPRETATION AND OPTIMISATION

The application of the developed simulation to the Spier plant and its results is discussed in this chapter. In the first step, the input variables are considered. Thereafter, the simulation output is provided and discussed with focus on sizing of the collector field and the resulting capital cost and LCOE.

5.1 Data input

The used simulation is described in the previous chapter. Input of power plant information was required to run the model. In this study, the collector field size and the rated turbine capacity were used as the levers to adjust the power plant output to the requirement of 2 785 MWh per year (contextual review). The input specifications are given in Table 4.

Table 4: Simulation input data

Element	Unit	Simulation input
Plant output	[MWh]	2 785
Plant location coordinates	[°]	-33.981517 N; 18.785877 E
DNI (hourly)	[kWh/m^{2}a]	2 342
Ambient temperature (hourly)	[°C]	16.5[1]
Steam turbine inlet temperature	[°C]	270
Condensing temperature	[°C]	15 above ambient
Thermal energy input for shutdown	[%]	30 of rated power
Piping length	[m]	3x20[2]
Pipe diameter	[m]	0.18[3]
Pipe insulation conductivity	[W/mK]	0.03[4]
Pipe insulation convection heat transfer coefficient	[W/m^{2}K]	10[4]
Capital cost power block	[R/kWe]	3 990[5]
Capital cost collector	[R/m^2]	1 140[6]
Insurance rate	[%]	1[7]
Debt interest rate	[%]	8
Depreciation period	[a]	25[8]
O&M cost	[R/kWe]	330[9]

[1)] Annual average, for simulation hourly temperature based on Meteonorm database [2)] Each from power block to collector, between the collectors (assuming 2 fields) and one back to the power block [3)] Based on (Häberle et al. 2002) [4)] Typical values for a good insulation material (Mills 1995) [5)] For simple once through saturated steam plant (Eck, Zarza 2006) [6)] For developing country (Lerchenmüller et al. 2004) [7)] In % of direct investment as (Häberle et al. 2002, Mertins 2009), hence capital cost minus 22.5% for engineering and licensing (Mertins 2009) [8)] Typically 25a (Morin et al. 2004) to 28a (Häberle et al. 2002) [9)] Number based on (Häberle et al. 2002) and based on developing world salaries

5.2 Results and interpretation

5.2.1 Plant dimensions

The power plant is required to produce 2 785 MWh of electricity for the mean year to supply Spier's demand (see contextual review). With the above introduced variables remaining fixed, the suitable size of the solar field to a correlating power block, or vice versa, can be found. The required collector field size over the power block dimension is illustrated in Figure 31.

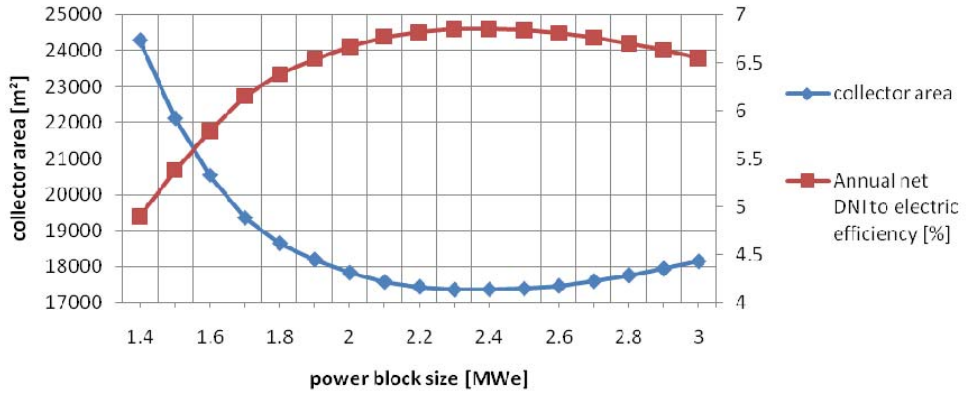

Figure 31: Collector field size and efficiency over power block size

As shown, the required collector area was at the minimum, with around 17 400 m² in a range of 2.3 MWe to 2.5 MWe rated power block capacity. This graph indicates that the annual average net efficiency was the highest in the same range at 6.9%[3]. The setup with a minimum utilisation of land (17 357 m²) was 2.3 MWe rated capacity with a net DNI-to-electricity net efficiency of 6.9%.

5.2.2 Production costs

Figure 31 shows that within a wide area of power block size (2.3 MWe to 2.5 MWe) the required land area did not change dramatically. To find the best power plant size it was important to incorporate cost into the sizing of the plant. The influence of the plant dimensions onto production cost is discussed in this section. The capital cost for each power block size is given in Figure 32.

[3] Applied definition of efficiency: ——— where P_{year} is the annual electricity production and A the collector aperture area.

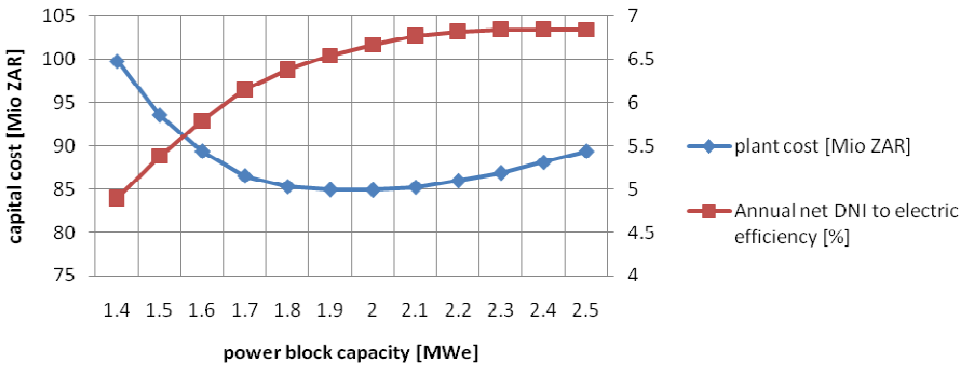

Figure 32: Capital costs for a first plant in Mio ZAR

The least expensive solutions, in terms of capital costs, were between 1.8 MWe to 2.1 MWe where the investment was above R28.3 million. However, this figure gives the cost for equipment, engineering and installation for a third plant. This means that mature systems are installed and the costs do not apply for a first plant or prototype plant. To represent additional effort, a correction factor of 3.0 was considered as a rule-of-thumb in the solar thermal research environment for a first plant (Gauché 2010).

The effect of the maturity of a technology is shown in Figure 33. If the entire plant is newly developed, a minimum capital investment of R84.9 million is needed. Usually, CSP technology developers do not engineer their own turbine systems but buy proven technology and fit the solar field to it. In this way, the capital cost can drop to R68.4 million (with different weight in cost, the optimum size shifts from 2.1 MWe to 2.3 MWe). If also a mature collector field exists, the cost can be further reduced to R28.3 million.

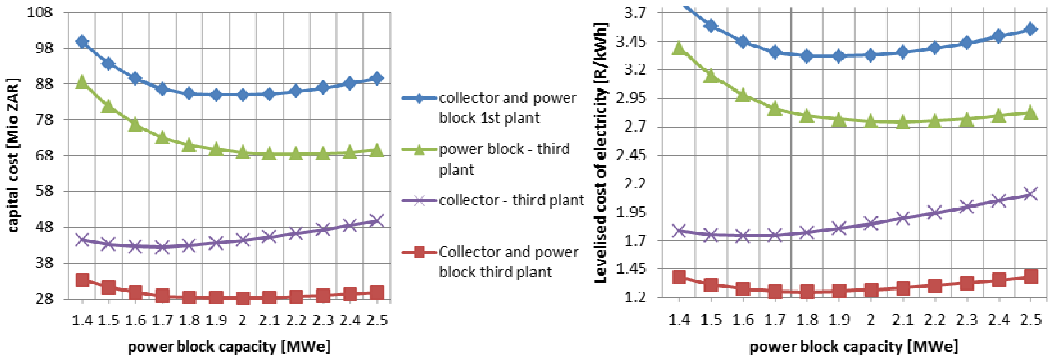

Figure 33: Capital cost in dependence of system maturity

The resulting LCOE is also given in Figure 33. For a newly developed first plant the LCOE was at its optimum at R3.32 per kWh (at 1.9 MWe power block size) and can potentially be brought down to R1.25 for a third plant (at 1.8 MWe power block size). The possible scenarios for an application can be found in the region of these results. A feasible scenario can be the purchase of a power block and a solar field developed in iteration steps. Opportunities to reduce power plant costs are discussed in Chapter 6.

5.3 Proposed plant design

Turbine development is not only a sophisticated field of science it is also a fairly old field. With high capital costs involved in construction of thermal power plants (conventional and renewable), efficiency improvements are taking place at an advanced level. As a result, it is a common approach to design a solar field around a purchased steam turbine (eSolar 2010, Mills, Morrison & Le Lievre 2004). For the proposed plant design it is assumed that a suitable steam turbine generator system can be purchased.

Further, the solar plant built at Spier will not necessarily be a first plant. First system prototyping can, for instance, take place at the solar roof of the University of Stellenbosch or on-site at Spier. For the dimensioning of the proposed plant it was assumed that through prototyping, knowledge is generated. Therefore, a reduced correction factor of 2 for the solar field was employed. The resulting effect on the LCOE is illustrated in Figure 34.

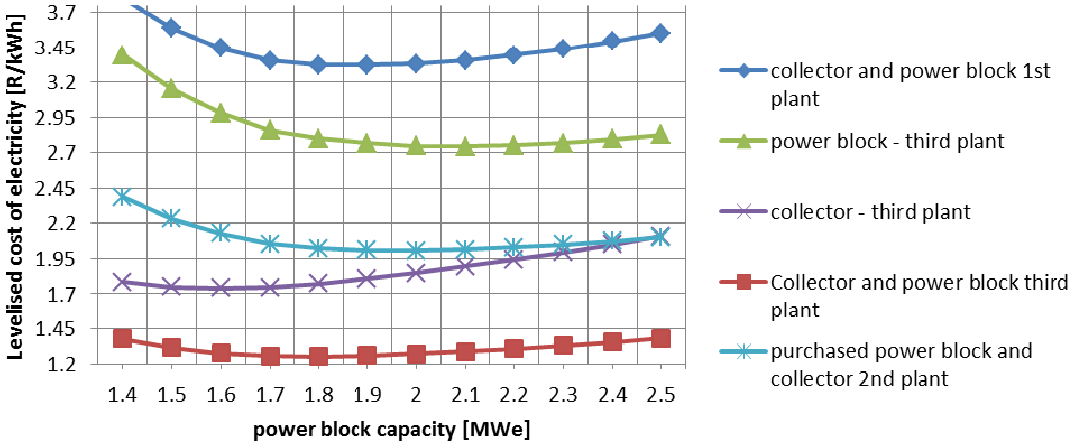

Figure 34: LCOE for the proposed design

The power plant setup with the lowest LCOE is summarized in Table 5.

Table 5: Proposed power plant setup

Element	Unit	Quantity
Power block size	[MWe]	2.0
Collector field area	[m^2]	17 828
Capital cost	[Mio ZAR]	50.3
Annual net solar to electricity efficiency	[%]	6.7
Electricity production	[MWh/a]	2 785
Levelised cost of electricity	[ZAR/kWh]	2.01

This simulation model was based on the Solarmundo prototype collector with a collector width of 24 m. This resulted in a total collector field length of 743 m. As introduced in the contextual review, about 100 000 m^2 are available at a slope of less than 1.75% and 33 000 m^2 at a slope of 1%. Multiple lines of the collector can theoretically be placed directly next to each other so that the required land is almost restricted to the dimension of the collector surface. The collector configuration is flexible with one to multiple parallel lines of the collector field possible. In a scenario with two parallel lines, the setup results in a length of 372 m per line, while four lines require 186 m. The proposed plant location for different quantities of lines is shown in Figure 35 (large scale pictures are given in Appendix J).

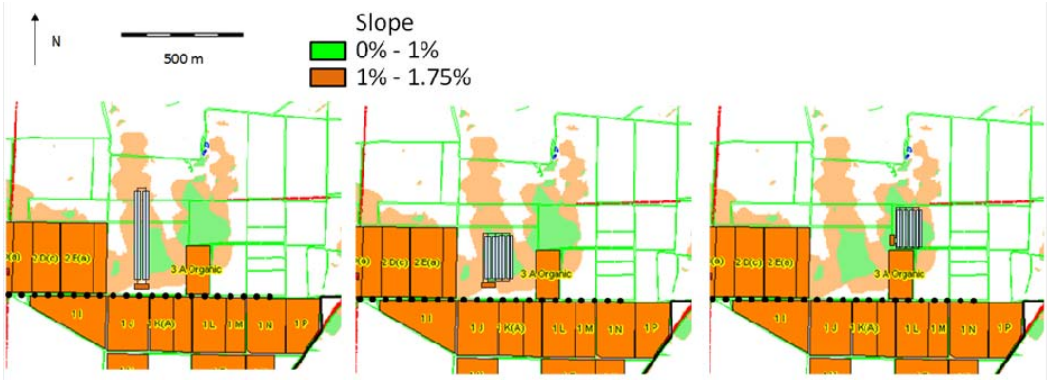

Figure 35: Possible linear Fresnel plant setup with two lines (left) and four lines (middle and right)

The sites were chosen because they not only fulfill the requirement of a slope with less than 1.75%, they also provide the least visual impact. The black dotted line given in Figure 35 represents a line of trees planted by Spier as a wind blocker. The trees also prevent visibility of the plant from the south. For these reasons the power block (marked orange) is positioned south of the collector field. The second positive facet of this location is that it is surrounded by two

hilltops, one from the western side and the other from the eastern side, as highlighted by blue circles in Figure 36 (large scale pictures for different plant locations is given in Appendix K). The western hilltop is with 77 m on the same level as the plant location at 75 m to 76 m, whereas the eastern hilltop reaches more than 100 m altitude.

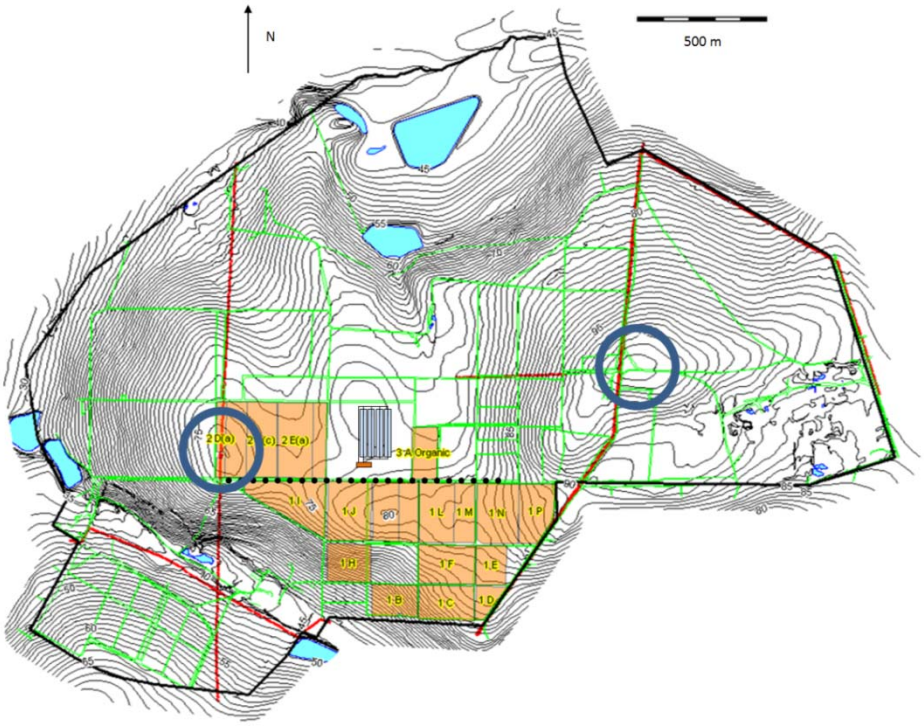

Figure 36: Proposed linear Fresnel plant location for setup with four lines with 1 m contour lines and hilltops (blue)

The vineyard to the west of the solar field provides additional visual protection. Visual impact is further discussed in Chapter 7. It has to be noted that sufficient land is available to accommodate linear Fresnel plants of dimension to supply the full current electricity demand (see Appendix L), hence twice as much as assumed for this study.

5.4 Comparison to Eskom price development

Spier Estate currently obtains its electricity directly from Eskom. Different units of Spier are operating on individual Eskom tariffs (Filander 2011). This leads to a combined average tariff of R0.428 per kWh for the business year 2010/2011 (based on Le Roux 2011). The Eskom price is not static, but will be undergoing rather radical tariff increases in the coming years. The approved average increases in Eskom tariffs is 25.9% for the financial years 2012/13 (ESKOM

2010b) and Eskom is further assuming 25.0%, each for 2013/14 and 2014/15 (Reuters 2010).

Solar thermal power stations are designed to operate for a minimum of 25 years. Therefore, the future development of Eskom tariffs needs to be predicted to allow for comparison. To do so, different scenarios were developed by the author to show the possible developments in the price for 10 years, from 2011 to 2020. The first scenario showed tariff increases at inflation rate after 2015 (the inflation rate of 2009 of 7.2% (USDOS 2011) was assumed to be constant). A second scenario showed further growth at 25.3% per year (which was the average increase for 2010 to 2015). A further intermediate scenario was developed with a 16.25% price increase. Bearing in mind that Eskom initially asked NERSA for tariff increases of 45% (M&G 2010a), the first scenario with a 25.3% increase does not represent a future worst case. Furthermore, the financing of the power station Kusile, that is currently under construction, is still unclear (M&G 2010b).

The resulting electricity tariffs are shown in Figure 37. By 2017, the year the solar thermal power plant needs to be commissioned, the projected Eskom tariff lies between R1.29 and R2.08 per kWh. By 2025, the inflation rate based scenario reaches R2.26 per kWh. For completeness the three developed scenarios are also compared to a linear Fresnel plant with a good research loan of 4% (see Chapter 6).

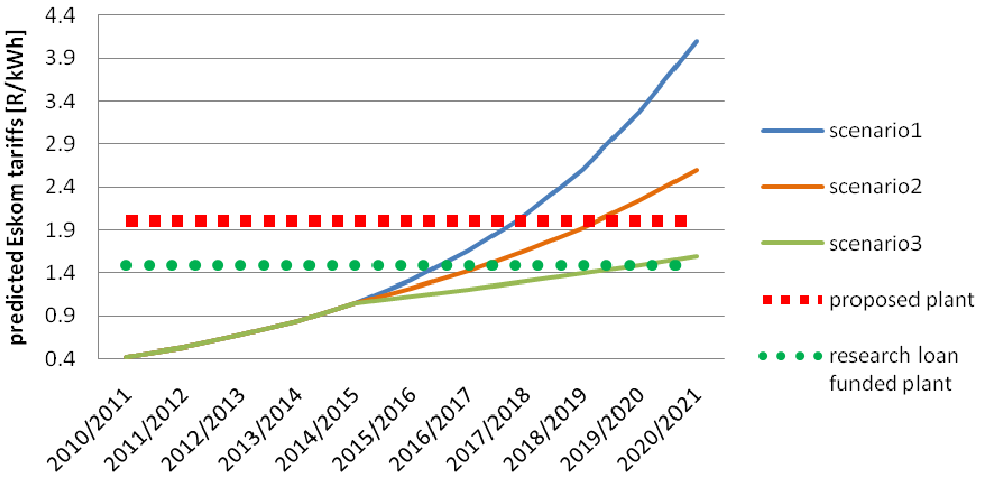

Figure 37: Eskom tariff prediction

The further the prediction is made into the future, the less accurate the projection becomes. It is unclear to which extent renewable energies, and other IPPs, will penetrate the market and whether ongoing cost escalation with regard to the erection of Medupi and Kusile can be absorbed by Eskom. The important point to note is that the proposed power plant producing at R2.01 per kWh can reach grid parity as early as 2017, the year of scheduled commissioning.

CHAPTER 6: POTENTIAL TO REDUCE LEVELISED COST OF ELECTRICITY

This chapter discusses approaches to reduce LCOE. Initially, the sensitivity of LCOE to external variables is investigated. Then the potential of cost reduction through local manufacturing is discussed. Thirdly, the opportunities due to improved funding are considered. As the final aspect, the potential LCOE reduction due to cogeneration is investigated. Possible additional income through commercially selling excess electricity to companies in the proximity of Spier (e.g. Technopark business park) is beyond the scope of this report and not discussed.

6.1 Sensitivity analysis

A sensitivity analysis was done on the proposed power plant as described in Chapter 5. The sensitivity of the LCOE to the parameters was investigated in a range of +/- 30% of the parameter value, as illustrated in Figure 38.

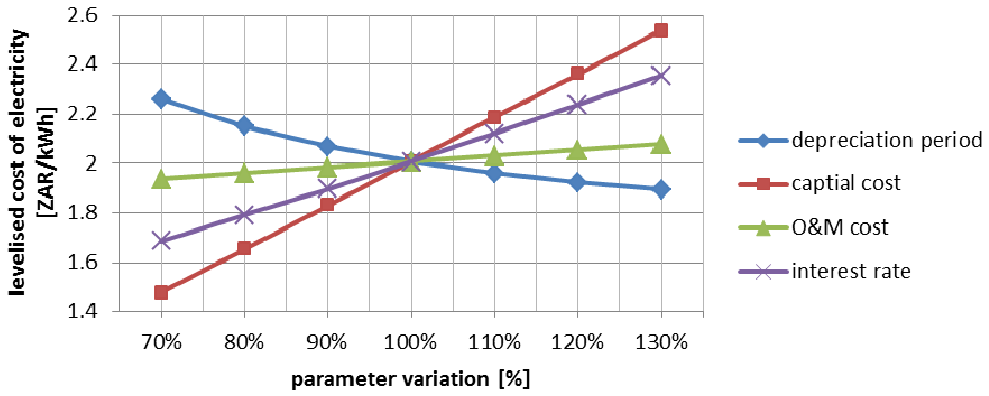

Figure 38: Sensitivity analysis on proposed power plant

This analysis showed that the capital costs and the interest rate on the loan had the biggest lever on the LCOE of the linear Fresnel plant. Sound research on the plant behaviour and the cost structure with low-cost South African labour could lead to reduced capital cost. A good understanding of these costs could also lead to lower interest rates for loans, due to the reduced risk of the investment.

6.2 Local manufacturing

Linear Fresnel has the highest potential of local manufacturing which is explained by the low complexity of the technology (Kaltschmitt 2007, Häberle et al. 2002, Lerchenmüller et al. 2004, Mertins 2009). The mirrors are either mounted flat or are delivered flat and mechanically bent on-site. The used cost figures for the collector field are already adjusted to developing countries (mostly Egyptian)

wages, while European figures are used for the power block. It is not assumed in this study that power block costs can be reduced, as the technology will likely need to be imported. However, it is probable that South African industry can perform more cost effectively. The linear Fresnel collector is both simple in terms of construction technique and optimal for automated mass production of the elements (Selig 2009). To further validate this point, quotes of preliminary designs are required.

A company named BBE Energy has constructed South Africa's first linear Fresnel prototype (van der Merwe 2010). BBE's claim is that the cost of their collector is about half that of the imported system. However, it is not stated with which system the comparison is made, nor is the cost of the BBE collector revealed. The collector generates direct steam for solar chilling purposes and is not designed to drive a steam turbine. With the limited information published and the different scope of the project, the transferability of the benefit of local production is not possible. Hypothetically, the effect of halving the collector field cost would cause the production cost to drop from R2.01 to R1.12 per kWh.

A Fresnel reflector's mirror field consists, for most part, of mechanically simple subsystems. These are the flat or mechanically bent mirror, brackets, bearings motor and control system, elevation construction, mirror cleaning machine (if required) and final assembly. None of these elements is unusual in engineering and manufacturing projects and, therefore, allows high domestic value gain. The collector tower assembly consists of the absorber pipe with selective coating, on-site welding assembly, secondary reflectors, the covering glass pane and brackets and further mechanical tower structure with its assembly. Besides the mirror, in this case the selective coating is a sophisticated product that can also need to be imported. The remainder is again no unusual manufacturing and assembly procedure.

Morin (2006) compares the effect of mirror quality on the Solarmundo prototype by simulation. Figure 39 shows the effect of mirror gaps and mirror quality on the LCOE. Figure 39 indicates tradeoffs in between, for instance, cheap local mirrors, compared to expensive more accurate imported products

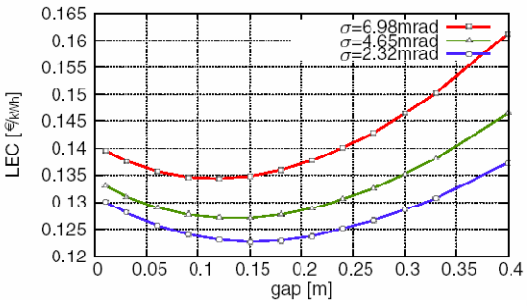

Figure 39: Effect of gap variation and mirror quality on LCOE (here LEC) (Morin et al. 2006)

6.3 Alternative funding options

A project of such a small scale is not suited to making use of the Clean Development Mechanism (CDM) under the Kyoto Protocol. The CDM application process is highly complex and very costly, restricting trading of prevented emissions to large scale-projects (Volschenk 2010). Furthermore, the Kyoto Protocol, and with it the CDM, is phasing out in 2012 with a subsequent mechanism not yet in place.

As introduced in the contextual review, an individual plant needs to be developed. In the cost section it is shown that the LCOE of a pilot plant are significantly higher than those of a turn-key plant. Thus, with the need for a technology to be developed, an attractive option is not to build it as a pilot plant, but as a prototype and research power station. This gives the stakeholders the opportunity to apply for national and international research funds, thereby significantly reducing the LCOE. Besides access to research funds, it is then possible to get loans with significantly better interest rates with 4% being a realistic outcome (Brent 2010). Such a loan would lead to a drop in LCOE to R1.49 per kWh. Research funds and grants often depend on specific programmes of institutions and need to be researched in depth if this project is brought further forward. For instance, the European Commission adjusts its supported research fields annually under the current 7th Framework programme. Grants are available to take off 60% of the capital cost on solar thermal steam generating plants (Brent 2010). A similar grant for solar thermal electricity production would drop the LCOE from R2.01 per kWh to R0.95 per kWh. In addition, smaller prototype plants to verify simulation and design results, as well as gain manufacturing experience, can be built into the process of project development. In such case, further reductions of costs and risks would be achieved.

A research plant at Spier has many appealing facets. Firstly, Spier itself offers a highly attractive site in terms of the sustainability context and public visibility. Secondly, the site is situated in the heart of the academic region of the Western Cape, with many universities and technikons in the region that can benefit from the developments. It is also close to political and government institutions, which is an important facet in terms of lobbying for support for this technology. Another feature that makes the idea of a research plant attractive is the land usage underneath the plant. The ability to use the land in this kind of two-fold fashion makes the linear Fresnel system such a promising technology in the context of sustainability. The land is not destroyed or blocked by the plant, and the land remains available for farming utilisation. The Spier farm, the Sustainability Institute and Stellenbosch University are all parties with a potential interest in research results in this field.

6.4 Investigation of potential for cogeneration

To get a picture of the cogeneration possibilities, the thermal energy dumping of the power plant is investigated in a first step. Then the possibilities of supplying the winery or hotel with heat not utilisable for electricity production are discussed.

6.4.1 Not utilisable heat energy

At times, when solar energy produces more steam than the turbine can utilise, excess thermal energy has to be dumped. At that time the turbine runs at rated power. Energy that is below a minimum of 30% rated turbine power has to be dumped, as it is not sufficient for the turbine to operate. Figure 40 illustrates the amount of thermal energy that is dumped.

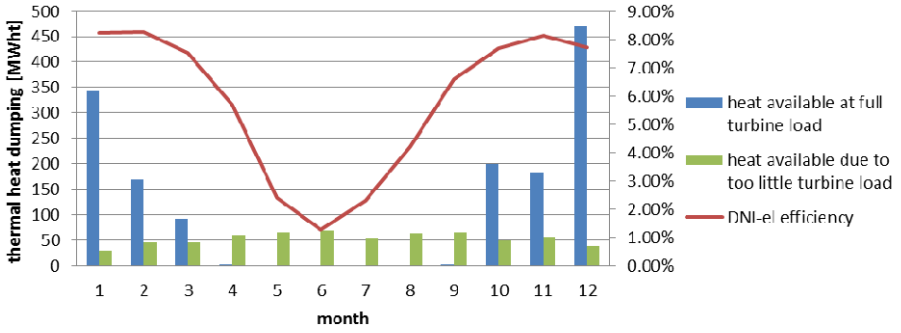

Figure 40: Thermal energy dumping for 2.0 MWe power block

As seen in Figure 40, with the proposed configuration (Chapter 5), the rated power of the turbine is only exceeded in the summer months of October to March. Dumping of heat energy due to too little steam availability occurs throughout the year, as there are phases in the morning or evening when sunlight is insufficient. Also, cloudy days lead to lower dumping which increases in winter.

6.4.2 Spier hotel

The electricity consumption of the Spier hotel is mainly driven by the hot water usage of the guests (Immelman 2010). The hotel at Spier has a capacity for 200 persons, with the average hot water consumption per occupant being 125 l per day, plus 4 400 l for the kitchen (Tekniheat 2010). Therefore, when the hotel is fully booked, its total hot water consumption peaks at 29 400 l per day. A look at the metering data given in Appendix B reveals the temporal demand for electricity. The morning peak consumption is shortly after 09h00, while the afternoon peak occurs after 18h00. With highest hotel occupancy in summer, this provides the possibility to supply a significant amount of that energy from the power plant. Figure 41 illustrates that during the summertime the simulated plant can already be producing at rated power by 09h00.

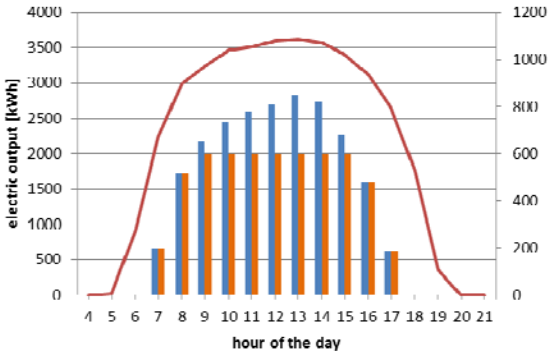

Figure 41: Plant production on January 1st

The economic sense of a cogeneration plant requires further diligent investigation. It needs to be kept in mind that large centralised storage tanks would be needed and the current geysers would still be required as back up. The power plant needs to be equipped with an additional heat exchanger and an isolated pipe that transports the hot water to the hotel. The distance is about 2 km

and the pipe needs to cross farm roads and a river. The cogeneration system competes with the installation of centralized heat pumps to meet the hotels hot water demand. At an initial investment of R969 000 the heat pumps can cut the hotel hot water cost to 30% of what is currently required (Tekniheat 2010). Concluding the cogeneration to supply the hotel hot water demand needs further investigation for feasibility. At this stage, with the given distance and the obstacles in between, it does not seem to be a solution promising a high return on the increased plant complexity.

6.4.3 Spier Wine Cellar

Heat can also be used for chilling purposes by use of solar chillers (absorption or adsorption chillers). While the hotel utilizes a multitude of independent air-conditioning systems, the wine cellars' main energy demand is large scale chilling. This is the cooling of grapes after harvest and of wines at two different temperatures in the barrels. The temporal correlation of winery electricity demand and the upper dumping (dumped thermal energy when turbine operates at rated power) of the plant is illustrated in Figure 42.

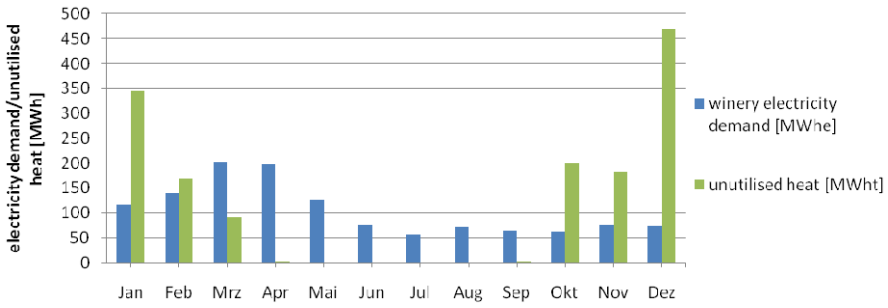

Figure 42: Electricity demand winery and upper dumping of energy

The energy demand of the winery is de-phased from the summer months. While thermal dumping peaks in December and January, the highest chilling demand from the winery is in March and April. No upper dumping occurs from May to September, while the winery reaches the low constant level in June/July. Technologies for solar thermal chilling systems are not in high maturity and mass production stage (Pierce 2011). Solar chilling is only economically feasible when free high temperature waste heat is available (Pierce 2011). The wine cellar is approximately 1 km south of the proposed power plant location and the isolated pipeline would need to cross multiple farm roads and a river. The solar chilling equipment requires the conventional chilling equipment as a backup. For these reasons, the additional plant complexity for cogeneration does not appear economically feasible. However, this aspect may need to be reconsidered at a later stage when chilling equipment prices drop.

CHAPTER 7: CSP AT SPIER AND THE ENVIRONMENT

This chapter briefly discusses the environmental impacts of a CSP plant on the Spier home farm in a micro Environmental Impact Assessment.

7.1 Construction

The first environmental impact occurs during plant construction phase. This contains civil works, cable placement, system assembly and commissioning. The construction phase is also accompanied by transportation/truck traffic.

7.2 Visual

The visual impact of a solar thermal power plant is inevitable, no matter which technology is chosen. The linear Fresnel mirror field is proposed to be elevated from the ground which allows dual utilization of the land, but increases its visibility. The reflected sunlight is directed onto the absorber which is mounted several meters above the mirrors. While the line of sight to the mirror field can be blocked by vegetation from places like roads, the collector on the towers would remain visible.

A mirror field of a solar thermal power station can be easily identified as a clean technology by spectators; the same does not necessarily apply to the power block. Especially for pilot plants and prototypes, the power block is typically visually unappealing. The plant site is exposed to views from the roads (Baden Powell drive and Annandale Road), farms and communities on surrounding hills. Also the recreational areas on the mountains allow high visibility of the power plant. Further investigation of communities and public areas impacted by the line of sight can be done by GIS tools. The visual impact seen from Helderberg and Stellenboschberg are highlighted in Appendix M and Appendix N.

7.3 Flora

The soil would be removed at places where the plant's pillars are mounted to the ground. Besides that, the flora underneath the mirror field would be affected by reduced insolation reaching the ground. The impact of that would be dependent on the type of vegetation currently growing. This leads, potentially, to the necessity of growing other types of plants and possibly opening up a new field of research on dual usability of linear Fresnel CSP plants.

As discussed, the visual impact of such a large structure in the Winelands cannot be avoided. This can partially be reduced by planting trees and bushes to block the line of sight from the roads and lower locations in the surrounding hills. The vegetation cannot be allowed to grow much higher than the mirror level, however, as it would then obstruct energy output.

7.4 CO_2 avoided

Over 90% of Eskom's capacity is generated by coal-fired power stations, one of the worst technologies in terms of CO_2 emissions (Fröhlich, Schwarz 2009). According to a company statement, Eskom-generated electricity leads to 0.9 kg of CO_2 per produced kWh of electricity (ESKOM 2007). Besides the construction of a 100 MWe solar power plant, Eskom is building two multi-GW coal-fired power stations, Medupi and Kusile. The carbon emissions per kWh generated by Eskom, therefore, are unlikely to undergo remarkable change in the future.

With annual assumed electricity consumption of 2 785 MWh, Eskom-generated power exhausts for 2 507 tonnes of CO_2 per year to supply Spier with electricity.

An estimate for current CSP plants is a causation of 33.4 grams of CO_2 per produced kWh (Viebahn, Lechon & Trieb 2010). This is a conservative figure, as it reflects a plant in the European environment with lower DNI. With that number, a CSP plant at Spier would annually be accountable for 93 tonnes of CO_2. This represents avoidance of 96.3% or 2 414 tonnes of CO_2 per year. The majority of that figure is caused by plant construction and distributed over the produced power through the plant lifetime. During operation, only O&M procedures cause marginal emissions.

For a more detailed analysis of the emissions caused by the proposed Spier linear Fresnel power plant, the reader is referred to the LCA (life cycle assessment) currently being produced as a Bachelor's thesis by André Lorenzen at the Sustainability Institute (Lorenzen 2011).

CHAPTER 8: RECOMMENDED STEPS TOWARDS A CSP PLANT AT SPIER

As a first step, Spier needs to make a decision, based on the presented LCOE and capital investment, whether the company sees this way of producing renewable energy as the most suitable for its purposes. The marketing benefits of running a carbon neutral sustainable wine estate outweigh a certain amount of additional costs for electricity. A discussion of this effect is beyond the scope of this study.

Building a power station on Spier Home Farms involves more than the actual design and construction of a power station. The first and most important step, following on a decision to further investigate the opportunity of a CSP plant, is to improve the chances of getting the construction of such a power plant approved by the municipality. According to the authorities, this process will include firstly, the rezoning of agricultural land, and secondly, the admission of building plans (Akhoma 2010). The latter is done by a committee. Therefore it is important to investigate the process thoroughly and to make sure that the members of the relevant committee are aware of the necessity and benefits of renewable energies in general, and the potential role of CSP specifically.

As the visual impact of such a plant cannot be avoided and because it will influence the decision making, it is recommended to set the plant styling as a high priority in further analysis or in a thorough feasibility study. The power plant must blend into the surrounding Winelands as well as possible and must under no circumstances look like an industrial plant, which might cause confusion. The plant should rather remind the spectator of the way forward towards an era not dominated by carbon emission exhausting industry as a representation of the current problems but rather of a sustainable technology. For this reason and also due to its extensive preparation time it is recommended to begin a full EIA at an early stage.

Also, a method of plant construction with least impact on soil is important to maintain the idea of sustainability. The visual impact also leads to the necessity of getting the neighbouring farms and communities positively attuned to the project and thus avoiding later unexpected or unwelcome headwind.

It is recommended to provide a preliminary design and request quotations from South African manufacturers to identify the full potential of cost reduction by domestic labour. Furthermore, thorough identification of research fields (within technology and dual usability) can increase opportunities of funding.

Besides further steps in the actual design and layout of the plant, it will be necessary to work on agreements with Eskom, Nersa and the municipality of Stellenbosch to find a feasible solution for using the municipality as power storage via the national grid.

A detailed energy audit on Spier is required with the target to identify the effect of different LCOE and future Eskom rates on energy efficiency and demand.

CONCLUSION

With the direct steam generating linear Fresnel technology, a system fitting to the requirements of plant operation in a sustainable environment on a farm was found. Due to the possibility of dual land usage underneath the mirrors for farming, the technology could further strengthen the sustainable approach at Spier. The site offers sufficient land for the collector field and insolation of strength superior to CSP locations in Spain. Water supply was also found to be sufficiently available.

The LCOE was identified with R2.01 per kWh. This is almost by a factor of five higher than the current R0.428 per kWh. Nevertheless, the reach of grid parity by 2017, the year of scheduled commissioning, is possible due to radically increasing utility rates. Allowing the university to utilise the system for research purposes, LCOE reduction would be achieved. The effect of a low interest rate of 4% would lead to LCOE reduction to R1.49 per kWh. With R49 million the capital costs involved would be high, but national and international funds and grants for research facilities could provide potential for further cost drop. For higher attractiveness of the project additional research could be done on the land usage underneath the mirror field.

The plant sizing on cost estimation was based on a simulation model, built on physics and literature results. Its applicability was verified with a single validation point – a prototype plant in Spain. Further development of the model is possible and would aid higher accuracy and allow more detailed plant sizing.

The Spier location offers a unique environment for a demonstration plant with its high public exposure and close access to Cape Town. This attractive location could further increase access ability to funding. A basic CSP plant as proposed for Spier would provide good potential as a first research station for institutions on their way to develop sophisticated utility scale projects.

However, it is important to understand the dimensions and the environmental impact, especially visual, of the plant. An evaluation would be needed if such a prominent structure would fit into the Spier philosophy. Furthermore, investigation on construction regulation and procedures would be required to identify risks of project refusal.

Based on the study, a CSP plant at Spier will be economically feasible and will be a capable of meeting the company's targets of carbon offsetting. It is recommended that the solution should be further pursued. The proposed way forward is a full scale feasibility study, including investigation of the domestic manufacturing industry and a detailed electricity demand prediction at Spier. The proposed linear Fresnel technology is economically competitive to an alternative PV solution. The linear Fresnel is proposed with R24 500 per kWe installed, while PV is predicted with R25 000 to R30 000 per kWe for large scale applications (Reinecke 2011). A CRSES developed PV tool predicts R1.99 per kWh (financed under the same conditions as the CSP plant as described in Chapter 5).

WORKS CITED

Abengoa Solar 2008, *Technologies - Concentrating Solar Power* [Homepage of Abengoa Solar], [Online]. Available: http://www.abengoasolar.com/corp/web/en/technologies/concentrated_solar_power/what_is_it/index.html [2010, 10/10].

Akhoma 2010, *Steps for approval of a solar thermal power plant at Spier* [Interview], Lubkoll, M., Stellenbosch.

Aora-Solar 2011, *Aora-Solar website* [Homepage of Aora-Solar], [Online]. Available: http://www.aora-solar.com/ [2011, 03/22].

Brent, A.C. 2010, *Financing of a prototype plant* [Interview], Lubkoll, M., Stellenbosch.

Brost, R. 2010, *Design of a High-Temperature Molten Salt Linear Fresnel Collector*, U.S. Department of Energy, Albuquerque.

Burkholder, F. & Kutscher, C. 2009, *Heat Loss Testing of Schott's 2008 PTR70 Parabolic Trough Receiver*, National Renewable Energy Laboratory, Golden.

Business Wire 2010, 29.12.2010-last update*, K Road Power Acquires 850 MW Calico Solar Project* [Homepage of Business Wire], [Online]. Available: http://www.businesswire.com/news/home/20101229005426/en/Road-Power-Acquires-850-MW-Calico-Solar [2011, 04/01].

CENERG 2011, 16.02.2011-last update*, SoDa service - Knowledge in solar radiation* [Homepage of CENERG], [Online]. Available: http://www.soda-is.com/eng/index.html [2011, 02/17].

Cohen, G. 2006, *An overview of the Concentrating Solar Power Industry*, Solargenix Energy, Las Vegas.

Curzon, F.L. & Ahlborn, B. 1975, "Efficiency of a Carnot engine at maximum power output", *American Journal of Physics,* vol. 43, pp. 22-24.

Deign, J. 2010, 19.07.2010-last update*, Will Schott call the shots in the Fresnel receiver market?* [Homepage of CSPtoday], [Online]. Available: http://social.csptoday.com/industry-insight/will-schott-call-shots-fresnel-receiver-market [2011, 04/11].

Derby, R.C. & Lazzara, S.P. s.a., *CENICOM SOLAR THERMAL POWER PLANT WITH THERMAL STORAGE*, Cenicom Solar Energy LLC, Ashford.

DOE 2009, *Concentrating Solar Power Commercial Application Study: Reducing Water Consumption of Concentrating Solar Power Electricity Generation - Report to Congress*, U.S. Department of Energy, Washington.

Donnelly, L. 2011, 18.03.2011-last update, *Power plant blast threatens supply* [Homepage of Mail & Guardian], [Online]. Available: http://mg.co.za/article/2011-03-18-power-plant-blast-threatens-supply [2011, 03/18].

DOW 2001, *DOWTHERM A - Synthetic Organic Heat Transfer Fluid - Liquid and Vapor Phase Data*, Dow Chemical Company, Midland.

Duffie, J.A. & Beckman, D.A. 2006, *Solar Engineering of Thermal Processes,* 3rd Edition edn, John Wiley & Sons Inc., Hoboken.

EC 2005, *SOLGATE - Solar hybrid gas turbine electric power system*, European Commission, Brussels.

Eck, M. & Hennecke, K. 2007, *Die solare Direktverdampfung–Vergleich mit anderen technologischen Optionen*, Deutschen Zentrums für Luft- und Raumfahrt (DLR) e.V., Stuttgart.

Eck, M. & Zarza, E. 2006, "Saturated steam process with direct steam generating parabolic troughs", *Solar Energy,* vol. 80, no. 11, pp. 1424-1433.

EPRI 2002, *Comparison of Alternate Cooling Technologies for California Power Plants: Economic, Environmental, and Other Tradeoffs*, EPRI and California Energy Commission, Palo Alto and Sacramento.

Eskom s.a., n.a.-last update, *Status report on capacity expansion projects* [Homepage of Eskom], [Online]. Available: http://www.eskom.co.za/live/content.php?Item_ID=9598&Revision=en/0 [2011, 03/28].

ESKOM 2007, *Eskom Annual Report 2007 - Directors' report - IMPACT ON THE ENVIRONMENT AND CLIMATE CHANGE* [Homepage of Eskom], [Online]. Available: http://www.eskom.co.za/annreport07/annreport07/directors_report_03.htm [2010, 09/03].

ESKOM 2010a, *Generation Connection Capacity Assessment of the 2012 Transmission Network (GCCA-2012)*, ESKOM, Pretoria.

ESKOM 2010b, *Frequently Asked Questions - 2010/11*, ESKOM, Sandton.

ESKOM 2011, *Guide for IPP grid application process - (TECHNICAL STANDARDS)*, ESKOM, Pretoria.

eSolar 2010, *Our Projects - Sierra Sun Tower* [Homepage of eSolar], [Online]. Available: http://www.esolar.com/our_projects/ [2011, 03/22].

Facão, J. & Oliveira, A.C. 2009, "Numerical Simulation of a Linear Fresnel Solar Collector Concentrator", ed. University of Porto, 8th International Conference on Sustainable Energy Technologies, Aachen, 03.08.2009.

Filander, O. 2011, *Electricity consumption of Spier* [Interview], Lubkoll, M. Spier.

Filander, O. 2010, *Availability of general resources at Spier home farm* [Interview], Lubkoll, M., Stellenbosch.

Ford, G. 2008, "CSP: bright future for linear fresnel technology?", *Renewable Energy Focus,* vol. 9, no. 5, pp. 48-49, 51.

Forristall, R. 2003, *Heat Transfer Analysis and Modeling of a Parabolic Trough Solar Receiver Implemented in Engineering Equation Solver*, National Renewable Energy Laboratory, Golden.

Fouilloux, J.P. & Otto, M. 2009, *Medupi and Kusile: supercritical giants of South Africa*, Alstom, Baden.

Fröhlich, T. & Schwarz, T. 2009, *Erneuerbare Energien in Südafrika*, Botschaft der Bundesrepublik Deutschland - Pretoria, Pretoria.

Gauché, P. 2010, *Operational experience of Solar Thermal Power Plants* [Interview], Lubkoll, M., Stellenbosch.

Gilman, P., Blair, N., Mehos, M., Christensen, C., Janzou, S. & Cameron, C. 2008, *Solar Advisor Model - User Guide for Version 2.0*, National Renewable Energies Laboratory, Godlen.

Google Maps 2010, 28.11.2010-last update*, Maps of the Western Cape* [Homepage of Google Maps], [Online]. Available: www.maps.google.co.za [2010, 11/28].

Gyso 2010, *Metering data Spier*, Spier, Stellenbosch.

Häberle, A., Zahler, C., Lerchenmüller, H., Mertins, M., Wittwer, C., Trieb, F. & Dersch, J. 2002, *The Solarmundo line focussing Fresnel collector. Optical and thermal performance and cost calculations.*, Fraunhofer ISE, Freiburg.

Haeger, M., Keller, L., Monterreal, R., Valverde, A. & de Almería, P.S. 1994, *PHOEBUS Technology Program Solar Air Receiver (TSA): Operational Experiences with the Experimental Set-up of a 2, 5 MWth Volumetric Air Receiver (TSA) at the Plataforma Solar de Almeria*, DLR, Plataforma Solar de Almeria (PSA).

Herrmann, U., Kelly, B. & Price, H. 2004, "Two-tank molten salt storage for parabolic trough solar power plants", *Energy,* vol. 29, no. 5-6, pp. 883-893.

IEA 2010, *Technology Roadmap Concentrating Solar Power,* International Energy Agency, Paris.

Immelman, C. 2010, *site visit on Spier hotel, conference and banqueting* [Interview], Lubkoll, M., Stellenbosch.

Incropera, F.P., DeWitt, D.P., Bergman, T.L. & Lavine, A.S. 1990, *Fundamentals of Heat and Mass Transfer,* Third Edition , John Wiley & Sons, New York.

Kalogirou, S.A. 2004, "Solar thermal collectors and applications", *Progress in energy and combustion science,* vol. 30, no. 3, pp. 231-295.

Kaltschmitt, M. 2007, *Renewable Energy - Technology, Economics and Environment,* 1st edn, Springer Verlag, Berlin.

Kearney, D., Kelly, B., Cable, R., Potroviza, N., Herrmann, U., Nava, P., Mahoney, R., Pacheco, J., Blake, D. & Price, H. 2003, *Overview on use of a Molten Salt HTF in a Trough Solar Field*, National Renewable Energies Laboratory, Golden.

Kruger, C. 2010, *Resources consumption of Spier* [Interview], Spier, Stellenbosch.

Küsgen, F. & Küser, D. 2009, 05.2009-last update*, Fresnel-Kollektoren an der Schwelle zur Marktreife* [Homepage of Energy20.net], [Online]. Available: http://www.mobility20.net/pi/index.php?StoryID=317&articleID=159100 [2010, 08/21].

Le Roux, B. 2011, *Spier electricity consumption* [Interview], Lubkoll, M., Spier.

Lerchenmüller, H., Mertins, M., Morin, G., Häberle, A., Zahler, C., Ewert, M., Fruth, M., Griestop, T., Bockamp, S. & Dersch, J. 2004, *"BMU-Fresnel"-Technische und wirtschaftliche Machbarkeits-Studie zu horizontalen Fresnel-Kollektoren: Abschlussbericht*, Fraunhofer ISE, Freiburg.

Lorenzen, A. 2011, *Bachelor Thesis: Life cycle analyses to establish the environmental and economic profiles of medium-scale concentrated solar power technologies: The case of a Linear Fresnel system on the Spier Estate*, Bachelor, Fachhochschule Kiel, Kiel.

Los Angeles Times 1999, 27.02.1999-last update*, Storage Tank at Solar Power Plant in Desert Explodes* [Homepage of Los Angeles Times], [Online]. Available: http://articles.latimes.com/1999/feb/27/news/mn-12205 [2010, 10/14].

M&G 2010a, 22.02.2010-last update*, Nersa set to announce Eskom hike decision* [Homepage of Mail&Guardian online], [Online]. Available: http://www.mg.co.za/article/2010-02-22-nersa-set-to-announce-eskom-hike-decision [2010, 10/01].

M&G 2010b, 11.11.2010-last update*, Eskom to get R20bn from state* [Homepage of Mail&Guardian online], [Online]. Available: http://www.mg.co.za/article/2010-11-11-eskom-to-get-r20-bn-from-state [2010, 11/20].

MEGS 2000, *N-Pentane - Material Safety Data Sheet*, MEGS, Montreal.

Mertins, M. 2009, *Technische und wirtschaftliche Analyse von horizontalen Fresnel-Kollektoren*, University of Karlsruhe.

Mills, A.F. 1995, *Heat and Mass Transfer,* first edn, CRC Press, Boston.

Mills, D. 2004, "Advances in solar thermal electricity technology", *Solar Energy,* vol. 76, no. 1-3, pp. 19-31.

Mills, D.R. & Morrison, G.L. 2000, "Compact linear Fresnel reflector solar thermal powerplants", *Solar Energy,* vol. 68, no. 3, pp. 263-283.

Mills, D.R., Morrison, G.L. & Le Lievre, P. 2004, *Design of a 240 MWe Solar Thermal Power Plant*, University of Sydney, Freiburg.

Morin, G., Lerchenmüller, H., Mertins, M., Ewert, M., Fruth, M., Bockamp, S., Griestop, T. & Häberle, A. 2004, "Plug-in Strategy for Market Introduction of Fresnel-Collectors", *Proceedings of 12th SolarPACES International Symposium on Solar Thermal Concentrating Technologies, Oaxaca, Mexico* Fraunhofer Institute for Solar Energy Systems, Freiburg.

Morin, G., Platzer, W., Eck, M., Uhlig, R., Häberle, A., Berger, M. & Zarza, E. 2006, "Road map towards the demonstration of a linear Fresnel collector using a single tube receiver", *13th SolarPACES Symposium*, ed. Fraunhofer-Institut für Solare Energiesysteme ISE, SolarPACES, pp. 20.

NERSA 2008, *NERSA Consultation Paper - Renewable Energy Feed - In Tarif*, National Energy Regulator of South Africa, Pretoria.

Nixon, J.D., Dey, P.K. & Davies, P.A. 2010, "Which is the best solar thermal collection technology for electricity generation in north-west India? Evaluation of options using the analytical hierarchy process", *Energy,* vol. 35, no. 12, pp. 5230-5240.

Novatec Biosol 2010, *Novatec Biosol AG - A solar revolution*, Novatec Biosol AG, Karlsruhe.

NREL 2010, 16.03.2010-last update*, Concentrating Solar Power Projects - Concentrating Solar Power Projects by Technology* [Homepage of National Renewable Energy Laboratory], [Online]. Available: http://www.nrel.gov/csp/solarpaces/by_technology.cfm [2010, 09/18].

Orosz, M.S. 2010, *Small scale solar ORC system for distributed power in Lesotho*, Massachusetts Institute of Technology, Cambridge.

Oxford University 2009, 20.02.2009-last update*, Safety (MSDS) data for pentane* [Homepage of Oxford University], [Online]. Available: http://msds.chem.ox.ac.uk/PE/pentane.html [2010, 10/18].

Pahwa, S. 2011, *Corporate Resiliance: A Case Study of Spier Group's search for a sustainable, lower carbon future*, PhD Thesis edn, School of Public Leadership, Stellenbosch University, Stellenbosch.

Paul, C. 2008, *Turnkey Solar Steam Generators for Process Heat and Solar Thermal Power Plants*, Novatec BioSol AG, Karlsruhe.

Pierce, W. 2011, *Interview: Economic feasibility of solar chilling*, Lubkoll, M., Stellenbosch.

Pitz-Paal, R. 2007, *Line Concentrators for Power Generation: Parabolic Trough and Linear Fresnel*, Deutsches Zentrum für Luft- und Raumfahrt, Stuttgart.

Prabhu, E. 2006, *Solar trough organic rankine electricity system (stores) stage 1: Power plant optimization and economics*, NREL, Golden.

Price, T. 2010, 04.06.2010-last update*, Fresnel specialist Novatec Biosol turns to superheated steam to boost efficiency by 50%* [Homepage of International Business Times], [Online]. Available: http://uk.ibtimes.com/articles/20100604/fresnel-specialist-novatec-biosol-turns-to-superheated-steam-to-boost-efficiency-by-50.htm [2011, 03/24].

Pye, J.D., Morrison, G.L. & Behnia, M. 2003, *Transient modelling of cavity receiver heat transfer for the compact linear Fresnel reflector*, University of New South Wales, Sydney.

Quaschning, V., Kistner, R., Ortmanns, W. & Geyer, M. s.a., *greenius - A New Simulation Environment for Technical and Economical Analysis of Renewable Independent Power Projects*, DLR, Plataforma Solar de Almeria.

Reinecke, J. 2011, Interview: *LCOE of a large scale PV application,* Lubkoll, M., Stellenbosch.

Reuters 2010, 07.07.2010-last update*, Eskom sees 25% increase in 2013, 2014* [Homepage of MONEYWEB], [Online]. Available: http://www.moneyweb.co.za/mw/view/mw/en/page295042?oid=485143&sn=2009+Detail [2011, 03/12].

Richter, C., Blanco, J., Heller, P., Mehos, M., Meier, A. & Meyer, R. 2010, *SolarPACES - Annual Report 2009*, SolarPACES, SolarPACES.org.

Romero, M., Buck, R. & Pacheco, J.E. 2002, "An update on solar central receiver systems, projects, and technologies", *Journal of solar energy engineering,* vol. 124, pp. 98.

Schott 2010, 02.06.2010-last update*, SCHOTT Solar CSP to supply direct steam receivers for Fresnel technology* [Homepage of Schott AG], [Online]. Available: http://www.schott.com/english/news/press.html?NID=2858 [2011, 04/11].

Scoccini, G. 2010, *Sustainable Energy in the framework of Sustainability Science. A case study in Africa*, Master of Engineering edn, University of Rome, Rome.

Selig, M. 2009, *PE1 - First Fresnel solar power plant in operation - Experiences and Outlook*, Novatec Solar, Karlsruhe.

Short, W., Packey, D.J. & Holt, T. 1995, *A Manual for the Economic Evaluation of Energy Efficiency and Renewable Energy Technologies*, National Renewable Energy Laboratory, Golden.

Sierra Club 2008, *Energy Facts - Compact Linear Fresnel Reflector (CLFR) Solar*, Sierra Club, San Francisco.

Sinai, J. & Fisher, U. 2008, *1 MW Solar Power Plant Using ORMAT ENERGY CONVERTER*, Ben-Gurion University of the Negev, Yavne.

Smit, F. 2010, *Energy consumption and efficiency at Spier cellar* [Interview], Lubkoll, M., Stellenbosch.

SolarPACES s.a., *Solar Power Tower*, SolarPACES.

SolarPACES 1998, *SOLAR DISH ENGINE*, SolarPACES, http://www.solarpaces.org/Library/AnnualReports/documents/AnnualReport2009Final_web.pdf.

Sopogy 2011, *The total solar solution* [Homepage of Sopogy], [Online]. Available: http://sopogy.com/solutions/ [2011, 03/22].

Spier 2008, *Spier Sustainability Report*, Spier, Stellenbosch.

Spliethoff, H. 2006, *The Organic Rankine Cycle - Power Production from Low temperature heat*, Technische Universität München, Munich.

Stancich, R. 2010a, 03.10.2010-last update*, AREVA Solar puts its money on the solar booster market* [Homepage of CSPtoday], [Online]. Available: http://social.csptoday.com/qa/areva-solar-puts-its-money-solar-booster-market [2010, 10.09].

Stancich, R. 2010b, 16.08.2010-last update*, Plug and Play CSP: Low impact, zero water, biofuel backed*. Available: http://social.csptoday.com/qa/plug-and-play-csp-low-impact-zero-water-biofuel-backed [2010, 09/20].

Stauffer, N. 2006, 18.10.2006-last update*, Engine on a chip promises to best the battery* [Homepage of Massachusetts Institute of Technology], [Online]. Available: http://web.mit.edu/newsoffice/2006/microengines.html [2011, 03/28].

Stine, W.B. & Geyer, M. 2001, *Power From The Sun*. Available: http://www.powerfromthesun.net/book.html [2010, 10/27].

Suntrace 2011, *DNI satellite truth? - How to handle the difference in values derived from different satellite data providers*, Suntrace, Hamburg.

Tecsia Lubricants 2010, *XCELTHERM 600 - HEAT TRANSFER FLUIDS*, Tecsia Lubricants Ptd Ltd., Singapore.

Tekniheat 2010, *Spier Hotel - Hot water, Heat Pump System*, Tekniheat, Bergvliet.

Tessera Solar 2011a, *Tessera Solar - SUNCATCHER ADVANTAGES* [Homepage of Tessera Solar], [Online]. Available: http://www.tesserasolar.com/north-america/advantages.htm [2011, 03/22].

Tessera Solar 2011b, *Imperial Valley Solar Project Acquired by AES Solar*, Tessera Solar, Houston.

Turchi, C. 2010, *Parabolic Trough Reference Plant for Cost Modeling with the Solar Advisor Model (SAM)*, National Renewable Energy Laboratory, Golden.

Tyner, C.E., Sutherland, J.P. & Gould, W.R. 1995, "Solar two: A molten salt power tower demonstration", *VDI BERICHTE,* vol. 1200, pp. 53-53.

Unitor 2008, *Sicherheitsdatenblatt R-245fa*, Unitor, Lysaker.

USDOS 2011, 11.03.2011-last update*, Background Note: South Africa* [Homepage of U.S. Department of State], [Online]. Available: http://www.state.gov/r/pa/ei/bgn/2898.htm [2010, 11/20].

van der Merwe, C. 2010, 16.11.2010-last update*, BBE builds locally developed linear Fresnel CSP plant* [Homepage of Engineering News Online], [Online]. Available: http://www.engineeringnews.co.za/article/bbe-energy-builds-locally-developed-linear-fresnel-csp-plant-2010-11-16 [2010, 11/19].

van Wylen, G.J., Sonntag, R. & Borgnakke, C. 1994, *Fundamentals of Classical Thermodynamics,* 4th Edition edn, John Wiley & Sons, Inc., New York.

Viebahn, P., Lechon, Y. & Trieb, F. 2010, "The potential role of concentrated solar power (CSP) in Africa and Europe--A dynamic assessment of technology development, cost development and life cycle inventories until 2050", *Energy Policy*.

Volschenk, J. 2010, *Renewable Energy Financing* [Lecture], University of Stellenbosch Business School, Stellenbosch.

von Wedel, H. 2011, 27.03.2011-last update, *Maschinenbau: Altes Motorenkonzept konkurriert in Nischenbereichen mit herkömmlichen Antriebsarten - Stirlingmotor fährt aus seinem Schattendasein* [Homepage of VDI Verland GmbH], [Online]. Available: http://www.vdi-nachrichten.com/vdi-nachrichten/aktuelle_ausgabe/akt_ausg_detail.asp?cat=2&id=327 [2011, 03/27].

Wagner, K. 2008, *Master Thesis: A graphic based interface to Endoversible Thermodynamics*, Chemnitz University of Technology.

Wey, E. 2011, *GHI et DNI Helioclim3 data time series for the site of Stellenbosch, South Africa - Lat/lon: -33.928, 18.865, Altidtude: 122m - Calibration from ground station measurements - Period June 23rd 2010 to January 24th 2011*, Transvalor S.A., Nice.

Winkler, H. 2007, "Energy policies for sustainable development in South Africa", *Energy for Sustainable Development,* vol. 11, no. 1, pp. 26-34.

World Bank 1999, *Cost Reduction Study for Solar Thermal Power Plants*, World Bank, Washington D.C.

Zarza, E., Valenzuela, L., Leon, J., Hennecke, K., Eck, M., Weyers, H.D. & Eickhoff, M. 2004, "Direct steam generation in parabolic troughs: Final results and conclusions of the DISS project", *Energy,* vol. 29, no. 5-6, pp. 635-644.

APPENDIX A – METERING DATA OF WINERY

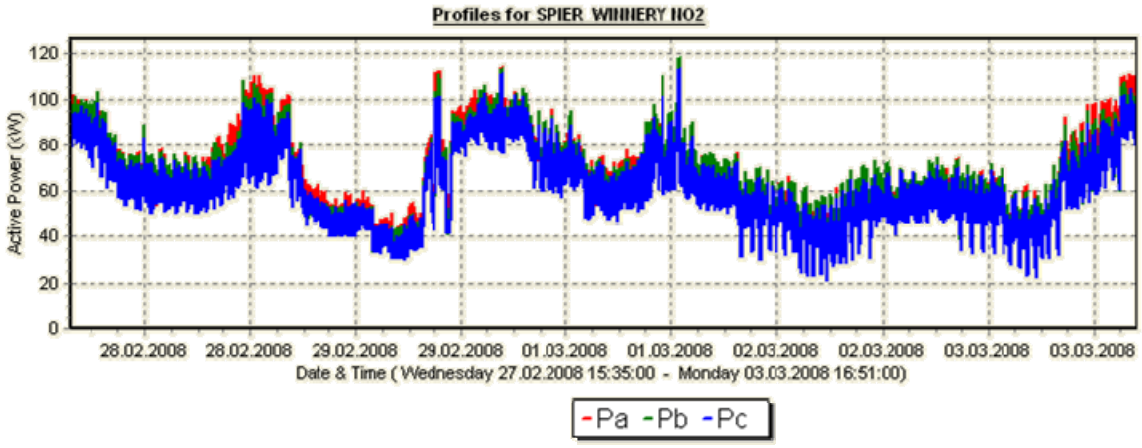

Figure 43: Metering data of the winery for February/March 2008 (Gyso 2010)

APPENDIX B – METERING DATA OF HOTEL

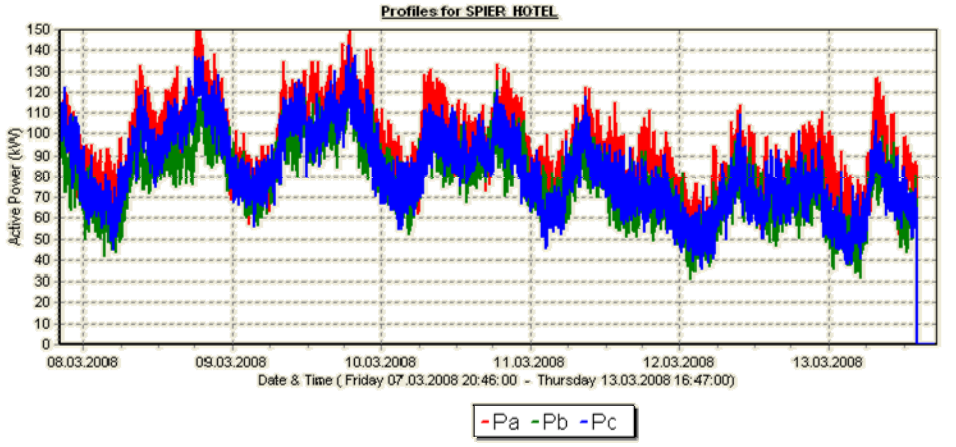

Figure 44: Metering data of the hotel for February/March 2008 (Gyso 2010)

APPENDIX C – SPIER FARM MAP

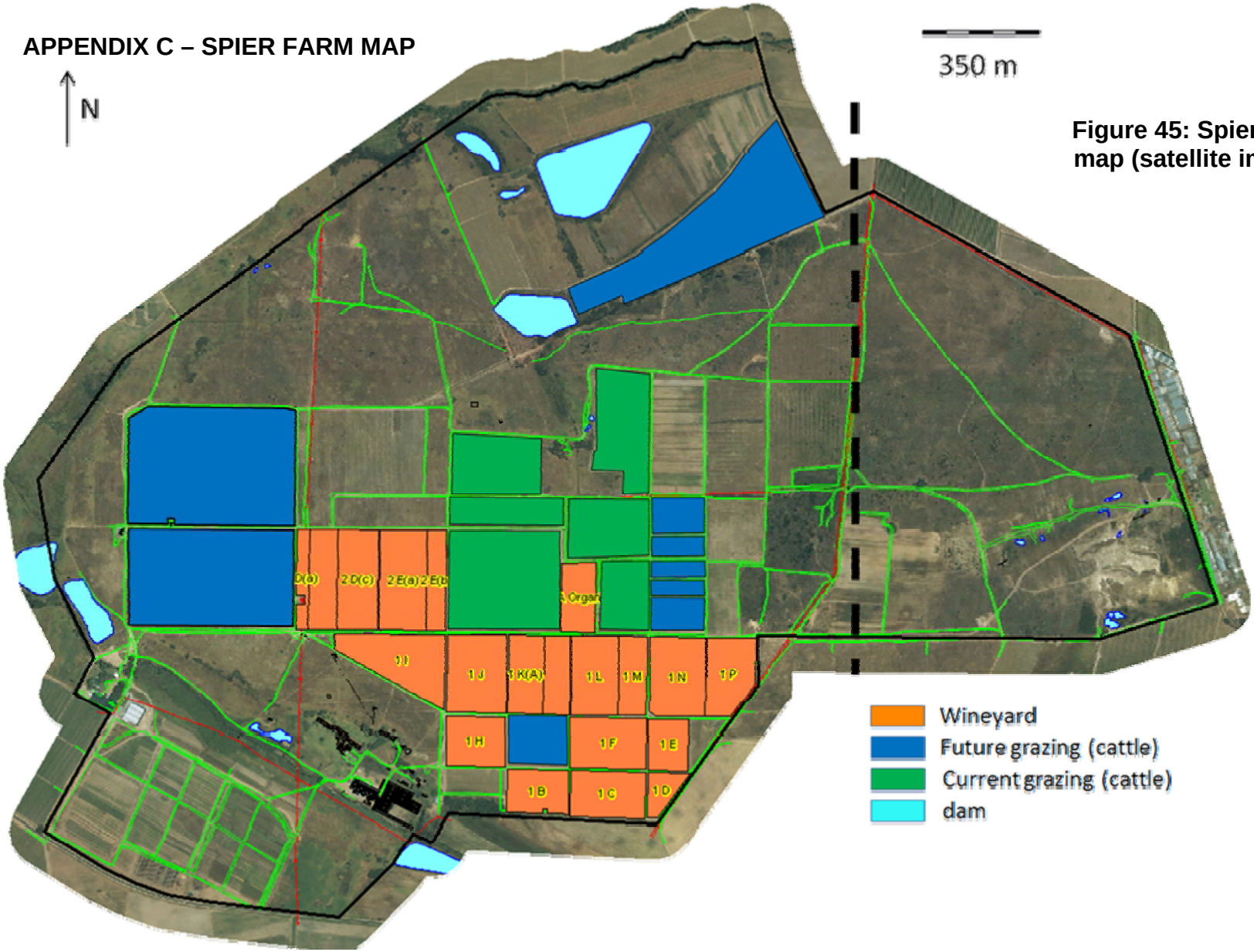

Figure 45: Spier farm map (satellite image)

APPENDIX D – SPIER FARM MAP SLOPE

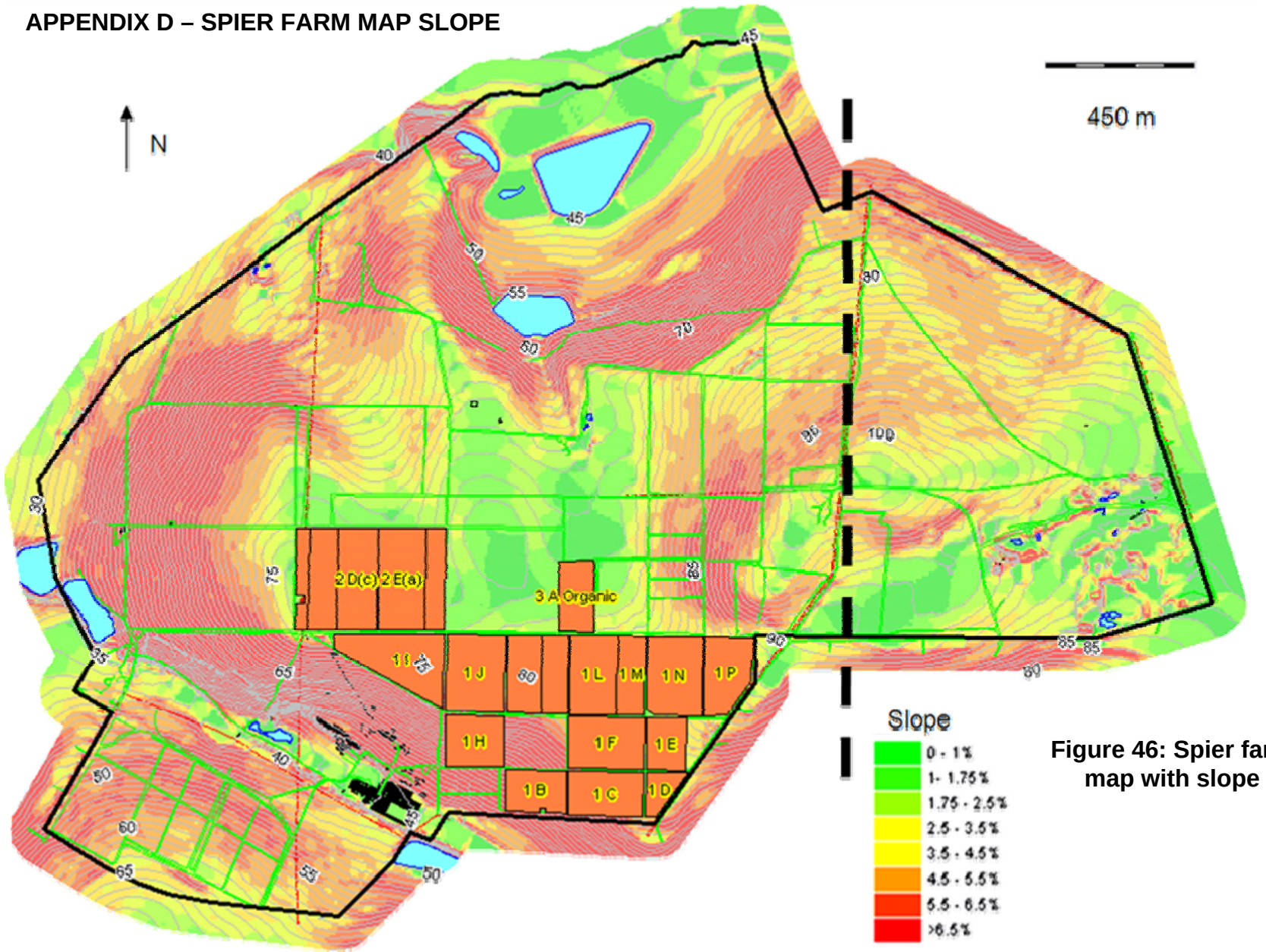

Figure 46: Spier farm map with slope

APPENDIX E – AREA AVAILABLE FOR TOLERABLE MAXIMUM SLOPES

As described in the contextual review and the technology review, different collector technologies can tolerate different amounts of maximum slopes. For the main CSP systems these are summarised in Table 6.

Table 6: Maximum slope tolerable by CSP collector technologies

CSP collector	Tolerable slope [%]
Parabolic trough	1[1]
Linear Fresnel	1.75[2]
Parabolic dish	10[3]
Central receiver	Depending on technology

[1)] (Turchi 2010) [2)] (Nixon, Dey & Davies 2010) [3)] (Tessera Solar 2011b)

Investigation of the farm satellite map shows significantly different areas available for different slopes tolerable, as illustrated in Appendix D. Given in Table 7 is a list of measured land available for different slopes.

Table 7: Area available for different slopes

Slope [%]	Area available [ha]
1	2.3 + 3.3
1.75	11.4 + 5.2
2.5	>28
5	>62

It can be seen that the more tolerable a technology is, the more land is potentially usable.

APPENDIX F – DNI

The most accurate and reliable source of DNI measurements are the readings of an installed, sun tracking measurement device situated at the location of the investigated plant. Another way to access DNI information without long term ground measurement is to analyse satellite data. An accessible resource is the HelioClim database, developed and operated by French research center “Centre Energétique et Procédés” (CENERG) that provides such a service with a database starting from 2004 with hourly irradiation data (CENERG 2011).

From June 2010 on, CRSES at Stellenbosch University operates a solar measurement station at the roof of the engineering department which is about 5.5 km linear distance apart from Spier. A comparison of the measured data from CRSES to the computed data of HC3v3 indicates that the actual DNI in Stellenbosch is about 10% above the data provided by CENERG (Table 8).

Table 8: Comparison of HC3v3 data set with CRSES-calibrated data

Year	CRSES HC3v3 calibrated [kWh/m2a]	CRSES HC3v3 Database [kWh/m2a]	Deviation [%]
2005	2 348	2 088	11.07325
2006	2 513	2 200	12.45523
2007	2 481	2 195	11.52761
2008	2 342	2 101	10.29035
2009	2 168	2 008	7.380074
2010	2 235	2 060	7.829978

This is not a surprising outcome, as satellite databases rely on complex algorithms and different databases deliver variation in results (Suntrace 2011). The previous update of the CENERG algorithm from HC3v2 to HC3v3 during the course of this work showed an increase of 10% in DNI Table 9.

Table 9: Comparison of HC3v2 and HC3v3 data for Spier location

Year	Spier HC3v2 Database [kWh/m2a]	Spier HC3v3 Database [kWh/m2a]	Deviation [%]
2005	1 859	2 026	8.242843
2006	1 948	2 211	11.89507
2007	1 941	2 222	12.64626
2008	1 861	2 137	12.91530
2009	1 767	2 035	13.16953

Based on the measured data for Stellenbosch by CRSES, an algorithm was developed which allows calibrating data of the previous years for the Stellenbosch University site with a mean absolute error of 5.0% for monthly DNI data (Wey 2011). This approach is not possible for the Spier wine farm, as no actual measured data exists for the site. The mean absolute error for hourly measurements is higher, due to punctual recorded satellite data compared to permanent measuring by CRSES device. In other words, short term atmospheric changes are well measured by the permanently recording device, but lead to an error with the hourly measurement, where this occurrence is either overlooked, or used for a full hour. In the long term those effects cancel out and lead to higher accuracy for monthly data sets.

Therefore, for Stellenbosch there now exist a calibrated HC3v3 database reaching back to 2004, while for the investigated site at Spier only the standard HC3v3 database is available. Comparing the satellite data for Spier and Stellenbosch University indicates a mean absolute error of 1.5% on monthly measurement Table 10.

Table 10: Comparison of the Spier and Stellenbosch HC3v3 dataset

Source	Spier HC3v3 Database [kWh/m2a]	CRSES HC3v3 Database [kWh/m2a]	Deviation [%]
2005	2 026	2 088	2.969349
2006	2 211	2 200	0.5
2007	2 222	2 195	1.230068
2008	2 137	2 101	1.71347
2009	2 035	2 008	1.344622

Concluding this, the most appropriate solution was, to use calibrated Stellenbosch data for the initial pre-feasibility study on the Spier CSP plant. The resulting mean absolute error was 5.2%. That this approach was valid is supported by a created DNI map of the region, as illustrated in Figure 47. This map was based on 30 data points, drawn from the HC3v2 version, closest to the Spier farm (with a radius of about 15 km).

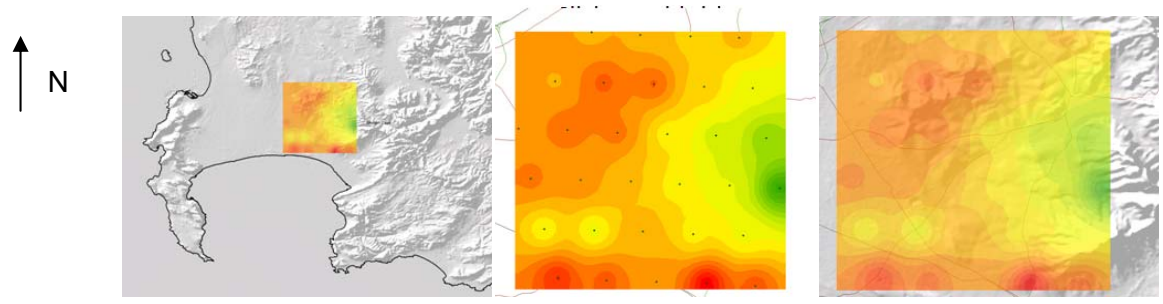

Figure 47: Size of the area of the utilised data points (left) the 30 data points and interpolated insolation (middle) and solar map with contour (right) (figures not scaled).

The map was generated on the basis of interpolation of the twelve closest points. Therefore the quality of the map is useful in the centre of the map where information of many points can be used, but not on the outer edges where little information for interpolation is available. The right-hand map in Figure 47 provides a good understanding of the quality of the interpolated map, as the annual insolation is influenced largely by the surrounding mountains. As can be read from Figure 47, the DNI on the western half of the estate is around 1 890 $\frac{\mathrm{kWh}}{\mathrm{m^2a}}$, and on the eastern half it is 1 880 $\frac{\mathrm{kWh}}{\mathrm{m^2a}}$, while CRSES at Stellenbosch University, where the measurement device is located, is exposed to around 1 850 kWh/m²a (note that this DNI map is based on HC3v2 data).

This way forward is acceptable for a pre-feasibility study. Recent research that compared several satellite algorithms with actual ground measurements concludes that the most accurate approach is the calibration of long term satellite data, supported by at least short term ground measurement (Suntrace 2011). Suntrace (2011) further states that application of a single satellite resource can lead to deviation of up to 30%. Should more detailed planning eventually become necessary, solid data will be gained by ground measurement on-site which can be used to accurately calibrate satellite data.

The mean year consisting of the calibrated data for Stellenbosch is available for the years 2004 to 2010. An average year, comprised from these six years, is approximated by fitting the specific months with the closest same monthly insolation from one of the five years. Thus, a mean year is generated and can be used for the simulation.

APPENDIX G – THE SOLAR BRAYTON CYCLE

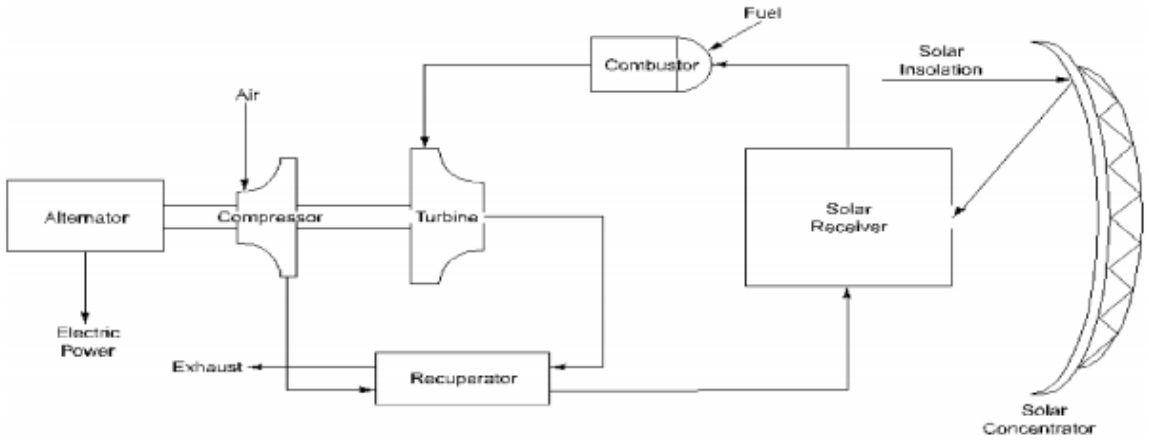

Figure 48: Configuration of a solar Brayton cycle (SolarPACES 1998)

APPENDIX H – INCIDENCE ANGLE MODIFIER

The incidence angle modifiers IAM_t and IAM_l are drawn from Häberle *et al*. (2002). In his document, a curve with the *IAM's* over the zenith angle for the Solarmundo linear Fresnel prototype plant is given, as shown in Figure 49.

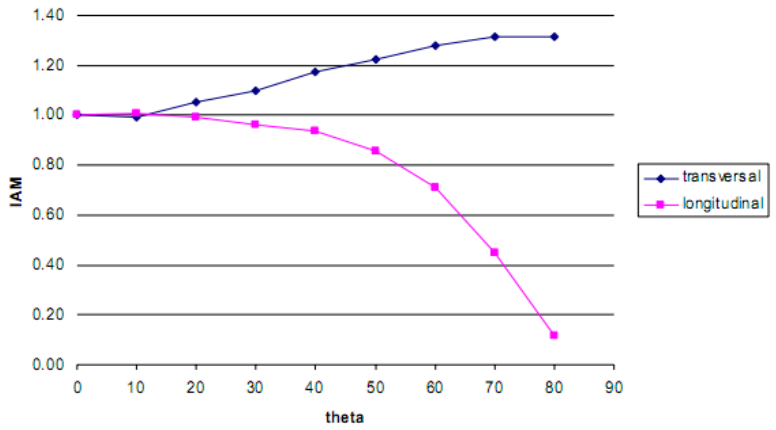

Figure 49: Incidence angle modifiers for the Solarmundo linear Fresnel prototype (Häberle et al. 2002)

To make use of the given points for the simulation, the points need to be expressed in functions of the incidence angle theta. A polynomial curve fit in Excel gives *IAM*-curves as given in Figure 50.

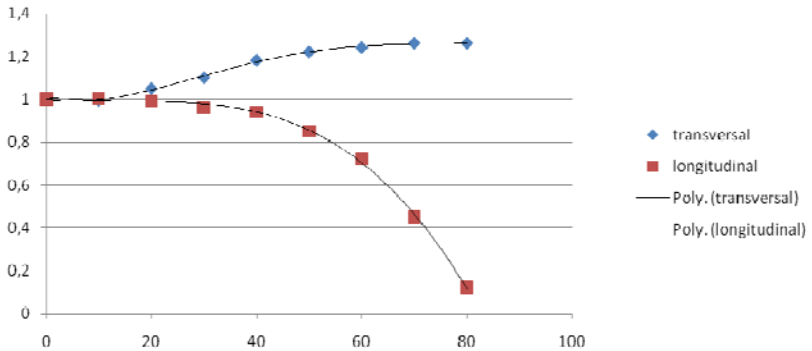

Figure 50: Incidence angle modifiers with polynomial best fit

The equation for the transversal polynomial fit is

$$IAM_t = 35.402 \cdot 10^{-9} \cdot \theta_t^4 - 71.500 \cdot 10^{-7} \cdot \theta_t^3 + 43.514 \cdot 10^{-5} \cdot \theta_t^2 - 39.096 \cdot 10^{-4} \cdot \theta_t + 99.961 \cdot 10^{-2} \quad \text{(G1)}$$

with θ_t as the transversal component of the incidence angle. The R^2 value for the fit is 0.997.

The equation for the longitudinal polynomial fit is

$$IAM_l = -33.123 \cdot 10^{-7} \cdot \theta_l^3 + 16.257 \cdot 10^{-5} \cdot \theta_l^2 - 29.233 \cdot 10^{-4} \cdot \theta_l + 1.0071 \quad \text{(G2)}$$

with θ_l as the longitudinal component of the incidence angle. The R^2 value for the fit is 0.999.

The author is aware that a higher order polynomial fit is not necessarily best engineering practice. For the scope of this simulation it gives a sufficiently accurate equation that can be used straightforwardly.

APPENDIX I – ABSORBER HEAT LOSS – THEORETICAL BACKGROUND

Before the usable solar energy is converted into thermal energy in the absorber pipe, it undergoes a series of heat losses. First of all the sun beams are reflected by the mirrors onto the absorber. The energy concentrated onto the absorber is then reduced to

$$I_{reflected} = \eta_{reflector} \cdot I_{usable} \qquad \text{(H1)}$$

with $\eta_{reflector}$ representing the optical efficiency of the mirror. If secondary reflectors are installed, or the beams travel through glass, these losses occur again at each of these stages, with $\eta_{optical}$ representing the reflectance of a mirror and the transmissivity of glass.

The losses in the absorber tube are commonly given in Watt per meter length of the pipe. Therefore, the energy input per meter is

$$\dot{q}'_{in} = I_{reflected} \cdot A \qquad \text{(H2)}$$

where *A* is the aperture of the reflector.

The desired thermal energy gain of the fluid in the pipe is then calculated as

$$\dot{q}'_{thermal\ in} = \dot{q}'_{in} - \dot{q}'_{loss} \qquad \text{(H3)}$$

In general, heat loss can be separated into three modes. These are conduction, convection and radiation (Incropera et al. 1990). For better understanding, a one-dimensional energy balance on an evacuated tube absorber is illustrated in Figure 51, where the glass envelope separates the absorber pipe from the ambient air.

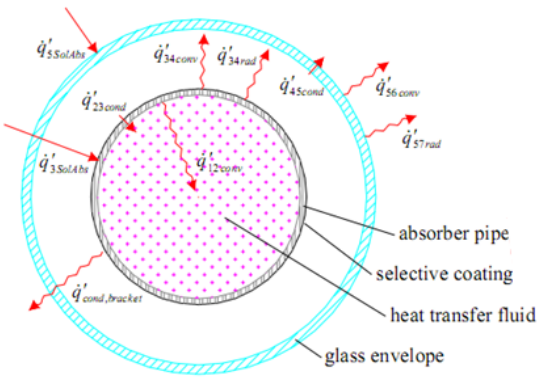

Figure 51: One-dimensional energy balance on evacuated tube absorber (Forristall 2003)

In the illustrated case, the thermal energy gain is

$$\dot{q}'_{thermal\ in} = \dot{q}'_{12conv} = \dot{q}'_{23\ cond} \tag{H4}$$

where

$$\dot{q}'_{23\ cond} = \dot{q}'_{3SolAbs} - \dot{q}'_{34\ conv} - \dot{q}'_{34\ rad} - \dot{q}'_{cond\ bracket} \tag{H5}$$

where $\dot{q}'_{cond\ bracket}$ are the conduction heat losses from the absorber pipe through the support bracket. $\dot{q}'_{34\ conv}$ and $\dot{q}'_{34\ rad}$ are the convection and radiation losses from the absorber pipe, where the convection part can be neglected in this scenario, as the space between the absorber and the glass envelope is evacuated. Furthermore

$$\dot{q}'_{3SolAbs} = \eta_{transenv} \cdot \dot{q}'_{in} \tag{H6}$$

where $\eta_{transenv}$ is the transmissivity of the glass envelope.

The heat loss of the one-dimensional segment is

$$\dot{q}'_{Heat\ loss} = \dot{q}'_{56conv} + \dot{q}'_{57rad} + \dot{q}'_{cond,bracket} \tag{H7}$$

where

$$\dot{q}'_{56conv} + \dot{q}'_{57rad} = \dot{q}'_{45cond} + \dot{q}'_{5SolAbs} \tag{H8}$$

with

$$\dot{q}'_{5SolAbs} = \dot{q}'_{in} - \dot{q}'_{3SolAbs} \tag{H9}$$

As a result the heat loss can be calculated depending on material properties, insolation and operating temperature of the absorber. For detailed theoretical analysis of the heat losses, the reader is referred to Forristall (2003). The heat loss of an evacuated receiver has been tested at NREL (Burkholder, Kutscher 2009) and is given in Figure 52.

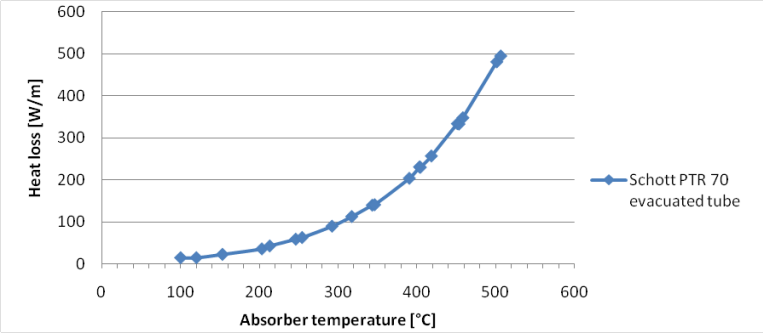

Figure 52: Heat loss of Schott 2008 PTR70 evacuated tube receiver (based on (Burkholder 2009))

APPENDIX J – PROPOSED POWER PLANT LOCATION (SATELLITE PICTURE)

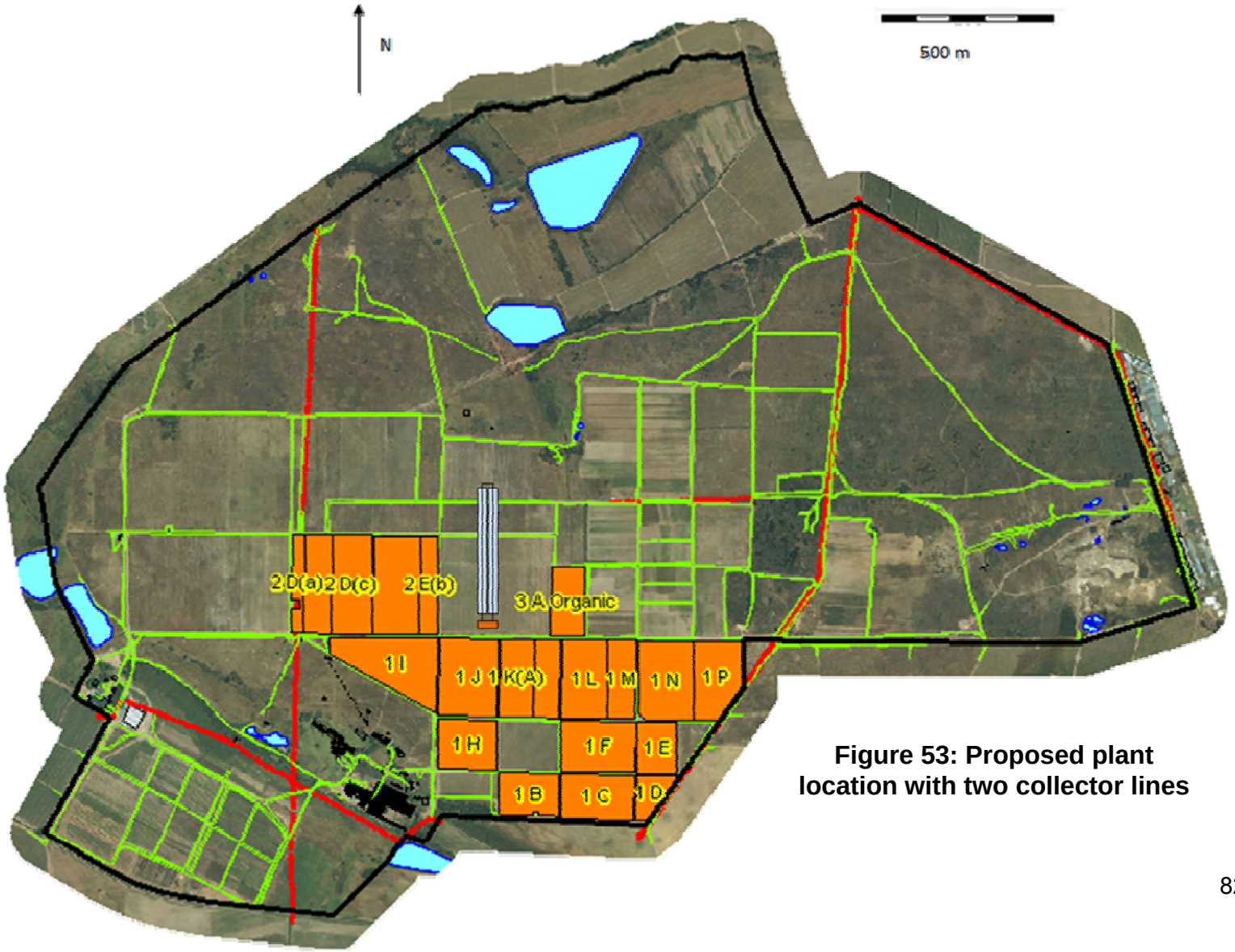

Figure 53: Proposed plant location with two collector lines

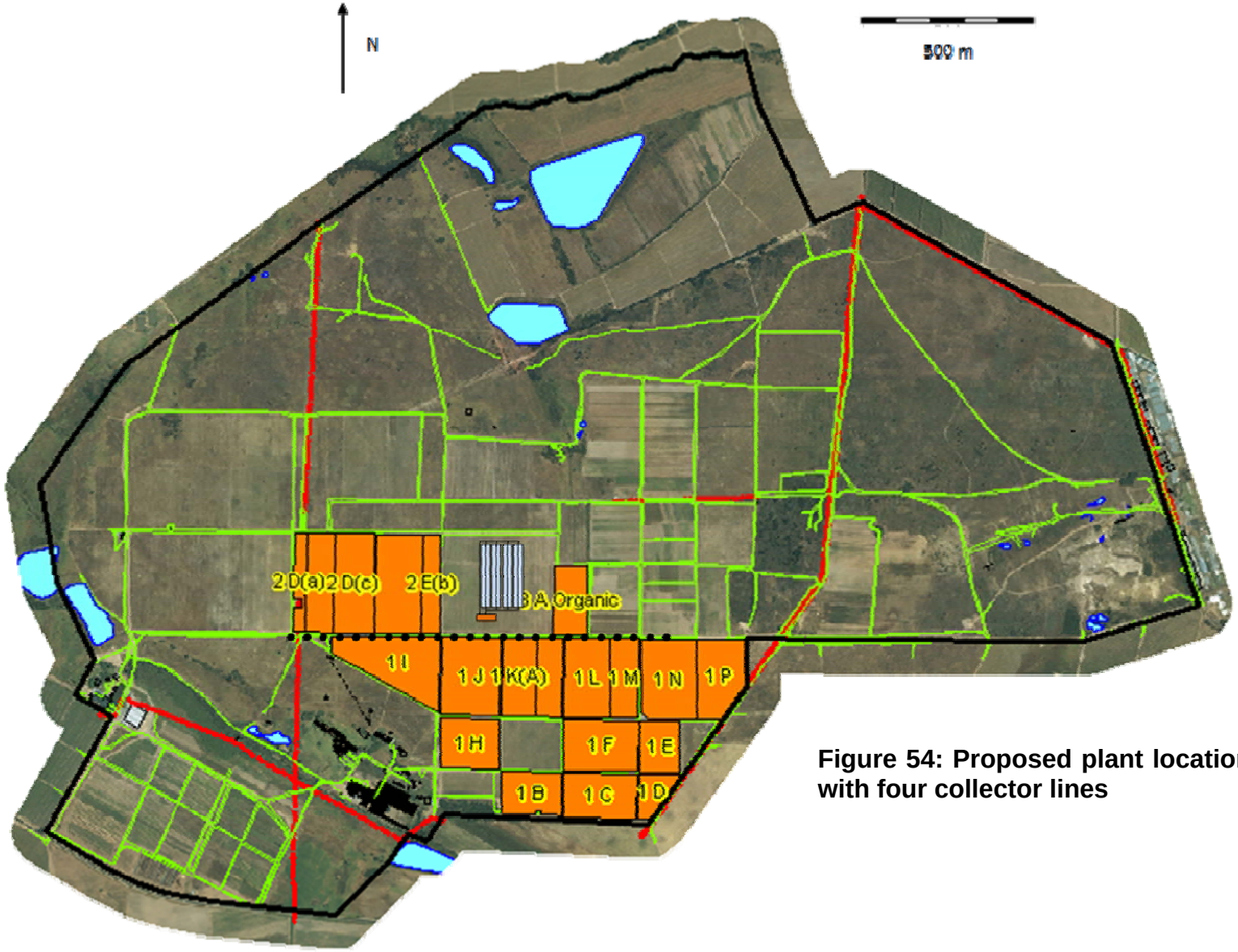

Figure 54: Proposed plant location with four collector lines

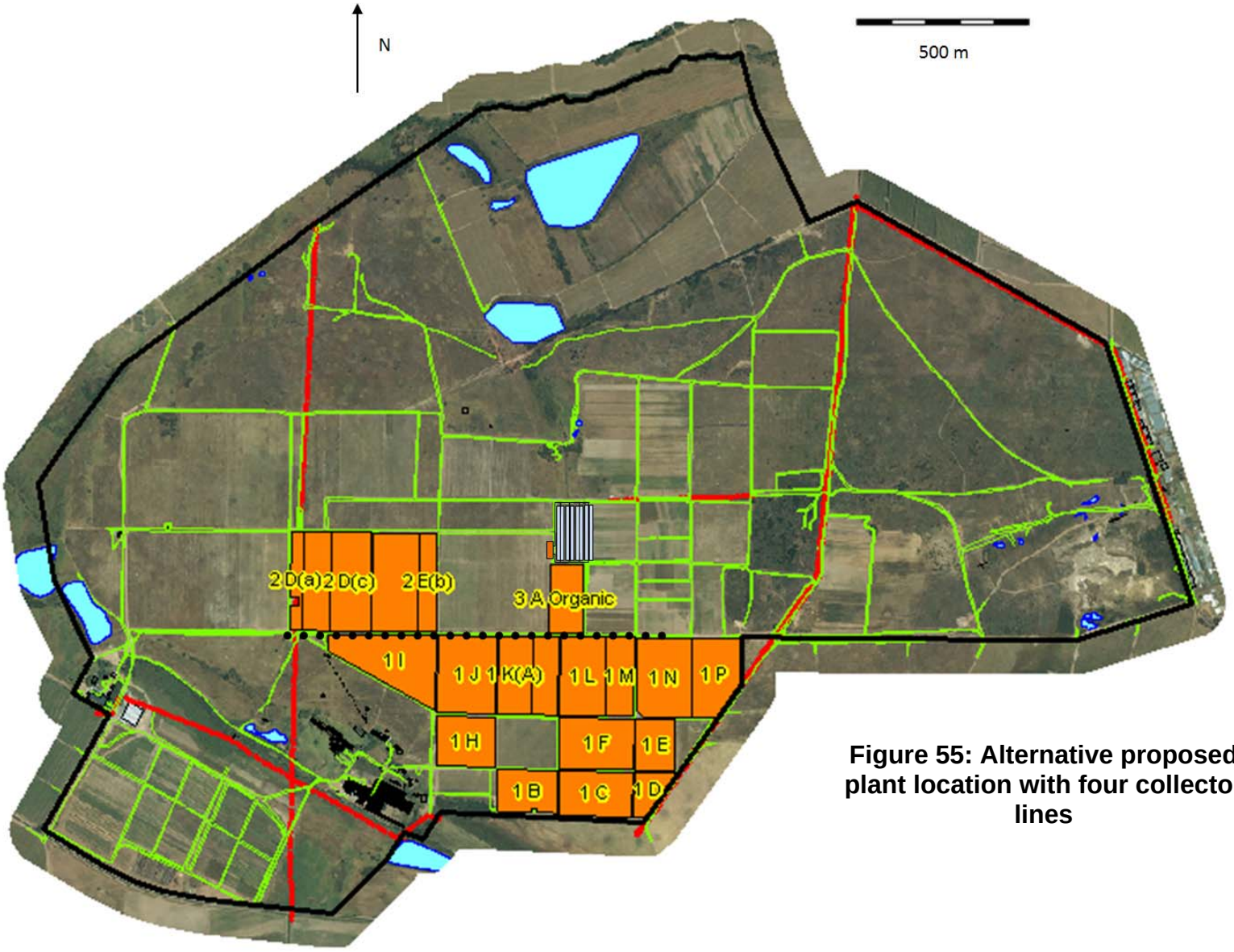

Figure 55: Alternative proposed plant location with four collector lines

APPENDIX K – PROPOSED POWER PLANT LOCATION WITH 1 M CONTOUR LINES

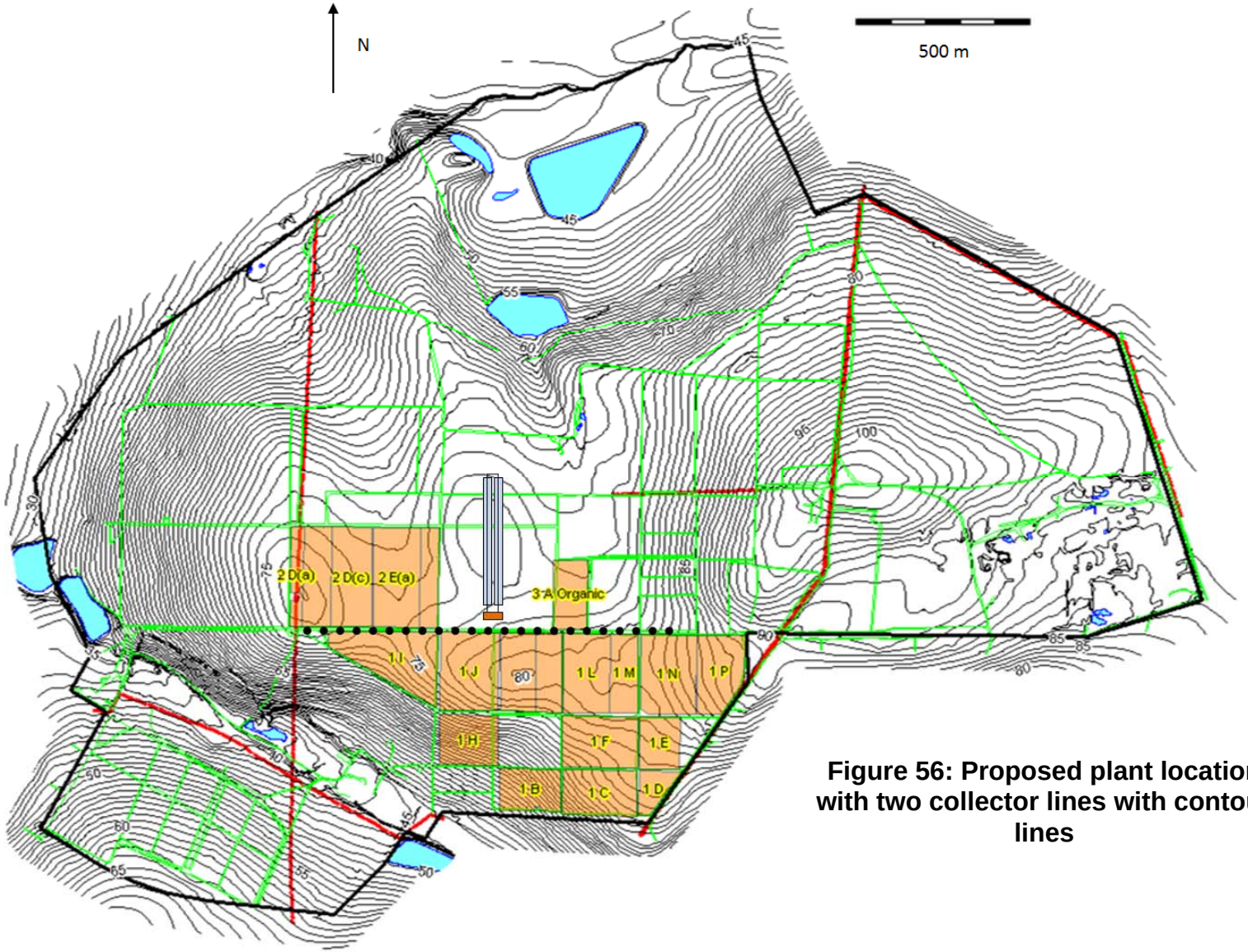

Figure 56: Proposed plant location with two collector lines with contour lines

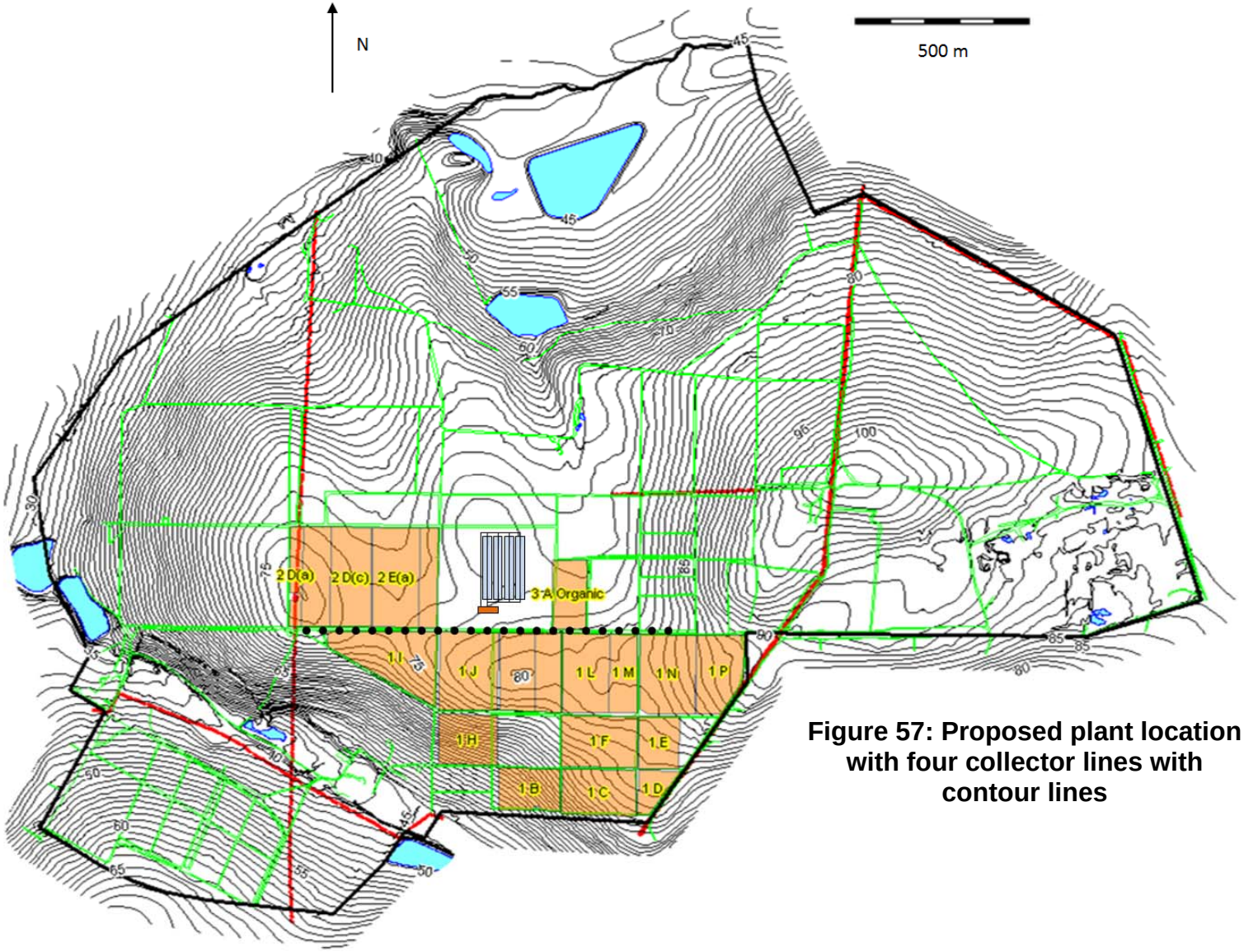

Figure 57: Proposed plant location with four collector lines with contour lines

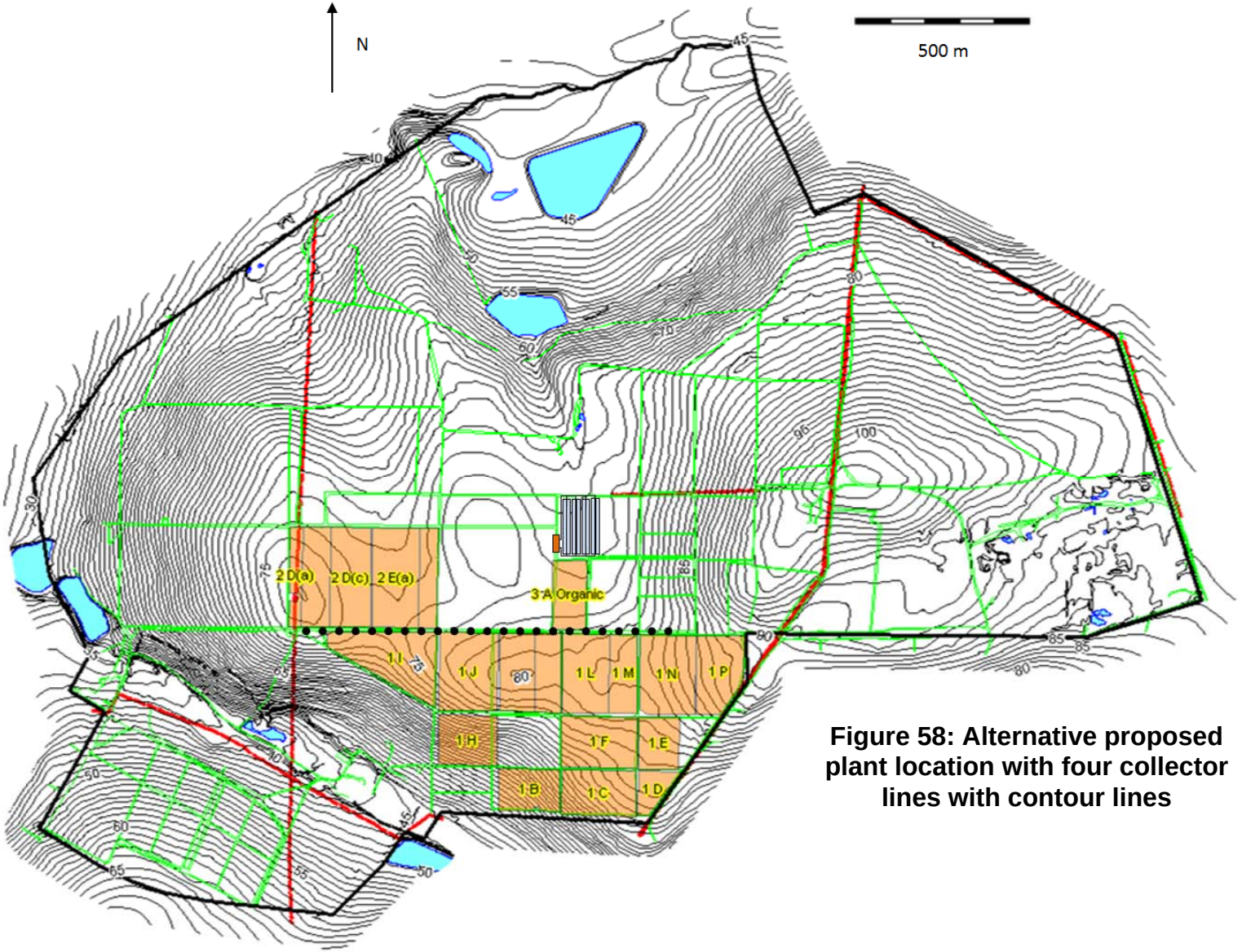

Figure 58: Alternative proposed plant location with four collector lines with contour lines

APPENDIX L – POSSIBLE POWER PLANT TO SUPPLY TODAY'S DEMAND

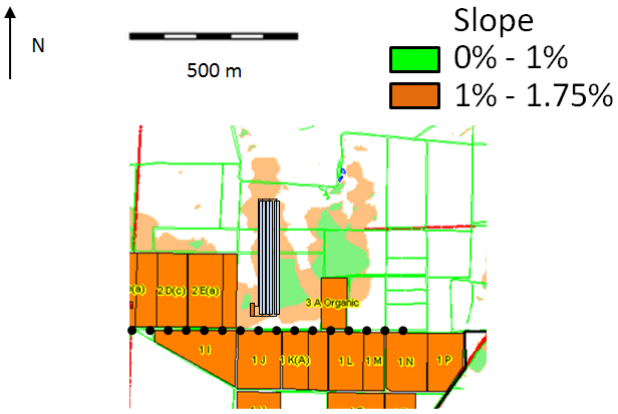

Figure 59 Power plant configuration with three lines, sized to supply 100% of today's electricity demand of 5 570 MWh per year

APPENDIX M – PROPOSED POWER PLANT LOCATION (PICTURE)

As seen from Helderberg southern summit (-34.038283°N,18.869054°E) with two collector line setup (Figure 60).

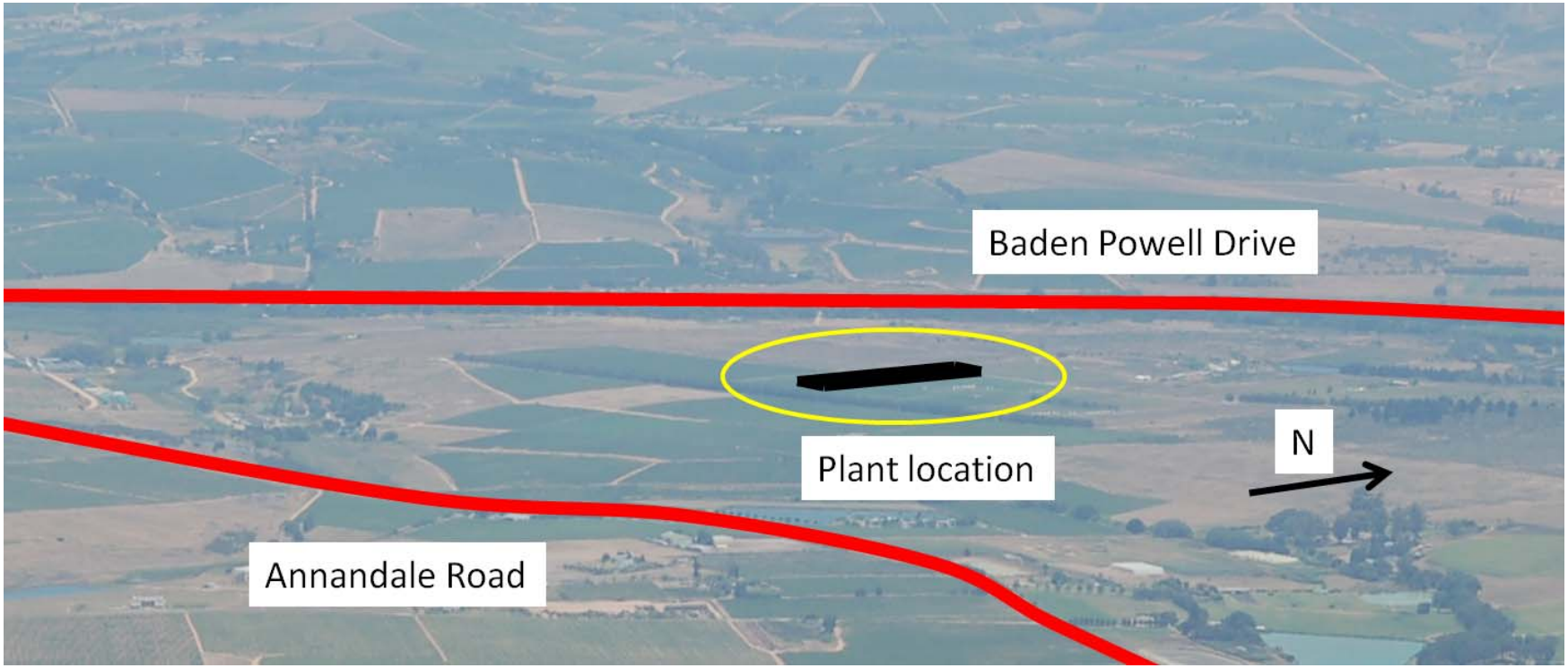

Figure 60: Proposed plant dimension with two collector lines seen from Helderberg

APPENDIX N – PROPOSED POWER PLANT LOCATION (PICTURE)

As seen from Stellenboschberg (-33.965598°N,18.892143°E) with two collector line setup (Figure 61).

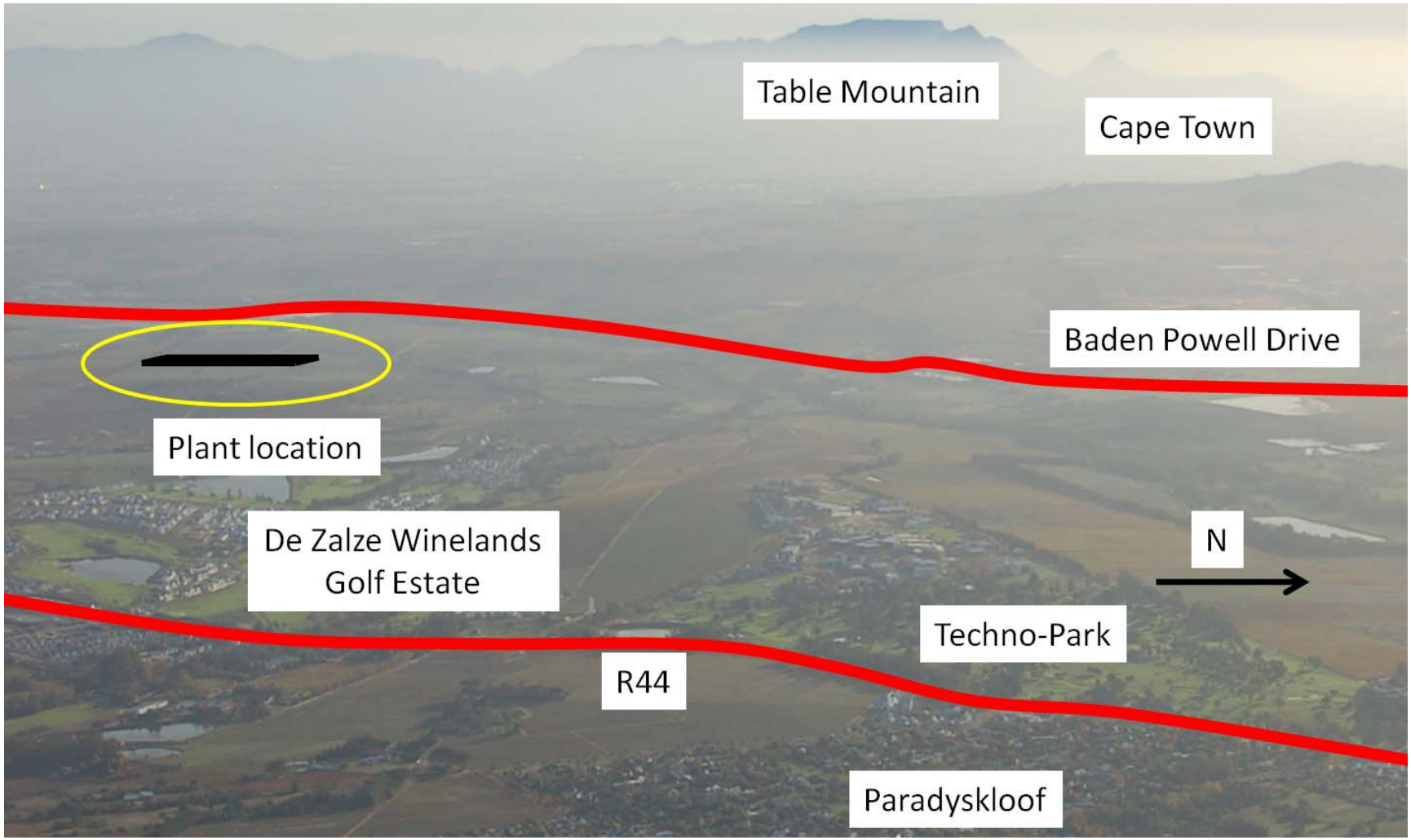

Figure 61: Proposed plant dimension with two collector lines seen from Stellenboschberg